RESEARCH REPORT

HEALTH EFFECTS INSTITUTE

Number 207
September 2022

Characterizing Determinants of Near-Road Ambient Air Quality for an Urban Intersection and a Freeway Site

H. Christopher Frey, Andrew P. Grieshop, Andrey Khlystov, John J. Bang, Nagui Rouphail, Joseph Guinness, Daniel Rodriguez, Montse Fuentes, Provat Saha, Halley Brantley, Michelle Snyder, Shams Tanvir, Kwanpyo Ko, Theophraste Noussi, Maryam Delavarrafiee, Sanjam Singh

ISSN 1041-5505 (print)
ISSN 2688-6855 (online)

Characterizing Determinants of Near-Road Ambient Air Quality for an Urban Intersection and a Freeway Site

H. Christopher Frey, Andrew P. Grieshop, Andrey Khlystov, John J. Bang, Nagui Rouphail, Joseph Guinness, Daniel Rodriguez, Montse Fuentes, Provat Saha, Halley Brantley, Michelle Snyder, Shams Tanvir, Kwanpyo Ko, Theophraste Noussi, Maryam Delavarrafiee, Sanjam Singh

---

with a Critique by the HEI Review Committee

Research Report 207

Health Effects Institute

Boston, Massachusetts

Trusted Science · Cleaner Air · Better Health

Publishing history: This document was posted at *www.healtheffects.org* in September 2022.

Citation for document:

Frey HC, Grieshop AP, Khlystov A, Bang JJ, Rouphail N, Guinness J, et al. 2022. Characterizing Determinants of Near-Road Ambient Air Quality for an Urban Intersection and a Freeway Site. Research Report 207. Boston, MA:Health Effects Institute.

CONTENTS

ABOUT HEI

The Health Effects Institute is a nonprofit corporation chartered in 1980 as an independent research organization to provide high-quality, impartial, and relevant science on the effects of air pollution on health. To accomplish its mission, the Institute

- Identifies the highest-priority areas for health effects research
- Competitively funds and oversees research projects
- Provides intensive independent review of HEI-supported studies and related research
- Integrates HEI's research results with those of other institutions into broader evaluations
- Communicates the results of HEI's research and analyses to public and private decision makers.

HEI typically receives balanced funding from the U.S. Environmental Protection Agency and the worldwide motor vehicle industry. Frequently, other public and private organizations in the United States and around the world also support major projects or research programs. HEI has funded more than 340 research projects in North America, Europe, Asia, and Latin America, the results of which have informed decisions regarding carbon monoxide, air toxics, nitrogen oxides, diesel exhaust, ozone, particulate matter, and other pollutants. These results have appeared in more than 260 comprehensive reports published by HEI, as well as in more than 2,500 articles in the peer-reviewed literature.

HEI's independent Board of Directors consists of leaders in science and policy who are committed to fostering the public–private partnership that is central to the organization. The Research Committee solicits input from HEI sponsors and other stakeholders and works with scientific staff to develop a Five-Year Strategic Plan, select research projects for funding, and oversee their conduct. The Review Committee, which has no role in selecting or overseeing studies, works with staff to evaluate and interpret the results of funded studies and related research.

All project results and accompanying comments by the Review Committee are widely disseminated through HEI's website (*www.healtheffects.org*), reports, newsletters and other publications, annual conferences, and presentations to legislative bodies and public agencies.

ABOUT THIS REPORT

Research Report 207, *Characterizing Determinants of Near-Road Ambient Air Quality for an Urban Intersection and a Freeway Site,* presents a research project funded by the Health Effects Institute and conducted by Dr. H. Christopher Frey of North Carolina State University, Raleigh, and his colleagues. The report contains three main sections.

The HEI Statement, prepared by staff at HEI, is a brief, nontechnical summary of the study and its findings; it also briefly describes the Review Committee's comments on the study.

The Investigators' Report, prepared by Frey and colleagues, describes the scientific background, aims, methods, results, and conclusions of the study.

The Critique, prepared by members of the Review Committee with the assistance of HEI staff, places the study in a broader scientific context, points out its strengths and limitations, and discusses remaining uncertainties and implications of the study's findings for public health and future research.

This report has gone through HEI's rigorous review process. When an HEI-funded study is completed, the investigators submit a draft final report presenting the background and results of the study. This draft report is first examined by outside technical reviewers and a biostatistician. The report and the reviewers' comments are then evaluated by members of the Review Committee, an independent panel of distinguished scientists who are not involved in selecting or overseeing HEI studies. During the review process, the investigators have an opportunity to exchange comments with the Review Committee and, as necessary, to revise their report. The Critique reflects the information provided in the final version of the report.

PREFACE

HEI's Research Program to Improve Assessment of Exposure to Traffic-Related Air Pollution

INTRODUCTION

Traffic emissions are an important source of urban air pollution. Emissions from motor vehicles and ambient concentrations of most monitored traffic-related pollutants have decreased steadily over the last several decades in most high-income countries as a result of air quality regulations and improvements in vehicular emission control technologies, and this trend is likely to continue. However, these positive developments have not been able to fully compensate for the rapid growth of the motor vehicle fleet due to growth in population and economic activity and increased traffic congestion, as well as the presence of older or malfunctioning vehicles on the roads.

In 2010, HEI published *Special Report 17, Traffic-Related Air Pollution: A Critical Review of the Literature on Emissions, Exposure, and Health Effects*. The report "identified an exposure zone within a range of up to 300 to 500 m from a major road as the area most highly affected by traffic emissions (the range reflects the variable influence of background pollution concentrations, meteorologic conditions, and season)" and estimated that 30% to 45% of people living in large North American cities reside within this zone. Based on a review of health studies, the report concluded that exposure to traffic-related air pollution was causally linked to worsening asthma symptoms. It also found "suggestive evidence of a causal relationship with onset of childhood asthma, nonasthma respiratory symptoms, impaired lung function, total and cardiovascular mortality, and cardiovascular morbidity" (HEI 2010).

Special Report 17 also noted that exposure assessment of traffic-related air pollution is challenging because it is a complex mixture of pollutants in particulate and gaseous forms, many of which are also emitted by other sources. Traffic-related air pollution is also characterized by high spatial and temporal variability, with the highest concentrations occurring at or close to major roads. Therefore, it has been difficult to identify an appropriate exposure metric that uniquely indicates traffic-related air pollution, and to model the distribution of exposure at a sufficiently high degree of spatial and temporal resolution.

The most commonly used exposure metrics are measured or modeled concentrations of individual pollutants considered to be indicators of traffic-related air pollution (such as nitrogen dioxide or black carbon) and simple indicators of traffic (such as distance of the residence from busy roads or traffic density near the residence).

A range of models — such as dispersion, land-use regression, and hybrid models — has been developed to estimate exposure. Some attempts to account for outdoor air entering buildings and how people spend time outdoors versus indoors have been made to refine such estimates. Many improvements in these exposure models have occurred over time, especially with the advance of geographical information system approaches and the application of more sophisticated statistical methods. However, their usefulness still depends on the model assumptions and input data quality. Few studies have compared the performance of different models and evaluated exposure measurement error and possible bias in health estimations.

To start addressing these issues, HEI issued a Request for Applications in 2013. To inform the development of the RFA, the HEI Research Committee held a workshop in April 2012 with experts in the areas of atmospheric chemistry, pollutant measurements, exposure models, epidemiology, and health assessment to discuss and identify the highest priority research questions.

Preface

OBJECTIVES OF RFA 13-1

RFA 13-1, Improving Assessment of Near-Road Exposure to Traffic Related Pollution, aimed to solicit studies to improve exposure assessment for use in future work on the health effects of traffic-related air pollution. The RFA had three major objectives:

- Demonstrate novel surrogates of near-road traffic-related pollution, taking advantage of new sensors and/or existing monitoring data.
- Determine the most important variables that explain spatial and temporal variance of near-road traffic-related pollutant concentrations at the personal, residential, and/or community levels, and explain the implications of these for future monitoring, modeling, exposure, and health effects studies.
- Improve inputs for exposure models for traffic-related health studies; evaluate and compare the performance of alternative models to existing models and actual measurements to quantify exposure measurement error.

DESCRIPTION OF THE PROGRAM

Five studies were funded under RFA 13-1 to represent a variety of geographical locations and cover the various RFA objectives; they are summarized below. The study by Frey and colleagues described in this report (Research Report 207) is the fourth to be published. In the meantime, HEI has funded additional studies on similar exposure assessment topics. All recent and ongoing exposure assessment studies are included in the Preface Table.

"The Hong Kong D3D Study: A Dynamic Three Dimensional Exposure Model for Hong Kong," Benjamin Barratt, King's College London, United Kingdom. Barratt and colleagues estimated exposure to traffic-related air pollution using a dynamic three-dimensional land use regression model for Hong Kong, which has many high-rise buildings, resulting in street canyons. Different exposure models were developed with increasing complexity (e.g., incorporating infiltration indoors, vertical gradients, and time–activity patterns) and applied in an epidemiological study to evaluate the potential impact of exposure measurement error in mortality estimates (*Research Report 194*).

"Enhancing Models and Measurements of Traffic-Related Air Pollutants for Health Studies Using Dispersion Modeling and Bayesian Data Fusion," Stuart Batterman, University of Michigan, Ann Arbor, Michigan. Batterman and colleagues evaluated the ability to predict traffic-related air pollution using a variety of methods and models, including a line source air pollution dispersion model and sophisticated spatiotemporal Bayesian data fusion methods. The study made extensive use of data collected in the Near-road EXposures and effects of Urban air pollutants Study (NEXUS), a cohort study designed to examine the relationship between near-roadway pollutant exposures and respiratory outcomes in children with asthma who live close to major roadways in Detroit (*Research Report 202*).

"Characterizing the Determinants of Vehicle Traffic Emissions Exposure: Measurement and Modeling of Land-Use, Traffic, Transformation, and Transport," H. Christopher Frey, North Carolina State University, Raleigh, North Carolina. In the study presented in this report, Frey and colleagues investigated key factors that influence exposure to traffic-related air pollution: traffic and its composition; built environment including road characteristics and land use; and dispersion, transport, and transformation processes. They made extensive measurements of fine particulate matter, ultrafine particles, oxides of nitrogen, and semivolatile organic compounds in various near-road locations in the Raleigh–Durham area.

"Developing Multipollutant Exposure Indicators of Traffic Pollution: The Dorm Room Inhalation to Vehicle Emissions (DRIVE) Study," Jeremy Sarnat, Emory University, Atlanta, Georgia Sarnat and colleagues evaluated novel multipollutant traffic surrogates by collecting measurements in and around two student dormitories in Atlanta and explored the use of metabolomics to identify possible exposure-related metabolites. The DRIVE study made use of a unique emission-exposure setting in Atlanta, on the Georgia Institute of Technology campus, with one dorm immediately adjacent to the busiest and most congested highway artery in the city (with more than 300,000 vehicles per day) and another dorm located farther away (*Research Report 196*).

"Evaluation of Alternative Sensor-Based Exposure Assessment Methods," Edmund Seto, University of Washington, Seattle, Washington. Seto and colleagues performed an evaluation of novel, low-cost air pollution sensors to characterize traffic-related air pollution in the San Francisco Bay area. They deployed various sensors — including Shinyei particulate matter sensors and Alphasense electrochemical sensors — for an extended period of time. Sensors were colocated with

reference monitors to evaluate sensor performance. This study resulted in an unpublished report, which can be obtained by contacting HEI at *pubs@healtheffects.org*.

FURTHER RESEARCH UNDERWAY

The studies funded under RFA 13-1 offer valuable lessons that can be integrated into new epidemiological research on the health effects of traffic-related air pollution. Thus, HEI issued *RFA 17-1, Assessing Adverse Health Effects of Exposure to Traffic-Related Air Pollution, Noise, and Their Interactions with Socioeconomic Status*, seeking studies to assess adverse health effects of short- and/or long-term exposure to traffic-related air pollution. The applicants were asked to consider spatially correlated factors that may either confound or modify the health effects of traffic-related air pollution, most notably, traffic noise, socioeconomic status, and factors related to the built environment, such as presence of green space. Three studies funded under RFA 17-1 are in progress as of the publication of this report (see Preface Table). In addition, HEI funded a related study under the Walter A. Rosenblith New Investigator Award to compare exposure estimates obtained from intensive air pollutant measurement campaigns with Google Street View cars with estimates from more conventional methods.

Subsequently, HEI issued *RFA 19-1, Applying Novel Approaches to Improve Long-Term Exposure Assessment of Outdoor Air Pollution for Health Studies* to address challenges in accurately assigning exposures of pollutants that vary highly in space and time to individuals, and to quantify the influence of exposure measurement error on estimated health risks. Five ongoing studies were funded under RFA 19-1. Three of the studies are combining measurements of air pollution from emerging sources — such as satellite data — and diverse exposure assessment approaches to improve exposure assignment in well-established cohorts. Two studies are testing the added value of incrementally more complex statistical modeling approaches to improving exposure assessment and how this may affect uncertainty in health effect estimates in epidemiological studies.

In addition, since the release of HEI's critical review of the traffic literature in 2010, many additional studies about traffic-related air pollution have been published, and regulations and vehicular technology have advanced significantly. In 2022, HEI published a new review of the epidemiological literature on selected health effects of long-term exposure to traffic-related air pollution: Special Report 23, *Systematic Review and Meta-analysis of Selected Health Effects of Long-Term Exposure to Traffic-Related Air Pollution* (HEI 2022). Further information on these activities can be obtained at the HEI website, *www.healtheffects.org/air-pollution/traffic-related-air-pollution*.

REFERENCES

Barratt B, Lee M, Wong P, Tang R, Tsui TH, Cheng W, et al. 2018. A Dynamic Three-Dimensional Air Pollution Exposure Model for Hong Kong. Research Report 194. Boston, MA:Health Effects Institute.

HEI (Health Effects Institute). 2010. Traffic-Related Air Pollution: A Critical Review of the Literature on Emissions, Exposure, and Health Effects. Special Report 17. Boston, MA:Health Effects Institute.

HEI (Health Effects Institute). 2022. Systematic Review and Meta-Analysis of Selected Health Effects of Long-Term Exposure to Traffic-Related Air Pollution. Special Report 23. Boston, MA:Health Effects Institute.

Sarnat JA, Russell A, Liang D, Moutinho JL, Golan R, Weber RJ, et al. 2018. Developing Multipollutant Exposure Indicators of Traffic Pollution: The Dorm Room Inhalation to Vehicle Emissions (DRIVE) Study. Research Report 196. Boston, MA:Health Effects Institute.

Seto E, Austin E, Carvlin G, Shirai J, Hubbard A, Hammond K, et al. 2018. Evaluation of Alternative Sensor-based Exposure Assessment Methods. Unpublished report. Boston, MA:Health Effects Institute.

Preface Table. Summary of Recently Completed, Ongoing, and Projected Studies Funded by HEI to Improve Exposure Assessment for Health Studies

Principal Investigator	Title	Study Status
RFA 13-1, Improving Assessment of Near-Road Exposure to Traffic Related Pollution		
Benjamin Barratt, King's College London, United Kingdom	The Hong Kong D3D Study: A Dynamic Three-Dimensional Exposure Model for Hong Kong	Research Report 194
Stuart Batterman, University of Michigan, Ann Arbor	Enhancing Models and Measurements of Traffic-Related Air Pollutants for Health Studies Using Dispersion Modeling and Bayesian Data Fusion	Research Report 202
H. Christopher Frey, North Carolina State University, Raleigh	Characterizing the Determinants of Vehicle Traffic Emissions Exposure: Measurement and Modeling of Land-Use, Traffic, Transformation, and Transport	Research Report 207*
Jeremy Sarnat, Emory University, Atlanta	Developing Multipollutant Exposure Indicators of Traffic Pollution: The Dorm Room Inhalation to Vehicle Emissions (DRIVE) Study	Research Report 196
Edmund Seto, University of Washington, Seattle	Evaluation of Alternative Sensor-Based Exposure Assessment Methods	Unpublished report
RFA 17-1, Assessing Adverse Health Effects of Exposure to Traffic-Related Air Pollution, Noise, and Their Interactions with Socioeconomic Status		
Payam Dadvand and Jordi Sunyer, Barcelona Institute for Global Health (ISGlobal), Spain	Traffic-Related Air Pollution and Birth Weight: The Roles of Noise, Placental Function, Green Space, Physical Activity, and Socioeconomic Status (FRONTIER)	Ongoing
Ole Raaschou-Nielsen, Danish Cancer Society Research Center, Copenhagen, Denmark	Health Effects of Air Pollution Components, Noise and Socioeconomic Status ("HERMES")	Ongoing
Meredith Franklin, University of Southern California, Los Angeles	Intersections as Hot Spots: Assessing the Contribution of Localized Non-Tailpipe Emissions and Noise on the Association between Traffic and Children's Health	Ongoing
RFA 16-1, Walter A. Rosenblith New Investigator Award		
Joshua Apte, University of Texas, Austin	Scalable Multi-Pollution Exposure Assessment Using Routine Mobile Monitoring Platforms	Ongoing
RFA 19-1, Applying Novel Approaches to Improve Long-Term Exposure Assessment of Outdoor Air Pollution for Health Studies		
Scott Weichenthal, McGill University, Montreal, Canada	Comparing the Estimated Health Impacts of Long-Term Exposures to Traffic-Related Air Pollution Using Fixed-Site, Mobile, and Deep Learning Models	Ongoing
Gerard Hoek, Utrecht University, The Netherlands	Comparison of Long-Term Air Pollution Exposure Assessment Based on Mobile Monitoring, Low-Cost Sensors, Dispersion Modelling and Routine Monitoring-Based Exposure Models	Ongoing
Kees de Hoogh, Swiss Tropical and Public Health Institute, Basel, Switzerland	Accounting for Mobility in Air Pollution Exposure Estimates in Studies on Long-Term Health Effects	Ongoing
Klea Katsouyanni, Imperial College, United Kingdom	Investigating the Consequences of Measurement Error of Gradually More Sophisticated Long-Term Personal Exposure Models in Assessing Health Effects: The London Study (MELONS)	Ongoing
Lianne Sheppard, University of Washington, Seattle	Optimizing Exposure Assessment for Inference about Air Pollution Effects with Application to the Aging Brain	Ongoing

*Current study.

HEI STATEMENT
Synopsis of Research Report 207

Air Quality Near a Freeway and an Urban Intersection

INTRODUCTION

Traffic emissions are an important source of urban air pollution, and exposure to traffic-related air pollution has been associated with various adverse health effects. However, exposure assessment is challenging because traffic-related air pollution is a complex mixture of many particulate and gaseous pollutants and is highly variable across locations and time. Developing accurate models of traffic-related air pollution for use in exposure assessment for epidemiological studies relies on understanding traffic activity and air flow at small spatial scales within cities.

Dr. H. Christopher Frey from North Carolina State University and his team proposed a study to explore how traffic activity metrics, land use parameters, and transport of pollutants influence near-road air pollutant concentrations. One question they posed was whether more detailed measurements of factors affecting near-road air pollutant levels can help with the development of models of concentrations of primary and secondary air pollutants within hundreds of meters of roads, and which of those measurements most improved the air quality model performance at different locations and times. They incorporated key concepts from various fields related to roads and air pollution, including transportation, mobile source emissions, traffic operations, and meteorology.

What This Study Adds

- The investigators conducted intensive measurement campaigns to explore detailed parameters that could potentially improve estimation of concentrations of six air pollutants (nitrogen oxides, nitrogen dioxide, ultrafine particles, black carbon, fine particles, and ozone) near a freeway and near an urban intersection.
- They developed parameters based on detailed real-time traffic intensity and novel traffic indices, real-world vehicle behavior (e.g., acceleration, breaking, and turning) and emissions, land use, and local meteorology.
- They developed statistical models of air pollutant concentrations based on these detailed parameters and output from a line source dispersion model reflecting traffic emissions on roads, meteorology, and other factors.
- Real-time local traffic, meteorological data, and dispersion model parameters contributed to statistical models of the six air pollutants near the freeway and urban intersection, with the parameters used in the final statistical models depending on the site and the pollutant.
- This study contributes a rich set of measurements on six air pollutants and shows that more detailed measurements can help with the development of enhanced near-road air quality models in specific situations.

APPROACH

The study aimed to explain variability in outdoor concentrations of six traffic-related air pollutants (nitrogen oxides, nitrogen dioxide, ultrafine particles, black carbon, fine particles, and ozone) at two sites near a heavily traveled freeway (140,000–145,000 vehicles per day) and a busy urban intersection (about 1,000 vehicles per day; Statement Figure). The investigators measured near-road air quality in both areas on selected days between July 2015 and May 2016. They used fixed and moveable monitors placed at various distances from traffic.

The investigators developed dispersion and statistical models of the measured air pollutants at both sites. They ran the U.S. Environmental Protection Agency's Research LINE source dispersion model (R-LINE) to test dispersion model output as inputs to the statistical models. They also tested many other potential statistical model inputs, including common inputs like distance to roads or land use, a new detailed assessment of land elevation and the built environment, and real-time local traffic and weather conditions. The study team compared different statistical models and selected as their final statistical models the simplest ones where the model predictions best matched the measurements (highest model R^2). The relative importance of all variables in the final statistical models was also reported.

This Statement, prepared by the Health Effects Institute, summarizes a research project funded by HEI and conducted by Dr. H. Christopher Frey at North Carolina State University, Raleigh, North Carolina, and colleagues. This report was completed before Dr. Frey took a position with the U.S. Environmental Protection Agency. Research Report 207 contains both the detailed Investigators' Report and a Critique of the study prepared by the Institute's Review Committee.

Statement Figure. Aerial photography of the freeway and urban intersection sites. Yellow dots show locations of fixed-site air quality monitors. Imagery source: OpenStreetMap.

MAIN RESULTS AND INTERPRETATION

Frey and colleagues compiled a comprehensive database of traffic-related and land use variables from measurement campaigns in two study locations (a freeway and a busy urban intersection) in North Carolina. Air pollutant concentrations were higher near the freeway than the urban intersection and decreased with increasing distance from traffic at both sites. Statistical model performance varied by both pollutant and site. At the freeway site, the models had moderate performance for black carbon, moderate to good for ultrafine particles, nitric oxide, and nitrogen oxides, and good for fine particles; at the urban intersection site, the models had poor performance for fine particles, moderate for ultrafine particles, and good for ozone. Local and real-time weather and traffic were useful parameters in statistical models of some of the pollutants, especially near the freeway.

Some other new potential parameters explored by the investigators (e.g., built environment and elevation) were not included in the final models because they did not contribute to the model R^2, most likely because the study areas were very small. Inclusion of dispersion model parameters improved the statistical models of the pollutants most strongly related to traffic at the freeway site but were less useful for predicting fine particle concentration at the freeway site or any of the pollutants measured at the urban intersection site.

In its independent review of the study, the HEI Review Committee concurred with the investigators that this study demonstrated that detailed characterization can sometimes be useful for developing statistical models that estimate near-road air pollutant concentrations. The Committee concluded that strengths of the study were the detailed characterization of the study areas and incorporation of the perspectives from transportation and other fields into the study of near-road air quality, the use of novel traffic indices with distance-weighted traffic activity, and the use of dispersion model parameters as contributors to statistical models of air pollution. However, they noted that there was not enough variation in some of the new parameters to include them in the statistical models. Additionally, the two sites evaluated might not be representative of other locations, and it is unclear how the models for those two sites represent exposure of nearby populations to air pollution.

CONCLUSIONS

Although the statistical models developed for this study are specific to the locations where the measurements were made, the intense measurement campaigns and evaluations of the value of new parameters that described land use, emissions, and local weather in detail contributed to an ongoing discussion of which detailed measurements are most valuable for developing better near-road air quality models of traffic-related air pollutants. Additional studies — including some ongoing studies funded by HEI — will be needed to explore whether the effort put into developing more complex models of traffic-related air pollution will benefit exposure assessment for epidemiological studies.

INVESTIGATORS' REPORT

Characterizing Determinants of Near-Road Ambient Air Quality for an Urban Intersection and a Freeway Site

H. Christopher Frey[1], Andrew P. Grieshop[1], Andrey Khlystov[2], John J. Bang[3], Nagui Rouphail[1], Joseph Guinness[1], Daniel Rodriguez[4], Montse Fuentes[1], Provat Saha[1], Halley Brantley[1], Michelle Snyder[4], Shams Tanvir[1], Kwanpyo Ko[1], Theophraste Noussi[3], Maryam Delavarrafiee[1], Sanjam Singh[1]

[1]North Carolina State University; [2]Desert Research Institute; [3]North Carolina Central University; [4]University of North Carolina, Chapel Hill

ABSTRACT

Introduction Near-road ambient air pollution concentrations that are affected by vehicle emissions are typically characterized by substantial spatial variability with respect to distance from the roadway and temporal variability based on the time of day, day of week, and season. The goal of this work is to identify variables that explain either temporal or spatial variability based on case studies for a freeway site and an urban intersection site. The key hypothesis is that dispersion modeling of near-road pollutant concentrations could be improved by adding estimates or indices for site-specific explanatory variables, particularly related to traffic. Based on case studies for a freeway site and an urban intersection site, the specific aims of this project are to (1) develop and test regression models that explain variability in traffic-related air pollutant (TRAP*) ambient concentration at two near-roadway locations; (2) develop and test refined proxies for land use, traffic, emissions and dispersion; and (3) prioritize inputs according to their ability to explain variability in ambient concentrations to help focus efforts for future data collection and model development.

The key pollutants that are the key focus of this work include nitrogen oxides (NO_x), carbon monoxide (CO), black carbon (BC), fine particulate matter ($PM_{2.5}$; PM ≤ 2.5 µm in aerodynamic diameter), ultrafine particles (UFPs; PM ≤ 0.1 µm in aerodynamic diameter), and ozone (O_3). NO_x, CO, and BC are tracers of vehicle emissions and dispersion. $PM_{2.5}$ is influenced by vehicle table emissions and regional sources. UFPs are sensitive to primary vehicle emissions. Secondary particles can form near roadways and on regional scales, influencing both $PM_{2.5}$ and UFP concentrations. O_3 concentrations are influenced by interaction with NO_x near the roadway. Nitrogen dioxide (NO_2), CO, $PM_{2.5}$, and O_3 are regulated under the National Ambient Air Quality Standards (NAAQS) because of demonstrated health effects. BC and UFPs are of concern for their potential health effects. Therefore, these pollutants are the focus of this work.

Methods The methodological approach includes case studies for which variables are identified and assesses their ability to explain either temporal or spatial variability in pollutant ambient concentrations. The case studies include one freeway location and one urban intersection. The case studies address (1) temporal variability at a fixed monitor 10 meters from a freeway; (2) downwind concentrations perpendicular to the same location; (3) variability in 24-hour average pollutant concentrations at five sites near an urban intersection; and (4) spatiotemporal variability along a walking path near that same intersection.

The study boundary encompasses key factors in the continuum from vehicle emissions to near-road exposure concentrations. These factors include land use, transportation infrastructure and traffic control, vehicle mix, vehicle (traffic) flow, on-road emissions, meteorology, transport and evolution (transformation) of primary emissions, and production of secondary pollutants, and their resulting impact on measured concentrations in the near-road environment. We conducted field measurements of land use, traffic, vehicle emissions, and near-road ambient concentrations in the vicinity of two newly installed fixed-site monitors. One is a monitoring station jointly operated by the U.S. Environmental Protection Agency (U.S. EPA) and the North Carolina Department of Environmental Quality (NC DEQ) on I-40 between Airport Boulevard and I-540 in Wake County, North Carolina. The other is a fixed-site monitor for measuring $PM_{2.5}$ at the North

This Investigators' Report is one part of Health Effects Institute Research Report 207, which also includes a Critique by the Review Committee and an HEI Statement about the research project. Correspondence concerning the Investigators' Report may be addressed to Dr. Andrew Grieshop, Department of Civil, Construction, and Environmental Engineering, Campus Box 7908, North Carolina State University, Raleigh, NC 27695-7908; e-mail: *apgriesh@ncsu.edu*. No potential conflict of interest was reported by the authors. This report was completed before Dr. Frey took a position with the U.S. Environmental Protection Agency.

Although this document was produced with partial funding by the United States Environmental Protection Agency under Assistance Award CR–83467701 to the Health Effects Institute, it has not been subjected to the Agency's peer and administrative review and therefore may not necessarily reflect the views of the Agency, and no official endorsement by it should be inferred. The contents of this document also have not been reviewed by private party institutions, including those that support the Health Effects Institute; therefore, it may not reflect the views or policies of these parties, and no endorsement by them should be inferred.

* A list of abbreviations and other terms appears at the end of this volume.

Carolina Central University (NCCU) campus on E. Lawson Street in Durham, North Carolina. We refer to these two locations as the *freeway site* and the *urban site*, respectively. We developed statistical models for the freeway and urban sites.

Results We quantified land use metrics at each site, such as distances to the nearest bus stop. For the freeway site, we quantified lane-by-lane total vehicle count, heavy vehicle (HV) count, and several vehicle-activity indices that account for distance from each lane to the roadside monitor. For the urban site, we quantified vehicle counts for all 12 turning movements through the intersection. At each site, we measured microscale vehicle tailpipe emissions using a portable emission measurement system.

At the freeway site, we measured the spatial gradient of NO_x, BC, UFPs, and PM, quantified particle size distributions at selected distances from the roadway and assessed partitioning of particles as a function of evolving volatility. We also quantified fleet-average emission factors for several pollutants.

At the urban site, we measured daily average concentrations of nitric oxide (NO), NO_x, O_3, and $PM_{2.5}$ at five sites surrounding the intersection of interest; we also measured high resolution (1-second to 10-second averages) concentrations of O_3, $PM_{2.5}$, and UFPs along a pedestrian transect. At both sites, the Research LINE-source (R-LINE) dispersion model was applied to predict concentration gradients based on the physical dispersion of pollution.

Statistical models were developed for each site for selected pollutants. With variables for local wind direction, heavy-vehicle index, temperature, and day type, the multiple coefficient of determination (R^2) was 0.61 for hourly NO_x concentrations at the freeway site. An interaction effect of the dispersion model and a real-time traffic index contributed only 24% of the response variance for NO_x at the freeway site. Local wind direction, measured near the road, was typically more important than wind direction measured some distance away, and vehicle-activity metrics directly related to actual real-time traffic were important. At the urban site, variability in pollutant concentrations measured for a pedestrian walk-along route was explained primarily by real-time traffic metrics, meteorology, time of day, season, and real-world vehicle tailpipe emissions, depending on the pollutant. The regression models explained most of the variance in measured concentrations for BC, PM, UFPs, NO, and NO_x at the freeway site and for UFPs and O_3 at the urban site pedestrian transect.

Conclusions Among the set of candidate explanatory variables, typically only a few were needed to explain most of the variability in observed ambient concentrations. At the freeway site, the concentration gradients perpendicular to the road were influenced by dilution, season, time of day, and whether the pollutant underwent chemical or physical transformations. The explanatory variables that were useful in explaining temporal variability in measured ambient concentrations, as well as spatial variability at the urban site, were typically localized real-time traffic-volume indices and local wind direction. However, the specific set of useful explanatory variables was site, context (e.g., next to road, quadrants around an intersection, pedestrian transects), and pollutant specific. Among the most novel of the indicators, variability in real-time measured tailpipe exhaust emissions was found to help explain variability in pedestrian transect UFP concentrations. UFP particle counts were very sensitive to real-time traffic indicators at both the freeway and urban sites. Localized site-specific data on traffic and meteorology contributed to explaining variability in ambient concentrations. HV traffic influenced near-road air quality at the freeway site more so than at the urban site. The statistical models typically explained most of the observed variability but were relatively simple. The results here are site-specific and not generalizable, but they are illustrative that near-road air quality can be highly sensitive to localized real-time indicators of traffic and meteorology.

INTRODUCTION

The goal of this research is to identify variables that explain spatiotemporal variability in near-road ambient air pollutant concentrations, based on case studies for a freeway site and an urban intersection site. The study boundary encompasses factors in the continuum from vehicle emissions to near-road ambient concentration, with a focus on factors that influence ambient concentrations of traffic-generated pollutants. These factors include land use, transportation infrastructure and traffic control, vehicle mix, vehicle (traffic) flow, microscale vehicle activity and emissions, meteorology, transport and evolution (transformation) of primary emissions and production of secondary pollutants, and their resulting impact on measured concentrations in the near-road environment. Near-road air pollutant concentrations to which people can be exposed can have both temporal and spatial variability. At the freeway site, we focused mainly on temporal variability of ambient concentrations near the freeway, supplemented with measurements of ambient concentration spatial gradients perpendicular to the freeway. At the urban site, we characterized spatial variability while also accounting for variations related to time of day. We considered seasonal variability at both sites.

We conducted case studies to identify factors that explain either temporal or spatial variability in pollutant concentrations at or near one freeway location and one urban intersection. Specifically, the case studies address factors influencing (1) temporal variability at a fixed monitor 10 meters from a freeway; (2) downwind concentrations perpendicular to the same location (estimated with a dispersion model, not regression); (3) variability in 24-hour average pollutant concentrations at five sites near an urban intersection; and (4) spatiotemporal variability along a walking path near that same intersection.

The use of fixed-site air pollutant concentration monitoring data in epidemiology studies is often convenient as a surrogate for personal exposure (Barcelo et al. 2016; Jandarov et al. 2017; Liu et al. 2017). However, the average personal exposure concentration to a pollutant such as $PM_{2.5}$ is often not the same as the mean ambient concentration. Variability in the ratio of personal exposure concentration to ambient concentration depends on factors such as the amount of time spent in different microenvironments, the infiltration of ambient air pollution into enclosed environments, and spatial variability in ambient concentration not characterized by a fixed-site measurement (Bergen et al. 2016; Burke et al. 2001; Dionisio et al. 2016; Lee and Sarran 2015; Özkaynak et al. 2009; Rich et al. 2018). Near-road ambient air pollution concentrations affected by vehicle emissions are typically characterized by substantial spatial variability with respect to distance from the roadway (Patton et al. 2014, 2017). Fixed-site monitors that produce long-term time series data are typically sparsely located relative to the need to characterize spatial variability in concentration gradients near roadways. Accurate quantification of spatial variability in ambient concentration can reduce bias in estimated concentration–response relationships (Hanigan et al. 2017).

Examples of techniques for quantifying spatial variability in ambient concentrations near roadways include land-use regression, dispersion modeling, chemical transport modeling, population-based exposure modeling, and field measurements (Chang et al. 2012; Di et al. 2016; Dons et al. 2012; Friberg et al. 2016; Patton et al. 2017; Rich et al. 2018). Here, the focus is on evaluating whether a relatively simple linear statistical modeling approach can estimate temporal variability in near-road ambient concentrations at both sites and spatial variability at the urban site. We assess spatial variability at the freeway site using a dispersion model. We identify potential explanatory variables and infer those that are the most helpful in explaining spatial or temporal variability in ambient concentration at the case-study sites.

Human exposure to TRAP emissions has been identified as a factor associated with adverse impacts on human health (e.g., Zhang and Batterman 2013). Key TRAPs and their effects are summarized. Key factors expected to contribute to variability in near-road air pollutant concentration are identified. Based on these considerations, the key hypothesis and specific aims of this project are presented.

TRAFFIC-RELATED AIR POLLUTANTS AND THEIR EFFECTS

In the United States, the on-road vehicle fleet is comprised mainly of light-duty gasoline vehicles (LDGVs) and heavy-duty diesel vehicles (HDDVs) (BTS 2017; Frey 2018). These vehicles emit a mix of pollutants, including regulated criteria pollutants, precursors to criteria pollutants, mobile-source air toxic (MSAT) pollutants, and greenhouse gases (FHWA 2016; Frey 2018; U.S. EPA 2017a,b).

Criteria pollutants are regulated under the NAAQS, and include NO_2, CO, $PM_{2.5}$, PM_{10} (PM less than 10 micrometers in aerodynamic diameter), sulfur dioxide, lead, and O_3. Vehicles emit a mixture of NO and NO_2, referred to as NO_x, of which the direct (*primary*) emissions are typically 95% by volume in the form of NO, except for some HDDVs that have post-combustion emission controls. Once released into the atmosphere, NO typically oxidizes to NO_2. The introduction of selective catalytic reduction for NO_x control of most new HDDVs since 2010 is substantially lowering the exhaust NO_x emissions of HDDVs (Sandhu and Frey 2012), a pattern that will continue for years to come as new vehicles enter the fleet and old vehicles leave the fleet (Frey 2018). On-road vehicles, and particularly HDDVs, emit primary $PM_{2.5}$. Since 2007, the vast majority of new trucks in the United States are equipped with diesel particulate filters that can lower truck PM emissions by well over 90%. On-road vehicles are not substantial contributors to PM_{10}, as particles emitted directly by vehicles tend to be within the $PM_{2.5}$ size fraction. Both gasoline and diesel fuels sold in the United States are subject to limits on sulfur content. These limits are in place to prevent degradation of post-combustion catalytic and filter-based emission control devices, but they also mean that SO_2 emissions from on-road vehicles are very small compared with other sources such as coal-fired power plants. Lead emissions from on-road vehicles are negligible as a result of leaded gasoline being phased out decades ago. O_3 is not directly emitted from vehicles, but some vehicle emissions are precursors to the formation of O_3 in the lower atmosphere. These vehicle emission precursors include NO_x, to a lesser extent CO, and volatile organic compounds (VOC).

The health effects of the criteria pollutants are summarized in the Integrated Science Assessments (ISA) developed by U.S. EPA staff for each pollutant. In the most recent ISAs, short-term exposure to NO_2 was found to be causal with respect to respiratory adverse effects, especially asthma exacerbation, and was likely to be causal for respiratory effects based on long-term exposures (U.S. EPA 2016). For CO, short-term exposures are likely to be causal for cardiovascular morbidity (U.S. EPA 2010). Short-term exposure to $PM_{2.5}$ was found to cause cardiovascular morbidity and premature mortality, and likely to be causal for respiratory morbidity (U.S. EPA 2019). There is generally insufficient evidence from which to assess whether short-term exposure to UFPs causes adverse health effects (e.g., respiratory, cardiovascular, and mortality from short- or long-term exposures), although recent studies indicate that UFPs may be associated with various effects such as reduced respiratory health, systemic inflammation, cardiovascular changes, and mutagenicity (Clifford et al. 2018; Devlin et al. 2014; Karottki et al. 2014; Landkocz et al. 2017; Rizza et al. 2019; Wolf et al. 2015). Short-term exposure to O_3 was determined to be causal for respiratory morbidity and likely to be causal for metabolic effects (U.S. EPA 2020).

The health effects of $PM_{2.5}$ are typically attributed to exposure to $PM_{2.5}$ mass concentrations. However, $PM_{2.5}$ is comprised of many chemical species, such as sulfate, nitrate,

elemental carbon, organic carbon, trace metals, and others. BC closely overlaps, but is not exactly the same as, elemental carbon, because these terms are defined operationally in terms of the detection methods used to measure them (Singh et al. 2014). At the time of the last science review for the NAAQS, there was not sufficient evidence to develop air quality standards based on particular PM species, such as BC. There is some evidence that adverse effects are associated with BC, but insufficient information to determine whether BC is simply an indicator of total $PM_{2.5}$ or other components (Luben et al. 2017). BC is typically a good indicator of primary emissions from diesel vehicles, since diesel PM is enriched in BC compared with particles from other sources, such as gasoline vehicles (Lambe et al. 2009).

VOC emissions include many species of hydrocarbons (HC) and other organic compounds, many of which are also deemed to be hazardous air pollutants. In addition, there is growing interest in the potential role of UFPs, either emitted directly from vehicles or formed in the atmosphere as a result of vehicle precursor emissions, such as VOCs. Vehicle organic gas emissions, from both gasoline and diesel vehicles, can lead to the formation of secondary organic aerosols (SOA) in the near-road environment (Gentner et al. 2017). Furthermore, changes in the vehicle fleet, such as a growing share of direct-injection gasoline vehicles, may increase primary PM emissions (Saliba et al. 2017), particularly for UFPs.

MSATs include hazardous air pollutants emitted from vehicles, such as benzene, formaldehyde, 1,3-butadiene, acetaldehyde, acrolein, and others (U.S. EPA 2007). Many of these pollutants, such as benzene, are emitted via combustion exhaust and from evaporative processes related to fueling, fuel storage, fuel transfer, and fuel transport. The key greenhouse gas emitted from vehicles is carbon dioxide (CO_2) (Frey 2018). CO_2 emissions are proportional to the rate of consumption of carbonaceous fuels such as gasoline and diesel fuel (Frey et al. 2010). CO_2 can also be used as an indicator of dispersion of vehicle exhaust.

Because exhaust emissions of vehicles are often related to vehicle power demand, as indicated by vehicle-specific power (VSP), and because multiple exhaust pollutants are emitted simultaneously, it is possible to focus on a subset of pollutants for the purpose of quantifying the effect of TRAP on near-road air quality. For example, CO_2, NO_x, CO, HC, and PM emission rates are proportional to VSP for both light-duty and heavy-duty vehicles (Frey et al. 2010; Sandhu et al. 2016). CO is a tracer of vehicle emissions near a roadway because it reacts slowly in the atmosphere. Although NO typically oxidizes to NO_2 relatively rapidly, especially in the summer, the mass of total NO_x is approximately constant in the near-roadway environment. Thus, both CO and NO_x are indicators of the dispersion of vehicle emissions. $PM_{2.5}$ is influenced by vehicle emissions but also is influenced by areawide contributions from regional emission sources. Thus, although $PM_{2.5}$ is highly significant with regard to health effects and current air quality regulations, it may be a relatively weak indicator of the contribution of traffic to near-road exposure to particles. In contrast, the formation of SOAs, including UFPs, is sensitive to primary vehicle emissions and can take place rapidly in the near-road environment. Thus, UFPs are of significant interest here. BC is also of interest as an indicator of diesel emissions.

SOURCES OF VARIABILITY IN NEAR-ROAD AIR QUALITY

Near-road ambient air pollutant concentrations are influenced by many factors, including land use, vehicle activity, emissions, and meteorology. Categorical surrogate exposure metrics, such as whether traffic flow is high or low, may not be able to explain as much variability in near-road air pollutant concentrations as continuous quantitative metrics, such as traffic density or predictions from a dispersion model (Batterman et al. 2014). Incorporation of a dispersion model into a land use regression model displaced two other input variables and improved model performance for sites with high ambient NO_x concentrations and close proximity to roadways (Michanowicz et al. 2016). Thus, dispersion modeling is taken here to be a benchmark for model performance.

Land Use

The built environment has been used as a surrogate for on-road emissions in land use regression models (e.g., Franklin et al. 2012; Henderson et al. 2007). The built environment has been identified as a causal factor that determines in part how people behave in space (e.g., Ewing and Cervero 2010). The built environment, such as building density, is a physical barrier or a facilitator to the dispersion of road-related emissions (e.g., Merbitz et al. 2012), often interacting with the natural environment. Thus, land use metrics are quantified.

Urban roadway configuration can affect near-road air quality. For example, there can be differences in near-road concentration for at-grade locations versus locations in which a roadway is embedded in a cut with higher surrounding terrain (Baldauf et al. 2013). Noise-barrier walls can create a downwind recirculation zone that affects downwind near-road concentrations (Ahangar et al. 2017). Vegetation downwind of the roadway can have different effects depending on the porosity of the foliage, with dense canopy improving air quality by 10% and high-porosity canopy deteriorating air quality by 15% near a roadway (Ghasemian et al. 2017). However, deciduous urban forests near roadways might have little impact on gaseous pollutant dispersion but some impact on PM dispersion (Yli-Pelkonen et al. 2017).

The literature suggests differences in UFP concentrations by level of overall urbanity, with more urban locations having higher concentrations of UFPs relative to less urban locations (Grana et al. 2017; Hagler et al. 2010; Kumar et al. 2014; Lanzinger et al. 2016; Tobias et al. 2018). At the same time, even within an urban area, there is heterogeneity in UFP concentrations (de Nazelle et al. 2017). Therefore, it is

particularly helpful to attempt to disentangle the explanatory factors associated with observed concentrations.

Recent efforts have begun to identify those specific factors. For example, proximity to roads and particular road characteristics such as width (Choi et al. 2016, 2018; Weichenthal et al. 2016), proximity to bus stops (Choi et al. 2018; Weichenthal et al. 2016), and proximity to specific land uses such as industrial uses and airports (Weichenthal et al. 2016) have been associated with increased UFP concentrations. By contrast, the presence of open spaces (Weichenthal et al. 2016; Xu et al. 2016) and particular building designs that promote higher ventilation (Choi et al. 2016) have been associated with lower UFP concentrations.

Vehicle Activity and Emissions

Vehicle emissions in the vicinity of an intersection are subject to second-by-second variability in emission rates, particularly those related to acceleration (Frey et al. 2003; Ritner et al. 2013; Unal et al. 2003, 2004). Traffic activity varies with the time of day, and there is typically variability in traffic volume, vehicle mix, and speed during a day (Batterman et al. 2015a). Variability in traffic volume based on 15-minute averaging times was shown to be correlated with near-road measurements of NO and NO_2 concentrations, including variability by time of day and by season; however, $PM_{2.5}$ mass measured near the roadway appeared to be more influenced by regional sources (Kendrick et al. 2015). Although traffic activity was an influential factor in near-road CO, NO_2, NO_x, and BC concentrations measured at a freeway site in Las Vegas, local meteorology was also a critical factor (Kimbrough et al. 2013). For example, concentration gradients at the Las Vegas freeway site were sensitive to atmospheric stability and wind direction (Richmond-Bryant et al. 2017). Vehicle travel demand and vehicle fleet composition affect near-road air quality (Alam et al. 2014).

Vehicle emissions source strength for a given vehicle varies primarily with respect to vehicle speed, acceleration, and road grade, and to a lesser extent with respect to ambient conditions. Speed and acceleration are influenced by traffic conditions, road geometry (e.g., ramps) and traffic control (e.g., intersections). From previous field studies, we have shown that vehicle emissions hotspots are associated with real-world situations such as signalized intersections at which accelerations occur repeatedly (Khan et al. 2020; Unal et al. 2003, 2004). Vehicle emissions are sensitive to steady-state versus transient speed, when comparing driving cycles with similar average speeds (Choi and Frey 2009). Here, we used portable emissions measurement systems (PEMs) (Frey et al. 2003, 2008) to collect data on *probe* vehicles operated in proximity to the air quality monitoring stations at the study sites. We quantified the spatial variability in emissions during travel along paths in proximity to the near-road sites, and we quantified temporal variability in vehicle emissions associated with different times of day. In combination with traffic count data, we quantified both spatial and temporal variability in emissions that contribute to near-road ambient pollutant concentration.

Transport and Transformation of Pollution Near a Road

Near-road concentrations of vehicular air pollution are influenced by complex dispersion and physicochemical transformations that differentially affect relatively inert species (e.g., CO, CO_2, NO_x) and more dynamic species (e.g., particle size distributions and chemical components) (Karner et al. 2010). These processes are influenced by many environmental parameters. The following have all been shown to influence the near-road concentrations and properties of particles: temperature and relative humidity (Charron and Harrison 2003; Jamriska et al. 2008), mixing height (and thus time of day), wind speed and direction (Charron and Harrison 2003; Kozawa et al. 2012; Zhu et al. 2002a,b), fleet composition, traffic volume and speed, roadway elevation and location of nearby buildings (Baldauf et al. 2013; Heist et al. 2009; Kastner-Klein and Plate 1999), and noise or vegetation barriers (Baldauf et al. 2008b; Beckett et al. 1998, 2000; Bowker et al. 2007; Buccolieri et al. 2009; Finn et al. 2010; Hagler et al. 2012; Lin and Khlystov 2012; Ning et al. 2010). Many of these papers focus on UFPs. Various studies have found sharper gradients in near-roadway air pollutants during early morning (before sunrise) hours (Durant et al. 2010; Gordon et al. 2012; Massoli et al. 2012; Zhu et al. 2002a), presumably due to a combination of low mixing height and large traffic volume. A number of studies have found the organic components of PM to be more dynamic (spatially and temporally variable) than other components (Massoli et al. 2012; Sun et al. 2012), in some cases showing an unexpected mild increase downwind of the roadway (Clements et al. 2009). Studies in Los Angeles of roadways with varying fleet composition have shown that semivolatile organic compound (SVOC) materials (indicated by evaporation of PM mass at elevated temperature) comprises a substantial portion of vehicle-attributed ambient aerosol (Biswas et al. 2007; Kuhn et al. 2005). The partitioning of semivolatile material may affect the toxicity of PM from vehicles (Biswas et al. 2007; Verma et al. 2011). Finding ways to model these processes using simple and computationally tractable approaches effectively and simply (Aggarwal et al. 2011) will provide a valuable tool for health assessments.

Dispersion

The effect of traffic emissions on near-road air quality depends on distance from the roadway. For example, filter-based $PM_{2.5}$ measurements 150 meters from a roadway in Maryland were found to have only a 12% to 17% contribution from roadway traffic (Ginzburg et al. 2015). Downwind of a highway, measured CO and UFP concentrations decreased with distance from the roadway, and in some cases were as low as urban background concentrations at 150 meters from the road (Hagler et al. 2010). A study of UFPs suggested that the contribution of traffic to downwind UFP concentrations may be discernible as far as 280 meters downwind of the road

(Jeong et al. 2015). Pollutant concentrations for NO, NO_x, CO, and $PM_{2.5}$ downwind of sites near I-93 in Massachusetts typically reached upwind background levels within 200 meters of the road, in the absence of other local sources, but the concentration spatial gradients differed among three neighborhoods (Patton et al. 2014). Thus, in terms of assessing the spatial gradient in TRAP concentrations, there is likely to be little utility in conducting measurements beyond several hundred meters from the roadway.

Although there are spatial gradients near roadways for many traffic-related air pollutants, these near-road concentrations have implications for human exposure. Approximately 10 million Americans live within 100 meters of a road with an annual average daily vehicle traffic count greater than 25,000; 60 million Americans live within 500 meters of such roads (Rowangould 2013). Nationally, minority and low-income households tend to be disproportionately located near roadways. Road proximity was associated with non-Alzheimer dementia in a recent population-based cohort study of neurological disease (Yuchi et al. 2020). In addition to residential microenvironments, other exposure microenvironments, such as schools, are located near roadways. Kweon and colleagues (2018) found that school proximity to highways was associated with adverse respiratory, neurological, and academic outcomes in students.

Steady-state Gaussian dispersion models are typically used to simulate air pollutant concentration gradients near roads. Key examples of such models are AERMOD, CALINE versions 3 and 4, ADMS, and the R-LINE) (Heist et al. 2013). Among these, R-LINE, AERMOD, and ADMS can predict meandering of vehicle-exhaust plumes upwind of a road during low wind speed conditions. R-LINE overall performance statistics comparable to the regulatory AERMOD dispersion model and to ADMS, and less scatter in concentration estimates than did the CALINE version 3 or 4 dispersion models. Patterson and Harley (2019) found that R-LINE responded "appropriately" to variability in seasonal meteorology and daily variations in emissions. Based on comparisons of model predictions to NO_x and BC concentrations measured for a year at two near-road monitoring sites, more than 90% of model predictions were within a factor of two, which was inferred to be good model performance. Thus, R-LINE is selected here as representative of the current state-of-the-art in near-road dispersion modeling.

R-LINE, developed by Snyder and colleagues (2013), has been used to model the dispersion of multiple TRAPs, including NO_x and $PM_{2.5}$, at a census-block level at locations in North Carolina and Oregon (Chang et al. 2015). HDDVs were found to contribute more than half of these pollutant concentrations near interstate highways. R-LINE has been used in a study of hourly $PM_{2.5}$ and NO_x concentrations for Detroit (Batterman et al. 2015b; Isakov et al. 2014). The use of dispersion models such as R-LINE require quantification of spatially and temporally resolved vehicle emissions and meteorology (Snyder et al. 2014). R-LINE has been found to be useful for estimating spatially and temporally resolved near-road ambient concentrations (Milando and Batterman 2018).

Studies that apply geographic and traffic-volume proxies in proximity-based or land use regression models to estimate ambient pollutant concentrations at high spatial resolution tend to provide better explanations of variations in exposure concentrations than do studies employing central-monitor air pollution measurements (Marshall et al. 2008). Improvements in estimation of near-road air quality have been reported by accounting for dispersion processes (Batterman et al. 2010; Franklin et al. 2012; Gordon et al. 2012) in addition to static geographic factors (e.g., roadway proximity or land use).

SPECIFIC AIMS

Based on case studies for a freeway site and an urban intersection site, the specific aims of this project are to:

1. explain variability in traffic-related air pollutant ambient concentrations at two near-roadway locations;
2. develop and test refined proxies for land use, traffic, emissions and dispersion; and
3. prioritize inputs according to their ability to explain variability in ambient concentrations, to help focus efforts for future data collection and model development.

Our key hypothesis is that modeling of near-road pollutant concentrations at the case-study sites, based on dispersion predicted by a representative dispersion model, could be improved by refining estimates or indices for explanatory variables, particularly those related to traffic.

Our approach is to test the hypothesis by collecting data regarding land use, traffic activity, vehicle emissions, and near-road ambient pollutant concentration for two case-study locations. These data were collected at a freeway site and an urban site in both winter and summer. At the freeway site, we focused mainly on temporal variability in near-road concentrations at a fixed location near a freeway, supplemented with spatial variability for a transect perpendicular to the freeway. At the urban site, we focused mainly on spatial variability at fixed locations surrounding an intersection, and for pedestrian transects in the vicinity of the intersection, with consideration of how the spatial variability may be influenced by time of day for the transects and by season for both the fixed locations and transects.

These data or indicators derived from these data were used to develop statistical models for near-road ambient concentrations at the case-study sites for selected pollutants. The relative contributions of characterizations of land use, traffic, emissions, and other determinants (e.g., meteorology) at the case-study sites were assessed in terms of their ability to explain variability in measured ambient concentrations.

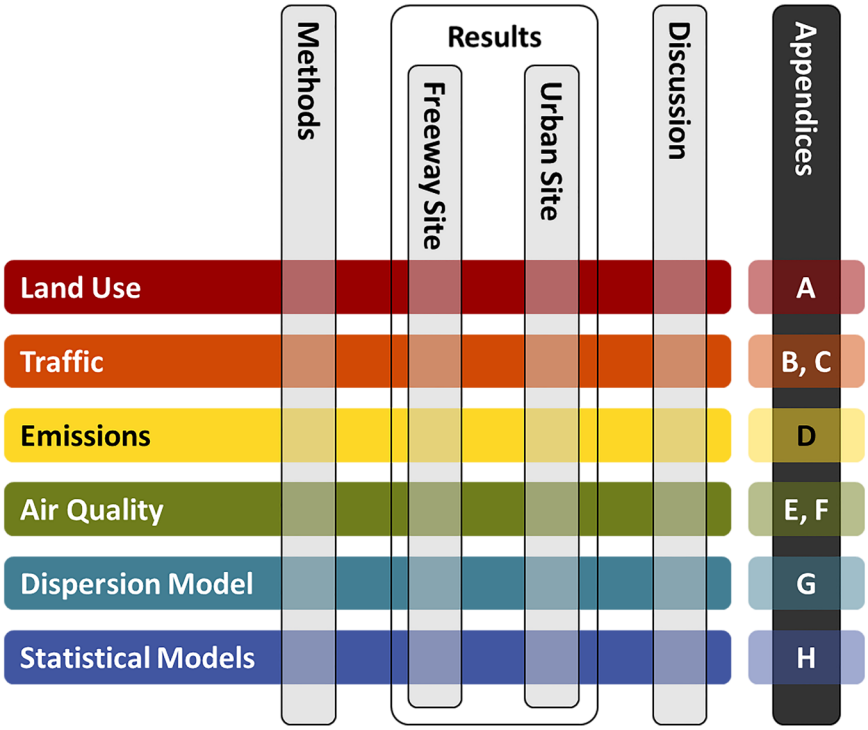

Figure 1. Organization of this report.

METHODS AND STUDY DESIGN

OVERVIEW

Organization of This Report

The organization of this report is illustrated conceptually in Figure 1. The major technical themes of this report are land use, traffic activity, vehicle emissions, measurement of air quality, dispersion modeling, and statistical modeling. These themes cut across all of the major sections of the report, including methods and study design, results, and discussion and conclusions. Furthermore, additional information pertaining to topics within each of these themes is available in Additional Materials Available on the HEI Website, Appendices A–H. This work features two field-study sites, including a freeway site and an urban site. Thus, the Results section is subdivided based on these two sites.

The appendices in Additional Materials include specific details that support the main points of the report. For land use, Appendix A includes a description of data sources, methods for use and validation of light detection and ranging (LIDAR) data to characterize the built environment in the vicinity of each site, and descriptive statistics for built-environment attributes.

For traffic analysis methods and results, high-level explanations and exhibits are given in the main report to define the method and demonstrate the results. Ancillary data used in method development along with their results, including site description, sensor data, and manually collected data are given in Appendices B and C for the freeway and urban sites, respectively. In addition, intermediate model details and results that contribute the final models shown in the main report are described in the appendices.

Appendix D includes details on the methods and results for field measurements of microscale vehicle tailpipe exhaust emissions, including details of study design and detailed results that quantify spatial variability in emissions at the two sites for selected times of day. Appendix E includes details on site selection and characteristics of the locations at which ambient concentration measurements were done at the freeway site, meteorological conditions at the site, diurnal patterns in traffic, measurement conditions for transect measurements of the spatial gradient in ambient pollutant concentration perpendicular to the freeway, determination of fleet average emission factors, and quality assurance (QA).

Appendix F includes supporting details regarding ambient concentration measurements made at the urban site, including QA procedures for sampling methods used at fixed sites and pedestrian transects, daily average $PM_{2.5}$ concentrations measured at fixed locations surrounding the intersection, meteorological conditions at the site, and pedestrian transect measurements. Appendix G provides details on dispersion model set-up, development of model input data, and results

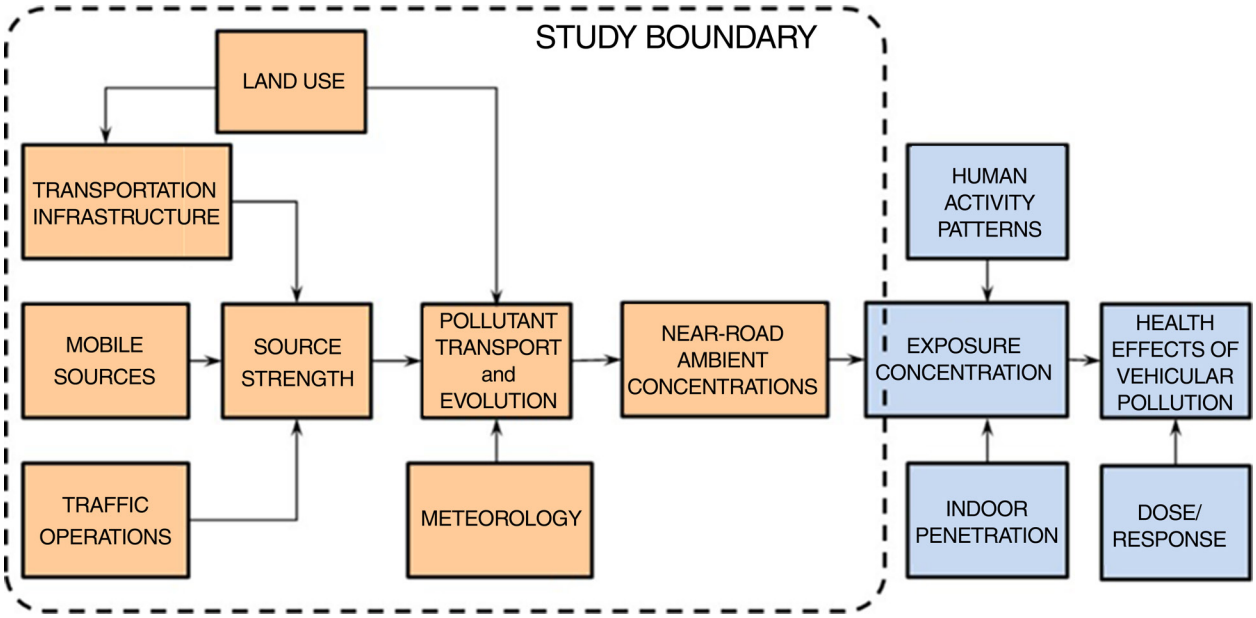

Figure 2. Conceptual overview of study scope. Boxes entirely within the study boundary were the focus of this research. Boxes outside the boundary informed choices regarding spatial and temporal resolution of upstream boxes but were not a main focus of this research.

for both the freeway and urban sites. Appendix H includes statistical models for pollutants at both sites, in addition to the models included in the main report.

Study Scope

The overall approach of this research is illustrated in Figure 2. The study boundary focuses on factors that influence ambient concentrations of traffic-generated pollutants at two specific sites. These factors include land use, transportation infrastructure and traffic control, vehicle mix, vehicle (traffic) flow, on-road emissions, meteorology, transport and evolution (transformation) of primary emissions and production of secondary pollutants, and their resulting impact on measured concentrations in the near-road environment (within 300 m of a highway or major artery).

There are some exposure factors that are not part of this research, but that are relevant to the potential use results of this work to improve exposure estimates for near-road microenvironments. These include human activity patterns, penetration of ambient pollution to indoor microenvironments within the near-roadway buffer, and consequent estimation of human contact with these concentrations, which constitutes exposure.

We conducted field measurements of traffic, vehicle emissions, and near-road ambient concentrations in the vicinity of fixed-site monitors. The freeway site fixed-site monitor is a station jointly operated by the U.S. EPA and the NC DEQ on I-40 between Airport Boulevard and I-540 in Wake County, North Carolina (i.e., U.S. EPA/NC DEQ). The urban site has a fixed-site monitor for measuring $PM_{2.5}$ at the NCCU campus on E. Lawson Street in Durham, North Carolina.

The freeway site was chosen for the following reasons: (a) the existing U.S. EPA/NC DEQ monitor already had electrical power; (b) there was sufficient room at the site to add a trailer in which additional instruments could be installed; (c) the site was very close to the edge of a highly traveled interstate; (d) a low traffic road perpendicular to I-40 could be used to measure spatial air quality gradients using an instrumented van; (e) a site was available on the other side of I-40 at which background monitors could be installed; and (f) real-time traffic data could be obtained using an existing traffic detector.

The urban site was chosen because: (a) it represented an urban intersection with pedestrian and vehicular traffic; (b) three quadrants were surrounded by residential housing; (c) a continuous PM monitor was located nearby that could be used for intercomparison with other instruments and to benchmark temporal trends; and (d) real-time traffic data could be obtained for the major through street of the intersection using the existing loop detectors.

The study design for field measurements and development of statistical models focuses on four main case studies: (1) temporal variability at a fixed monitor 10 meters from a freeway; (2) downwind concentrations perpendicular to the same location (estimated with a dispersion model, not regression); (3) variability in 24-hour average pollutant concentrations at five sites near an urban intersection; and (4) spatiotemporal variability along a walking path near that same intersection.

Our methods and study design include measurement and quantification of land use, traffic, vehicle emissions, and ambient concentrations at the freeway and urban sites. Different methods were used for the study design between the two sites because of differences in site characteristics. For example, temporal variability in traffic data were quantified at the freeway site using data from an existing Remote Traffic Microwave Sensor (RTMS) radar detector that was used to quantify vehicle counts in all lanes in both directions on I-40. In contrast, existing traffic detectors at the urban site measured temporal variability in vehicle counts on only one of the two intersecting roads. Therefore, supplemental video was collected at the urban site from which temporal variability in traffic flow on the cross street, as well as all turning movements at the intersection, could be quantified.

The freeway site air quality measurements included characterization of temporal variability in PM concentration at a fixed site and spatial variability in concentration for a transect perpendicular to I-40, whereas the urban site included characterization of spatial variability in ambient concentrations in the neighborhoods and campus in the vicinity of the intersection. The urban site air quality measurements included fixed locations surrounding the intersection and a pedestrian transect.

Spatial variability in on-road vehicle emissions was quantified at both sites based on measurements of real-world tailpipe emissions of selected vehicles using a portable instrument. Dispersion model predictions were made to help explain temporal and spatial variability in air quality ambient concentrations at both sites. We developed statistical models of air quality ambient concentrations for multiple pollutants for the freeway and urban sites. These models focused on temporal variability at the freeway site and on spatiotemporal variability at the urban site.

Experts of different backgrounds may use similar terms to describe different things. Here, we intentionally use terms related to *estimation* and *explanation* to describe the output of the statistical models developed in this work. We conceptualize these models as quantifying the key sources of variability in our observations, based on site-specific data. We infer whether a variable is *useful* or *important* based on whether it contributes to explaining variability in measured ambient concentrations. The key insight sought is regarding which inputs explain or contribute more variability in ambient concentrations than others. These insights are developed based on regression modeling and analysis of variance (ANOVA). For the regression models, a contribution to R^2 is estimated. Based on ANOVA, the relative ranking of key sources of variance is inferred.

Evaluations of internal validity include assuring that our results are not compromised by methodological errors, and that the data and models for the sites represent the truth of variations at the sites. To assure the internal validity of our measurements, we conducted measurements according to accepted QA and quality control (QC) approaches, and we subjected our study design and data interpretation to peer review. We assessed the internal validity of the statistical models using cross validation and, for temporal variability at the freeway site for selected pollutants, comparisons of model estimates to independently measured pollutant concentrations at the same site.

We did not quantitatively assess the external validity of the models, such as by comparing model estimates to measured values for other sites. For this reason, we conceptualize the models as being focused on explaining variability in measured concentrations at the sites for which the models were calibrated. However, with regard to both internal and external validity, we qualitatively considered whether the direction (mathematical sign) and magnitude of model coefficients for explanatory variables was consistent with prior findings. This latter type of evaluation is useful for confidence building but does not quantify model errors.

LAND USE

Land use was characterized for the freeway and urban study sites using a variety of data sources. The characterization of land use is potentially relevant to quantifying spatial variability in ambient concentrations. In-situ measurements were conducted to validate elevation data. Data from multiple sources were processed and joined to create a high-resolution grid that describes the built environment proximate to each study site. For both study locations, data were examined regarding bus stops, airport location, roads, tree canopy, housing units, land uses (commercial, community service, industrial, public service, recreation, residential, residential–multifamily, street, vacant, and wild), and type of employment if present (office, retail, industrial, and both service-low and service-high [with either low or high trip generation or attraction]). These data sources are listed in Additional Materials Table A.1. The data were transformed into explanatory variables, as detailed in Additional Materials Table A.2, for use in spatial analysis for the urban site.

We collected preprocessed LIDAR elevation data for the study area for the year 2007. A Digital Surface Model (DSM) grid with a 1-meter cell size was interpolated from the points by using the linear triangulated irregular network (TIN) interpolation method. We validated the LIDAR data as detailed in Additional Materials Appendix A. The LIDAR showed fair to moderate agreement with site visits and with oblique photography.

Once the built environment data were collected, and for both the freeway and urban sites, we created grid cells of 5 m × 5 m within 2,000 feet (609 meters) of each study site and calculated a number of different variables. Additional Materials Table A.2 shows how the input data were connected to the resulting explanatory variables. In brief, the variables developed included: (a) distances of each cell to the data collection site, nearest bus stop, Raleigh–Durham International

Airport (RDU), nearest street, near street arterial or above, to I-40/NC 55 centerline; (b) proportion of each cell's area covered by a building, tree canopy, and not covered; (c) the number of housing units, employees (for Durham only) attributed to each cell (through interpolation), and buses per hour servicing the nearest bus stop; (d) predominant type of land use and employment, if applicable; and (e) average and standard deviation of height of any structure (canopy of building) in cell.

TRANSPORTATION

Temporal variability in traffic activity was quantified at the highway and urban sites, along with spatial and temporal variability in microscale (second-by-second) measured vehicle-exhaust emission rates at both locations. Traffic activity data were obtained from existing side-fire radar detectors at the freeway site and from existing magnetic loop detectors at the urban site. Additionally, video recording was performed to verify and supplement the detector data that was available only on the main road. Additional traffic-related variables not measured directly with sensors were statistically estimated. Pollutant concentrations at the mesoscale spatial resolution (i.e., road link average) are expected to be sensitive to traffic activity. These include the number of vehicles passing a point per unit time, vehicle class (car versus trucks), and link average speed as well as vehicle proximity to the measurement points. Traffic count and the mix of vehicle type can vary by location, time of day, day of week, or season. Speeds and accelerations are influenced by traffic conditions, road geometry, and traffic control configuration (e.g., intersections). We also collected data for microscale vehicle trajectories and exhaust emission rates from which to quantify spatial and temporal variability in emission source strength at the two study sites.

Mesoscale Traffic Activity — Freeway Site

To characterize the temporal trends of multiple traffic-related air pollutants, month-long *summer* and *winter* measurement campaigns were conducted 1 June–2 July 2015 and 18 January–20 February 2016 at a field site near Interstate 40 (I-40), in Raleigh, North Carolina. Traffic volume by lane, composition, and speed were collected at the I-40 near-road monitoring site using an existing RTMS detector located within 50 meters of the U.S. EPA/NC DEQ fixed-site monitor. The sensor produces traffic measurements on I-40, which has four through lanes in each direction.

The RTMS station generates reports at multiple time aggregations (1 min, 5 min, 15 min, 1 hour), depending on user request (See Additional Materials Tables B.1–B.3 and Additional Materials Figure B.1 for more details on RTMS data). The system creates vehicle classifications based on the length of detected vehicles and converts the information to four classes representing passenger cars (class 1), commercial vehicles (class 2), single-unit trailers (class 3), and multiple trailer trucks (class 4). HVs include class 3 and class 4 vehicles. At 1-minute time resolution, vehicle classification and average speeds were available by direction and lane. At longer averaging times, lane-by-lane data were not available. All mesoscale traffic-related variables observed at a 15-minute aggregation interval were summarized as an observation set. The traffic-activity data for the freeway site includes 2,880 summer observation sets and another 2,880 winter observation sets. QA and QC of the RTMS data were done using video data collected at the same location (details are given in the Results section).

Two sources of bias were identified from the RTMS detector reports: (a) an undercount of total volume in the traffic lanes nearest to the sensor, even though the total directional count was correct, and (b) a systematic undercount of HV for the direction closer to the sensor. Coifman (2006) stated that the performance of RTMS detectors may differ according to their lane position because the nearest lanes have a smaller detection zone and the furthest lanes have an occlusion issue. Therefore, validation was performed with video recording to verify and correct the RTMS data. A video camera was installed at the same location with RTMS for four hours. Additional Materials Figure B.2 shows the framework used in correcting inconsistencies in RTMS data.

In addition to the need to predict lane counts on the basis of 15-minute aggregated counts for all lanes, as well as to address the undercount of total volume in the lanes nearest the sensor, a multinomial log-linear model was developed to predict the lane volume distribution that could be applied to both directions. The model was validated with observations from another nearby, far-side sensor. Similarly, to predict lane distribution of HVs and to address the systematic undercount of HVs for the direction closer to the sensor, which is the westbound direction, a multinomial log-linear model was developed to estimate the distribution of total HV counts by lane. Both models use observed 15-minute volume observations, time of day, and directional average speed as explanatory variables and the fraction of traffic in each lane as the dependent variable. See Additional Materials Tables B.4–B.6 and Additional Materials Figure B.3 for more details on the models and the model predictions. The contribution of pollutants from traffic-related sources was assumed to be directly related to the amount of traffic passing through a road section, the extent of HV presence in the stream, and the average speed of the facility. In addition, traffic physically closer to the monitoring site was expected to have a stronger impact on the observed diurnal pattern of pollutant concentrations than traffic farther away from the monitoring station. Thus, four basic indicators of vehicle volume, composition, speed, and distance from the monitoring site were used to develop three diurnal traffic indices. Proximity to the monitoring site was incorporated as a simple weighting factor, which is the inverse of the orthogonal distance from the centerline of each lane to the monitoring site position. Three indices are estimated using Equation 1: (1) volume index, total volume in vehicles per hour (vph); (2) HV index, total HV volume in vph; and (3) density index, in vehicles per mile (vpm):

$$I_t^r = \sum_i \frac{P_{it}^r}{D_i} / \sum_i \frac{1}{D_i} \quad (1)$$

where,

r type of index e.g. volume, HV, or density

t estimation time period (15-minute interval; 96 such periods per day)

i lane number

I_t^r index value at time t of type r

P_{it}^r traffic variable associated with lane i at time t of type r

D_r distance from the centerline of lane i to the monitoring station.

Sources of input data for the traffic indices include RTMS sensors, video, geometric design maps, and model estimates. Table 1 summarizes the inputs and corresponding sources.

Mesoscale Traffic Activity — Urban Site

Traffic activity data at the urban site were measured near the NCCU campus in Durham, North Carolina. The site represents mostly stop-and-go movements in the vicinity of a signalized intersection. Moreover, the presence of a university campus in close proximity created microenvironments in which a greater number of pedestrians were exposed to traffic compared with the freeway site. Data collection was focused on the intersection of Alston Avenue (NC 55) and E. Lawson Street, which is at the northeastern corner of the NCCU campus. Alston Avenue has two through lanes and one lane left-turn pocket near the intersection in both directions. Lawson Street has one shared lane and left-turn pockets in both directions. Traffic data were archived from magnetic-loop detectors used for signal operation at the intersection. In addition, video recordings were performed during August 2015, January 2016, and May 2016. See Additional Materials Figures C.1–C.3 for more details on the location of the urban site.

Intersection traffic control is maintained by the city of Durham. Inductive-loop detectors permanently exist on all approaches to the intersection. However, all of Lawson Street and the left-turn lane detectors on Alston Avenue are presence detectors, which are intended to actuate signals. To help validate the total counts from these detectors, and to record HV presence and turning movements, video cameras were installed at the northwest and southeast corners of the intersection.

Validation of loop detector vehicle counts was performed with video recording. Two-day directional counts were extracted manually from video. The detector counts were similar to those inferred from the video. All missing directional counts were estimated from manual counts from video. The estimated flow fractions were time-of-day dependent and covered the morning peak hours (07:00–09:00), midday hours (09:00–16:00), evening peak hours (16:00–18:00) and nonpeak hours (0:00–07:00 and 18:00–24:00). Thus all twelve movement counts were estimated for the days where manual counts were not available.

Spatial and temporal variation of pollutant concentrations was investigated two ways: (1) pedestrian transects with portable monitors on sidewalks on the south side of Lawson Street and west side of Alston Avenue; and (2) fixed receptor pollutant concentration monitoring located in quadrants surrounding the intersection. Consequently, traffic data collection was focused around both approaches.

Video-based vehicle counts on the south and west approaches of the intersection were archived during the periods when pedestrians equipped with personal environmental monitors (PEM) were traversing those segments. This constituted the traffic activity index for comparison with pedestrian transects. Details are given in Additional Materials Table C.1.

Table 1. Sources of Input Data Used to Generate Three Traffic Indices for the Freeway Site

	Source of Input Data by Type of Traffic Index		
Traffic Index Input	HV Index	Volume Index	Density Index
Number of lanes per direction	M	M	
Distance from each lane CL to monitor	M	M	M
Distance from CL of directional road to monitor			M
Total vehicle count per period per lane		S, V	S, V
Total HV count only (or count estimate) per lane	S, V, E		
Average vehicle speed per direction			S, V

CL = centerline; E = estimate from model; M = map; S = sensor; V = video.

For the comparison to the fixed monitors in each quadrant, which measured daily average pollutant concentrations, traffic activities were estimated based on daily averages. Each of the movements through the intersection has different acceleration and deceleration patterns (e.g., for turning movements, decelerate upon entry, accelerate upon exit) and thus may have different impacts on concentrations. Four indices were developed to help assess which traffic-related factors explain variability in near-road ambient concentrations: (1) traffic-volume index; (2) distance-adjusted traffic-volume index; (3) VSP-adjusted traffic-volume index; and (4) distance- and VSP-adjusted traffic-volume index.

Figure 3 depicts the twelve movements used to develop the traffic indices for the fixed-site receptors, based on assessing the proximity to an example quadrant receptor (Q4). The measured concentration at Q4 could be influenced by twelve directional movements on the closest roads, which include the north-leg and west-leg of the intersection. To calculate an index that accounts for these movements, class 1 and class 2 vehicles were assumed to be equivalent to passenger cars and class 3 and class 4 vehicles are assumed to be HV. HV were weighted as being equivalent to 6.8 passenger car units using estimated national average NO_x emission rates per vehicle-by-vehicle type (U.S. DOT 2012).

Indices were estimated using Equation (2):

$$I_d^r = \Sigma_i \Sigma_j \frac{w_{ij}^r \times V_{ijd}^r}{d_i^r} \qquad (2)$$

where,

- ***r*** type of index (e.g., traffic-volume, distance-adjusted traffic-volume, VSP-adjusted traffic-volume, or distance- and VSP-adjusted traffic-volume)
- ***d*** estimation day
- ***i*** approach label for NB, SB, EB and WB approaches ***(i = 1 to 4)***
- ***j*** turning movement type: through, left-turn or right-turn, ***(j = 1 to 3)***
- I_d^r index for day ***d*** for index type ***r***
- V_{ijd} traffic volume on approach i for turning movement j on day d
- d_i orthogonal distance, centerline of movement on approach ***i*** to the monitoring station
- w_{ij}^r VSP weighting factor applicable to approach ***i*** and movement ***j***.

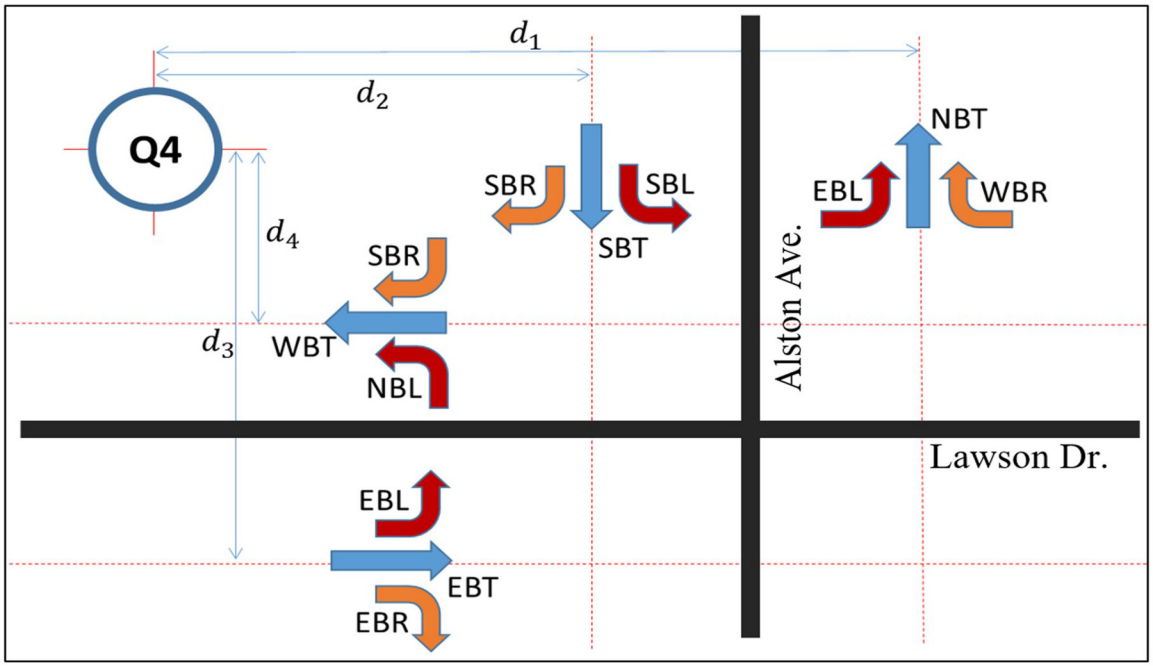

Figure 3. Schematic of the contributing traffic movements and their separations (d_1 to d_4) for generating traffic indices for receptor Q4. Movements are labeled based on direction (EB = eastbound, NB = northbound, SB = southbound, WB = westbound); and whether turning (L = left, R = right) or through (T) (e.g., SBL means southbound left turn). Separations are shortest distances from each through lane to the receptor. Dotted red lines indicate the position of through lanes.

The unweighted traffic-volume index is the result of aggregating twelve traffic volumes based on the movements indicated in Figure 3 and shown in Additional Materials Table C.2. The weighting factors (w_{ij}) for power demand, which were estimated based on VSP, and distance (d_i) was set to 1.0 in the traffic-volume index. The distance-adjusted traffic-volume index is the sum of the ratio of each traffic volume and its distance from the receptor. The weighting factor (w_{ij}) was also set to one when only the influence of distance is considered. The VSP-adjusted traffic-volume index is the sum of the product of traffic volume multiplied by a VSP factor (w_{ij}). The distance value (d_i) was set to one when the index accounts only for the influence of VSP. The typical spatial distribution of VSP along each movement was estimated from a series of sample vehicle runs in the vicinity of the intersection of Alston and Lawson streets at a 0.05-mile resolution (see the next section). The highest VSP value across all runs per movement and approach was applied as the weight. Finally, a distance- and VSP-adjusted traffic volume index was estimated by summing terms across all relevant turning movements (j) and intersection approaches (i) in a given day (d). This process was repeated for the sensors on all four quadrants, since the movements, distances, and VSP estimates vary across quadrants. Table 2 summarizes the collected mesoscale traffic data at the urban site.

Microscale Vehicle Emissions

Vehicle operation is subject to spatial variability in proximity to the I-40 air quality monitoring site and at the Durham site. For example, the U.S. EPA air quality monitor is located just downstream of a ramp from Airport Boulevard that merges to I-40 west. Especially during rush hour, it may be possible that vehicles merging from the ramp onto I-40 west may encounter some delay and concurrent variability in speed and acceleration that could lead to elevated emissions near the monitor. At the Durham site, which includes several intersections, the typical stop-and-go driving pattern could lead to emission hotspots in the vicinity of intersections that might help explain spatial variability in measured air quality.

Field measurements were conducted to measure the real-world speed, acceleration, road grade, power demand, and exhaust emission rates for selected LDGVs. Details of the measurement methods, QA, and results are given in Additional Materials Appendix D. Second-by-second vehicle activity and tailpipe exhaust NO, CO, and HC concentrations were measured using portable emissions measurement systems (Frey et al. 2003). NO_x emissions for LDGVs are typically composed of 95% by volume of NO. Thus, NO is an excellent surrogate for total NO_x. Vehicle-activity and engine data were recorded using an onboard diagnostic scan tool. Second-by-second data on latitude, longitude, and elevations were recorded using global positioning system (GPS) receivers with barometric altimeters.

Real-world data were collected for four LDGVs for five days during off-peak, morning peak, (~07:00–09:00), and evening peak (~16:00–18:00) for each site. In earlier work, we have demonstrated quantitatively that the second-by-second speed, acceleration, and power demand achievable by any typical LDGV is comparable to that of another LDGV, based on analysis of measurements we have done previously on 100 LDGVs (Liu and Frey 2015a). Thus, it is not necessary to have a large sample of LDGVs for the purpose of obtaining typical vehicle trajectories.

For I-40, the key focus of the study design was to quantify vehicle activity on the freeway segment between Airport Boulevard and I-540 that includes the U.S. EPA/NC DEQ monitoring site. We created multiple circulating routes that included vehicle movements at the ramps closest to the U.S. EPA/NC DEQ site, movements on nearby roads including Aviation Parkway and Slater Road, and through movements in each lane. Examples of three of these routes are shown in Figure 4.

Table 2. Sources of Input Data Used to Generate Four Traffic Indices for the Urban Site

	Source of Input Data by Type of Traffic Index[a]			
Traffic Index Input[b]	Traffic Volume	Distance-Adjusted Traffic Volume	VSP-Adjusted Traffic Volume	Distance- and VSP-Adjusted Traffic Volume
Contributing traffic movement volumes (see Figure 3)	V, S	V, S	V, S	V, S
Distance from each impacting movement CL to monitor		M		M
Highest measured VSP to monitor			GPS	GPS

[a] CL = centerline; GPS = 1 Hz GPS for estimating VSP; M = map; S = sensor; V = video; VSP = vehicle specific power.

[b] If no video is available, deployed sensors may be used to estimate overall segment volumes without turns.

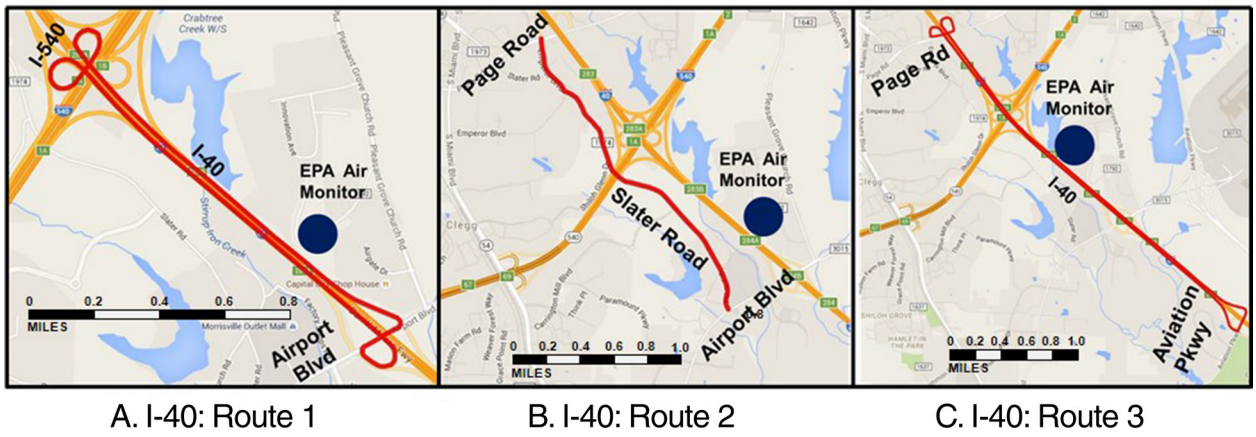

Figure 4. Designated routes for real-world vehicle tailpipe emission measurements at I-40 site: A: Route 1 — includes ramps nearest to the monitor; **B**: Route 2 — focuses on an arterial road upwind of I-40; and **C**: Route 3 — focuses on through movements on I-40 in multiple lanes in both directions.

The vehicle trajectory study design for the Durham site, illustrated in Figure 5, was motivated by the need to measure all of the possible movements through the intersection of E. Lawson Street and S. Alston Avenue. There are a total of 12 possible movements. For vehicles traveling southbound on Alston, they can continue straight, turn right onto Lawson, or turn left on Lawson. Likewise, vehicles traveling northbound on Alston can make one of three movements at the intersection with Lawson. Vehicles traveling eastbound or westbound on Lawson can make one of three movements in each direction. Furthermore, the study design was motivated by the need to obtain data along Lawson Street between Fayetteville Street and Alston Avenue, and along Alston Avenue between Lawson and Cecil Street, which include paths approximately concurrent with the pedestrian transects for air quality measurements.

Details regarding the vehicles measured, how many runs were made by each vehicle for each study location, route, and time of day, are given in Additional Materials Table D.1.

AIR QUALITY

The study design for air quality measurements is described for the freeway site and the urban site. Additional details regarding study design are in Additional Materials E for the freeway site and Additional Materials F for the urban site.

Freeway Site

Additional details given in Additional Materials Appendix E for the freeway site include the rationale for site selection, meteorological conditions, QA procedures, examples of

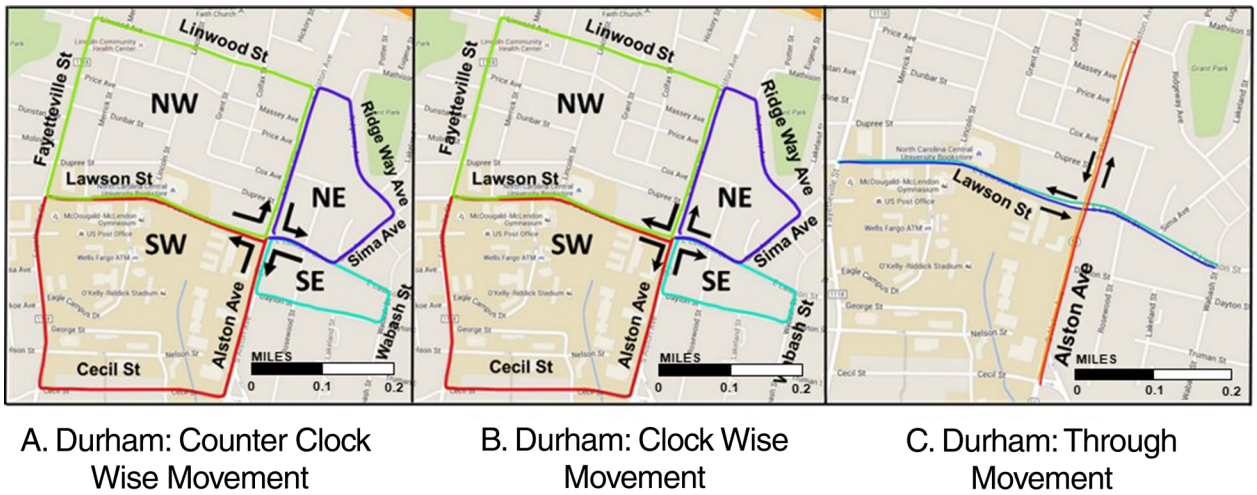

Figure 5. Designated routes for real-world vehicle tailpipe emission measurements at the urban site: A. counter clock wise movements; **B.** clock wise movements; and **C.** through movements.

calibration and intercomparison results, and the method for inference of fleet average vehicle emission factors. At the freeway site, measurements focused on quantifying temporal variability at a near-road fixed location, supplemented with transect measurements of the spatial gradient for a transect perpendicular to the freeway.

We conducted measurements next to Interstate 40 (I-40), near Durham, North Carolina, USA (Figure 6), where it is an eight-lane highway with an annual average daily traffic volume of 140,000–145,000 vehicles per day. At the measurement location, a low-traffic rural road (Triple Oak Drive, Morrisville, North Carolina) runs almost perpendicular to the highway, in line with the dominant wind direction. This configuration enabled us to run downwind transects with a mobile lab (van) for several hundred meters downwind to quantify the spatial gradient in ambient concentration. A key reason for selecting this site was that it was already established as a monitoring site by the NC DEQ and the U.S. EPA Office of Research and Development. The established site was within ~5 meters of the interstate with power, internet, and security in place.

One possible concern regarding the location of these sites is the influence of the relatively nearby RDU, with runways approximately 2 kilometers from the Triple Oak Drive sampling site. However, we did not observe an impact of aircraft operations on the measurements. See Additional Materials Appendix E for more discussion of the site, the rationale for its selection, and an evaluation of the lack of impact of aircraft operations on the measurements (Additional Materials Figure E.1).

Measurements were collected at three locations: (1) temporal variability in pollutant concentrations at a fixed-site monitor located 10 meters from the highway edge, (2) temporal variability in pollutant concentrations at a stationary background site located on the opposite side of the highway, about 400 meters away from the highway, and (3) spatial variability in pollutant concentrations measured during downwind transects on Triple Oak Drive using a mobile platform. The background site was located in a commercial building with sampling inlet on the roof. The fixed-site monitor is an existing monitoring site operated jointly by the U.S. EPA and NC DEQ. The U.S. EPA/NC DEQ fixed-site monitor continuously monitors CO, NO, NO_x, O_3, BC, and a set of basic meteorological parameters. The U.S. EPA provided a supplemental trailer, for use in this project, approximately 10 meters to the east of the existing U.S. EPA/NC DEQ fixed-site monitor, and also approximately 10 meters from the highway edge (see Figure 6). Our team used the supplemental trailer, which we refer to as the North Carolina State University (NCSU) trailer, to install our own set of instruments.

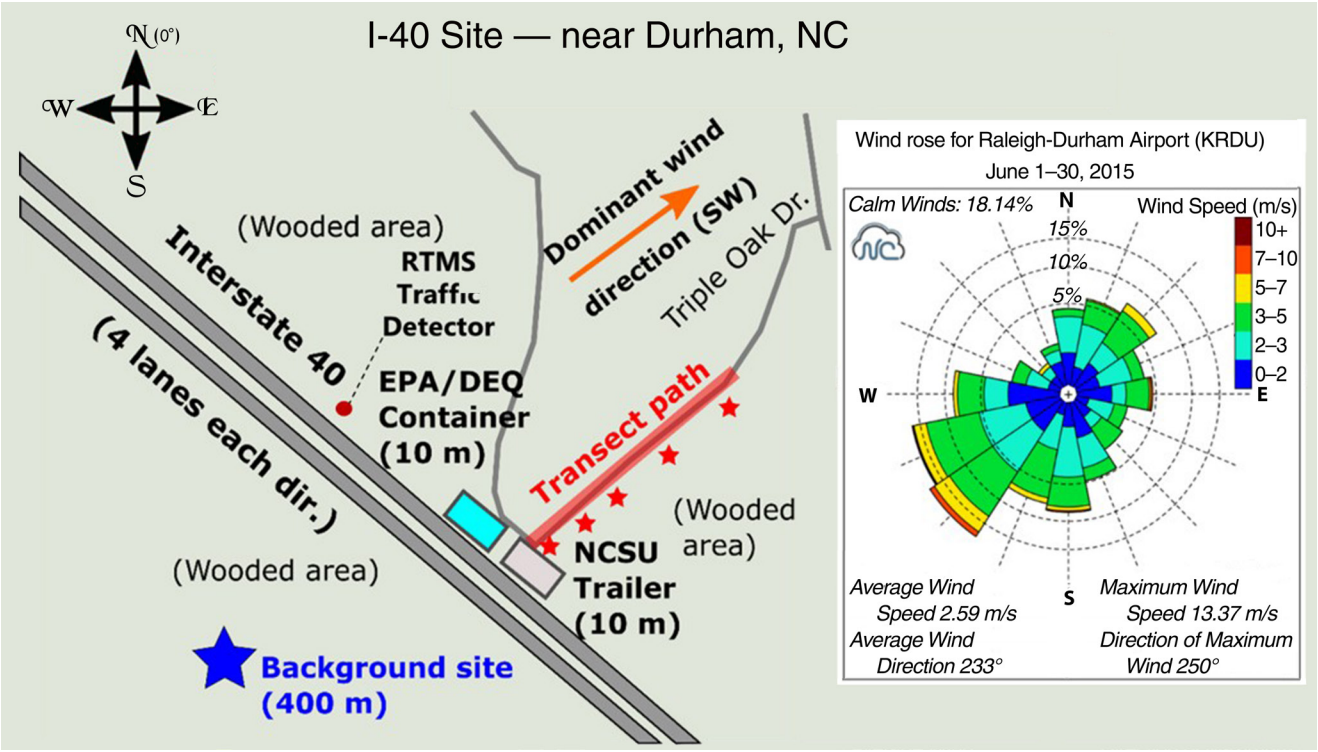

Figure 6. Study area map showing the relative locations of the fixed-site monitor (EPA/DEQ container), the trailer provided by the U.S. EPA for use by North Carolina State University (NCSU trailer) to install additional air quality instrumentation, the upwind background site (star), the transect path for air quality measurements on Triple Oak Drive, and the RTMS traffic detector. The wind rose (insert) illustrates that the predominant wind direction is from the southwest during summer.

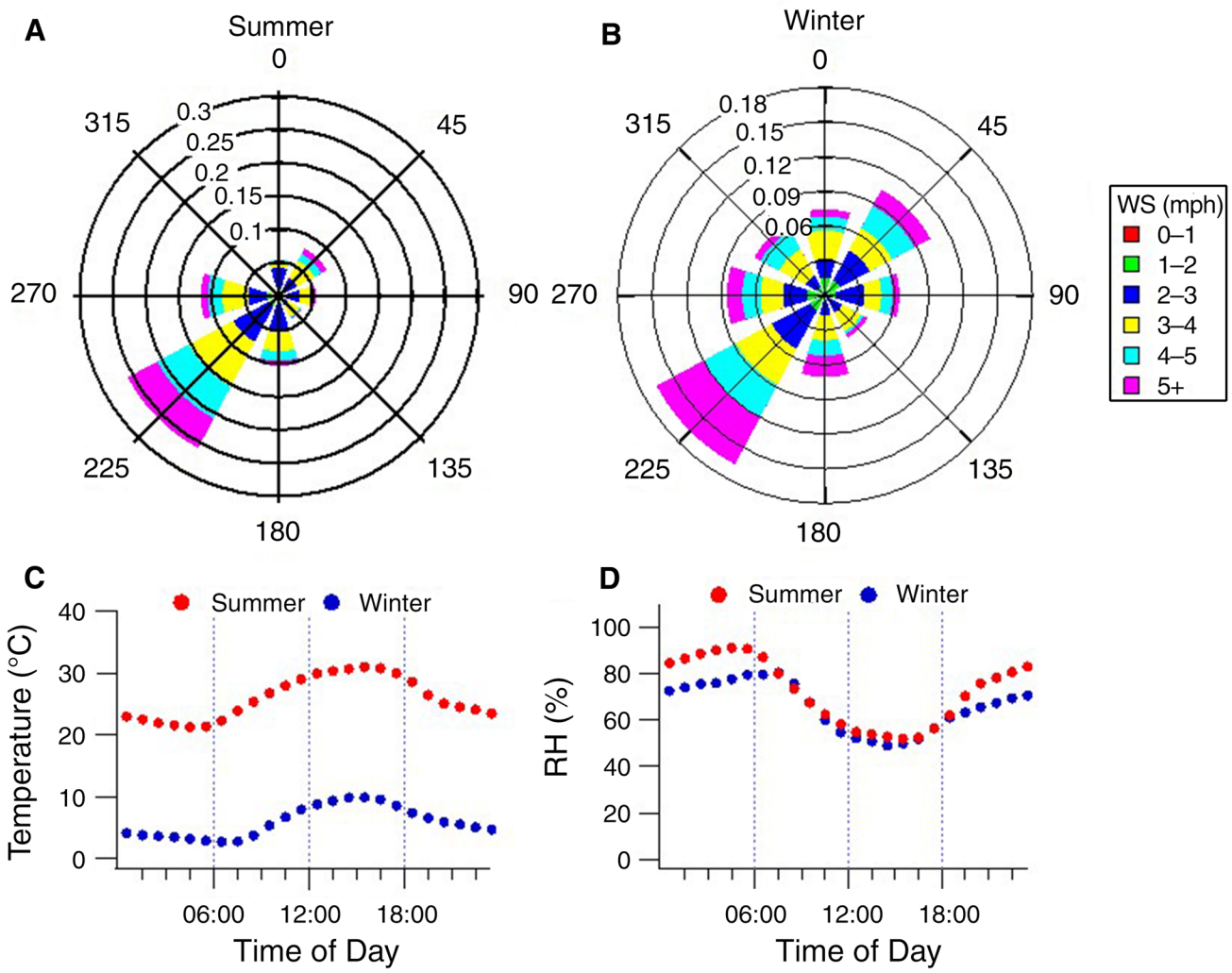

Figure 7. Campaign-average meteorological conditions during the I-40 summer and winter campaigns. RH = relative humidity; WS = wind speed. (Reprinted from Saha et al. 2018a, with permission from Elsevier)

The main meteorological conditions during the summer and winter measurement campaigns are summarized in Figure 7; these are discussed further in Additional Materials Appendix E (Figures E.2 and E.3, Table E.1). Instruments and methods used in these campaigns are listed in Table 3. Data were collected at the NCSU trailer and background sites continually during these periods, with only momentary interruptions to allow for instrument maintenance or intercomparison measurements. Downwind transect measurements on Triple Oak Drive were collected on selected days (summer: 4 days; winter: 3 days, see Additional Materials Table E.1 for details) within a window of continuous stationary measurements. Transect days were selected based on favorable weekday weather forecasts for no precipitation and southwest winds (coming from and perpendicular to the roadway). On these days, two to three transect runs were typically completed per day, during times with distinctive traffic and meteorological conditions: morning rush hour (~07:00–09:00), mid-day (~12:30–14:30) and evening rush hour (~16:30–18:30). For the downwind transect runs, a van equipped with a subset of instruments from the near-road trailer was used. The instruments temporarily taken from the trailer for use in the van included a scanning mobility particle sizer spectrometer (SMPS; TSI, Inc., 3787 condensation particle counter paired with 3081 differential mobility analyzer) for measuring ambient particle size distribution, a multitube thermodenuder (TD) coupled with an SMPS for particle volatility, and instruments for measuring BC, NO, NO_x, and CO_2. Aerosol size distribution measured by SMPS and concentrations of BC (microAeth, AE51), NO_x, and NO (Ecotech 9841 NO_x analyzer) were continuously measured at the background site during each campaign.

Data collected during the summer and winter campaigns have undergone QA procedures to ensure data quality and

Table 3. Particle and Gas Instrumentation at the Freeway Site, Raw Data Time Resolutions, and Data Quality Assurance (QA) Approach

Measurement Locations	Parameters	Instrumentation	Raw Data Time Resolution	QA Approach
Near-Road Trailer (10 m)				
	Aerosol chemical speciation	ACSM (Aerodyne Research)	10 min	Pre- and post-campaign standard response factor (NO_3 IE) calibration
	Particle size distribution	SMPS (TSI); 3010 CPC, 3081 DMA	2.5 min	Pre- and post-campaign co-location of all SMPSs used in this study
	Black carbon	PAX (λ= 870 nm) (DMT Inc.)	1 sec	Calibration with Fullerene shoot
	NO_X, NO	Two-B tech NO/NO_X monitor (Model 410, 401 NO_2 converter)	5 min	Calibrated with standard NO cylinder gas; Air gas
	Aerosol volatility	Multi-tube Thermodenuder with SMPS (TSI); 3010 CPC, 3081 DMA; 4 temperature points: 60, 90, 120, and 180°C; 30 sec mean residence time	10 min	Empirical particle loss characterization as a function of TD temperatures using non-volatile NaCl particles
	CO_2	LI-820 (Li-Cor)	1 sec	Calibrated with standard CO_2 cylinder gas; Air gas
Background Site (400 m)				
	Particle size distribution	SMPS (TSI Inc); 3787 CPC, 3081 DMA	2.5 min	Pre- and post-campaign co-location of all SMPSs used in this study
	Black carbon	Micro-Aeth AE 51 (AethLab)	1 sec	Co-located with PAX
	NO_X, NO	Ecotech NO_X analyzer (EC 9841)	1 min	Calibrated with standard NO cylinder gas; Air gas
Downwind Transects (10, 50, 100, 150, 220 m)				
	Particle size distribution	SMPS (TSI); 3010 CPC, 3081 DMA	2.5 min	Pre- and post-campaign co-location of all SMPSs used in this study
	Black carbon[a]	PAX (λ= 870 nm) (DMT)	1 sec	
	NO_X, NO[a]	Two-B tech NO/NO_X monitor (Model 410, 401 NO_2 converter)	5 min	
	Aerosol volatility[a]	Multi-tube Thermodenuder with SMPS (TSI); 3010 CPC, 3081 DMA; 4 temperature points: 60, 90, 120, and 180°C; 30 sec mean residence time	10 min	
U.S. EPA/NC DEQ Fixed Site Monitor (10 m)				
	CO		1 min	U.S. EPA standard QA protocol
	NO, NO_X		1 min	
	O_3		1 min	
	Black carbon		1 min	

[a] Same instrument shared between transect van and near-road trailer; no data at near-road trailer during transect measurements.

ACSM = aerosol chemical speciation monitor; CPC = condensation particle counter; DMA = differential mobility analyzer; IE = ammonium nitrate ionization efficiency calibration; NO_3 = nitrate; PAX = photoacoustic extinctiometer; SMPS = scanning mobility particle sizer spectometer; TD = thermodenuder.

intercomparability of data from different sites and instruments, as described in Table 3. QA approaches and examples of calibration and intercomparison data are given in Additional Materials Appendix E (Figures E.11–E.16 and related discussion). All identified correction factors (calibration factors, instrument intercomparison factors, and particle loss factors for TD data) were applied to raw data for subsequent analyses. Data intercomparisons were also made with the available data from instruments operated at the U.S. EPA/NC DEQ station where applicable (e.g., NO_x, see Additional Materials Figure E.16). A good overall agreement was found between the data collected in the two side-by-side trailers. For subsequent analyses, the long-term data collected from the near-road trailer and background site were averaged to hourly resolution, while for a particular transect run, data collected at each transect location were averaged over ~20 minutes.

Quality-assured data were analyzed for downwind concentration gradients of gaseous and particulate air pollutant concentrations, the downwind evolution of particle size distribution and particle volatility, diurnal profiles of pollutant species, and the correlations of pollutant concentrations with traffic and meteorological parameters. Comparisons between summer and winter results were made to assess seasonal variability. In several analyses discussed below, BC is used as an inert tracer for vehicle-emitted particles; we take this approach to separate particle transport and dilution from other processes (e.g., reactions, particle evaporation and condensation). However, we acknowledge that differential deposition may affect interpretation of results of this analysis. Fleet average vehicle emission factors were also inferred from near-road concentrations using methods described briefly in the Near-Road Dispersion Modeling section and in more detail in Additional Materials Appendix E (Figures E.5–E.10, Tables E.3 and E.4, and related discussion).

Urban Site

To provide data on urban air pollution ambient concentrations, field measurements were conducted in an urban environment near the NCCU campus (Figure 8) in Durham, North Carolina. More detail on QA and QC procedures, measured concentrations, and seasonal wind roses are given in Additional Materials Appendix F.

Measurements were conducted between summer 2014 and summer 2016 and were staggered between sampling periods at the freeway site. Both stationary and mobile measurements were conducted. Air pollution exposure concentration measurements at the urban site focused primarily on spatial variability based on simultaneous measurements made at five stationary locations surrounding the intersection and pedestrian transect measurements made along a walking path in the vicinity of the intersection. Measurements were repeated on multiple days in each season from which temporal trends could be assessed. The stationary sites were selected to represent four quadrants (Q1 to Q4) surrounding the intersection

Figure 8. Urban sampling sites located in Durham, North Carolina. 24-hour average $PM_{2.5}$, O_3, NO_x, and NO_2 concentrations were measured at sites Q1–Q5. Yellow arrows show the pedestrian transect route. The location of the beta attenuation monitor (BAM) for hourly $PM_{2.5}$ measurements is shown. The locations of loop detectors and video cameras used to quantify vehicle flow are also indicated. Distance between pairs of quadrants: Q1–Q2 450 ft; Q2–Q3 300 ft; Q3–Q4 300 ft; Q1–Q4 310 ft; Q4–Q5 100 ft. Tree buffers were present between streets and the Q1 and Q2 sites. (Map and aerial image attributed to OpenStreetMap contributors under Open Database License with cartography licensed as CC BY-SA; *www.openstreetmap.org/copyright.*)

of interest at Alston Avenue and Lawson Street, as well as to leverage existing monitoring sites at the northeastern corner of the NCCU campus close to the intersection (Q5) and at a parking deck on Lawson Street west of the intersection. At the latter, a beta attenuation monitor (BAM) measures hourly $PM_{2.5}$ concentrations. The BAM is a federal equivalent method instrument and was also used to benchmark the PEM filter-based $PM_{2.5}$ samplers that were deployed at the quadrant sites. The Q1, Q2, and Q4 quadrants represent near-road residential areas. Q3 and Q5 are in the same quadrant. Q3 is a near-road site and Q5 is a near-intersection site. The mobile measurements were made by pedestrians carrying portable instruments and are referred as *pedestrian transects*. The pedestrian transect pathway was designed to enable comparisons of the effects of land use patterns — including buildings, bus stops, vegetation, and road proximity, as well as traffic patterns and weather conditions — on ambient concentration.

Each field sampling season lasted for approximately two weeks, and measurements were made for winter and summer seasons. At least two weekend days were included during each two-week long sampling period so that ambient concentrations could be compared based on the day of the week. Field sampling was conducted during time periods when NCCU was in session to reflect the typical traffic and ambient conditions around the area. Sampling during days with extreme weather conditions, especially in the winter sampling period, was curtailed for the safety of the volunteers engaged in pedestrian transects.

The instruments used at the urban site are listed and described in Table 4. Air pollutants measured included PM of different sizes (UFPs and $PM_{2.5}$), NO_x, NO_2, O_3, CO, and CO_2. However, not all of these pollutants were measured at all locations. Data regarding weather conditions (including wind speed, wind direction, and humidity) were collected to assess the impact of meteorological variables on air pollution ambient concentration. The table also indicates the key aspects of the QA procedures for each instrument. In general, standard operation procedures for each instrument were followed based on the instrument manual, including procedures for calibration and operation of the instruments. Additional Materials Figure F.2 gives an example of hourly average $PM_{2.5}$ concentrations measured hourly with the same BAM used to evaluate the PEM instruments.

The PEM units at the quadrant sites, Q1–Q5, collected daily average $PM_{2.5}$ concentrations. Except for Q3 and Q5, these sites were located at residences based on cooperation from local residents. To reduce the burden to the residents, and for the security of the instruments, measurements were made with small samplers that could be easily hidden and had low power requirements. $PM_{2.5}$ was measured with a PEM from SKC Ltd. This PEM is an inertial impaction sampler for measuring time-averaged particle concentration on a filter. The PEM requires a known flow rate of sample air that was supplied by an AirCheck pump. Daily average concentrations of NO_x, NO_2, and O_3 were measured using Ogawa passive samplers (Ogawa USA). The collection pads were replaced each day. The pads removed from the sampler were placed in prewashed individual sample vials and placed in a refrigerator until they were hand-delivered to RTI International for sample analysis. An additional stationary site, located at a parking deck along East Lawson Street to the west of the intersection of interest, measured $PM_{2.5}$ on an hourly basis using a BAM. To help evaluate temporal trends in the $PM_{2.5}$ measurements in the vicinity of the intersection, the $PM_{2.5}$ measurements from the PEM units located at each of sites Q1–Q5 were compared with the BAM located just a few hundred feet away from the intersection at the parking deck. The BAM is located on an edge of the top level of the parking deck.

Data were collected along the pedestrian transect using real-time portable monitors that were carried by student research assistants. Instruments used to measure $PM_{2.5}$ included SidePak (TSI Inc) and DustTrak (TSI Inc). DustTrak data were collected consistently in both seasons. UFP concentrations were measured using P-Trak (TSI Inc), which use a condensation particle counter detection method. O_3 was measured using a Portable Ozone Monitor (POM) (2BTech Inc). A Q-Trak (TSI Inc) was used to measure CO, CO_2, temperature, and relative humidity. A GPS receiver was used to record locations. Most of the instruments recorded data at 1 Hz.

As part of QA, calibration and instrument checks were completed for each instrument one week before sampling started in each season. QA for each instrument was conducted according to their respective operating manual or other established standard operation procedure, as further detailed in lists of QA procedures given in Additional Materials Appendix F for Ogawa samplers, PEMs, the POM, DustTrak, and P-Trak.

For example, the POM was kept in its operating temperature range in the winter by wrapping it with insulation. It was carried in a protective backpack and was warmed up prior to collecting data. The instrument was stored in the laboratory at a controlled temperature. The instrument readings were typically well above the detection limit of 2.0 ppb. Thus, there were no data handling issues related to values below the detection limit for this instrument. The measured values from the POM were benchmarked to ambient O_3 measured at the nearest regulatory fixed-site monitor, and were judged to be comparable in magnitude, taking into account the potential for spatial variability, and given that O_3 levels can be highly variable because of distance from the regulatory monitor and proximity to roads.

QA and QC procedures for the Ogawa samplers included: (a) detailed procedures for cleaning the diffusion end cap, stainless steel screen, sampler body, and sampler clip; (b) storage of precoated sampling pads for O_3, NO_x, and NO_2 according to manufacturer instructions; (c) insertion of sampling pads and field blanks into the sampling body on the morning of a measurement; (d) transport of sample bodies with pads or field blanks to and from the site in sample vials and zip-lock bags in an icebox; and (e) transport of sample

Table 4. Particle and Gas Instrumentation at the Urban Site, Averaging Time, and Quality Assurance Approach

Measurements	Instruments Used	Averaging Time	Quality Assurance
Particulate matter ($PM_{2.5}$)	PEM (Personal Environmental Monitor) (SKC)	24-hr daily Rush hour	• AirCheck pump calibration was performed using DryCal before sampling. • Calibration of PEM by leak check followed by DryCal when AirCheck pump is connected to each PEM unit. • Compared to BAM (Met One Instruments) for validation (see below and Appendix F for BAM).
	SidePak (TSI) -portable	1 Hz	• SidePak. zero-cal and cross check with other units. • Zero calibration per manual. Inter-comparison of two SidePaks for consistency check.
	BAM	Hourly, daily-hourly average, continuous	• Federal Equivalent Method (FEM) BAM (Met One Instruments). Calibration performed by company technician. • BAM data from Durham, NC (Armory location) was also used for background.
	DustTrak -portable	1 Hz	• DustTrak manual/SOP was followed for zero calibration and operation.
Particulate matter (UFP PN)	P-Trak (TSI) -portable	1 Hz	• Performed zero-calibration. Registered ultrafine counts from two units were compared.
NO_X, NO_2, O_3	Ogawa samplers	24-hr daily	• SOP based on manual was followed to clean and assemble the units. • Chain of Custody: logsheet filled each time sample was handled, including before sampling and during transfer to RTI International for analysis. • Ogawa Field blanks.
	POM -portable	10 sec	• O_3 zeroing scrubber calibration was performed before use.
CO, CO_2, temperature, humidity	Q-Trak (TSI) -portable	1 Hz	• Three units of Q-Traks were run simultaneously and the registered values were compared several times before actual sampling.
Wind direction, speed, and other meteorological variables	Onsite weather station	24-hr continuous	• Compared information (wind direction/speed, temperature, precipitation).
Spatial identification	GPS	1 Hz	• Data from the GPS unit was compared with smartphone GPS data

BAM = beta attenuation monitor; POM = portable ozone monitor; SOP = standard operating procedure.

vials in a small icebox to an analytic lab at RTI International with a chain of custody document. QA and QC procedures for the Ogawa sampling were based on those published by Ogawa and developed at the Harvard TH Chan School of Public Health, as noted in Additional Materials Appendix F. Field blanks for Ogawa sampling were deployed. Background levels based on the blanks were incorporated into the analysis of field samples.

For the DustTrak, the effect of zero drift was minimized by zero calibration of the unit prior to each transect measurement. The reported measurement range for the DustTrak for $PM_{2.5}$ is 0.001–150 mg/m^3 according to the operating manual. The lowest nonzero value that can be reported by the DustTrak is 0.001 mg/m^3. We treated all measured values as observations, including zero values, and checked observations for indications of potential data quality problems (e.g., negative values).

PEM filters for daily average $PM_{2.5}$ concentration measurements were preconditioned in a humidity- and temperature-controlled HEPA filter chamber for at least 24 hours before their use. The filters were post-conditioned for a day before weighing to minimize the humidity effect. Meteorological data during each sampling period were collected from a weather station on the NCCU campus four blocks from the intersection of interest. Pedestrian transect measurements were conducted in a consistent way in terms of start and stop times and walk speed.

The BAM was located on the roof of a 4-story parking deck. The third and fourth levels of the parking deck were not used during the first two days of BAM data collection. The first two levels of the parking deck of the same building were also almost empty during the week in which BAM data were used for comparisons with other measurements. The vehicles that used the parking deck were exclusively light-duty vehicles. In the United States, gasoline cars and light trucks comprise 95% of the on-road fleet (Chambers and Schmitt, 2015). Thus, it is highly unlikely that many diesel vehicles used the parking deck. LDGV tend to have very low primary $PM_{2.5}$ mass emission rates (Frey 2018). Much of the primary particle emissions from LDGV are in a submicron size range, such as below 300 nm, which contributes very little to $PM_{2.5}$ mass concentration. For this reason, the potential impacts from the parking deck on $PM_{2.5}$ values registered at the BAM monitor are believed to be very minimal.

NEAR-ROAD DISPERSION MODELING

As part of the statistical model development for near-road ambient concentrations described later, we explored whether the near-road dispersion model helps to explain spatial and temporal variability in ambient concentrations. We chose the R-LINE model developed by the U.S. EPA (Snyder et al. 2013) to simulate the downwind dispersion of roadway emissions. Additional Materials Appendix G provides details of R-LINE and how it was configured to represent each of the study sites and documentation of input data.

Prior to applying the model, we evaluated how well the model was able to simulate the measured temporally and spatially resolved near-road air quality observations. R-LINE was used with surface meteorology measurements taken at RDU, with upper air soundings (measurements of the vertical distribution of meteorological properties) from the Greensboro airport. Meteorological measurements were taken every minute with a 0.5 meter/second minimum wind threshold, averaged over the hour using AERMINUTE, then surface dispersion parameters were calculated using AERMET (Cimorelli et al. 2005). R-LINE was run for the freeway site and season-specific meteorological conditions. R-LINE was run with two-line sources spatially centered in the middle of the I-40 eastbound and westbound roadway, each with four 3.6 meters wide lanes (two on either side of each source). The sources were one kilometer in length with a height of two meters and an initial vertical spread of 1.5 meters to simulate an average emission height and uniform mixing due to traffic turbulence on the roadway. Model receptors were located perpendicular to the highway 10, 50, 100, 150, and 220 meters downwind from the edge of the highway to be consistent with the transect measurement locations. R-LINE was run using a unit emission rate of 1 g/m/sec. Measured traffic volumes and derived fleet-average emissions factors were used to estimate fleet-average emission rates. The latter were used to scale unit-emission-rate R-LINE output to obtain estimated ambient concentrations. The extracted fleet-average fuel-based emission factors (g/kg) were converted to a distance-based value (g/mile) for this analysis. This conversion calculation assumed an average fuel efficiency of light- and the heavy-duty vehicles of 30 and 8 miles per gallon, respectively, and the fraction of light- and heavy-duty vehicles in the campaign-average fleet of 94% and 6%, respectively. The approach for estimating fleetwide emission rates is described in more detail in Additional Materials Appendix E.

R-LINE was also used to model roadway impact on concentrations along the walking paths used for pedestrian transects at the urban site. We used the road-network around the walking paths and simulated each roadway with an average annual daily traffic of 1,000 vehicles per day (which can be scaled to actual traffic counts). R-LINE outputs were grouped by roadway name; thus, adjustment to traffic volumes can be made without rerunning R-LINE.

STATISTICAL METHODS AND DATA ANALYSIS

Statistical models were used to quantify the contribution of metrics such as land use, traffic activity, meteorology, dispersion, and vehicle emissions to variability in measured concentrations. Statistical model development focused on the following cases: temporal variability at a fixed monitor 10 meters from a freeway; variability in 24-hour average pollutant concentrations at five sites near an urban intersection; and spatiotemporal variability along a walking path near that same intersection. A statistical model was not developed for the downwind concentrations perpendicular to the freeway; instead, for this case, the role of the dispersion model in predicting the spatial gradient was evaluated. The physical plausibility of statistical model coefficients was evaluated. For freeway site models, it was possible to compare model estimates to independent data at the same site for selected pollutants, which raises confidence that those models could be used to estimate concentrations at that site. The models are not intended, however, to be used for predictions for other sites.

We used best subset selection with 50-fold cross validation to choose the simplest model that retained the optimal explanatory power. The best model containing a given number of input variables was selected based on minimizing the residual sum of squared errors (SSE) of the training data. The best overall models were chosen as the most parsimonious models whose mean SSE for the validation data were no more than one standard error above the minimum SSE (James et al. 2013). By using this method, we were able to identify the combination of metrics that provided the most explanatory power while still being interpretable. All statistical models were fit using the statistical analysis software R version 3.2.2.

Freeway Site

The statistical model for the freeway site focused on quantifying temporal variability at a fixed location. Five response variables were considered at the freeway site, including concentrations of BC, ultrafine particle number (UFP PN), PM mass, NO, and NO_x, measured at the site 10 meters from the freeway. Measurements were collected at 1-second intervals for BC concentration, 2.5-minute intervals for UFP PN and PM concentrations, and 5-minute intervals for NO and NO_x concentrations. All responses were averaged to 60-minute intervals to coincide with wind measurements at RDU. All of the pollutant concentration distributions were right skewed. To reduce the potential for skewness in distributions of model residuals, the pollutant concentrations were transformed. Response variables were increased by 0.1 (to reduce left skewness and to avoid taking the log of zero in the case of observed values equal to zero) and log-transformed (to reduce right skewness) before the analysis. We further standardized all of the input variables to have mean zero and unit variance. Standardizing the input variables allowed us to compare the effect estimates on the same scale and to interpret the intercept as the overall mean of the transformed concentrations.

Nineteen input variables were compared. These inputs include: (a) traffic indices described earlier; (b) predicted concentrations from the R-LINE dispersion model; (c) cosine of the wind direction centered so that wind perpendicular from the road to the monitor was 0 degrees; (d) temperature; (e) wind speed; (f) first and second harmonics of time of day; and (g) indicators for summer versus winter sampling campaign and weekend versus weekday. The predicted concentrations from R-LINE are source strengths of 1 g/m/sec or a linear function of each of the traffic indices. The background concentrations and R-LINE predictions were also increased by 0.1 and log-transformed to maintain an approximately linear relationship with responses. Wind direction and speed were available both from the sonic anemometer located adjacent to the monitors and from RDU. Wind direction and speed were collected at 1-second intervals by the sonic anemometer and averaged to 60-minute intervals. Hourly measurements collected at RDU (KRDU Station) were available from the State Climate Office of North Carolina CRONOS database.

We modeled the responses as:

$$Y(t) = X(t)\beta + \varepsilon(t) \qquad (3)$$

where $Y(t)$ is a log response at hour t (i.e., BC, UFP PN, PM, NO, or NO_x), $\mathbf{X}(t)$ is a 1-by-k row vector of input variables at hour t, as described in the previous paragraph, β is a k-by-1 column vector of regression coefficients, and $\varepsilon(t)$ is a random error term, assumed to follow a stationary autoregressive moving average (ARMA) process of autoregressive (AR) order p and moving average order q (ARMA(p,q)).

Before fitting the time-series models described in equation 3, input variables that explained variability in ambient concentrations were selected using best subset selection with 50-fold cross validation. All possible models were compared using the leaps R package (Lumley 2017). The best model containing a given number of input variables was selected by minimizing the SSE of the training data. Because the SSE of the training data will always decrease as more input variables are added, models of different sizes were compared using the SSE of the validation data, averaged across all 50 validation sets. As the size of the models (number of input variables included) increased, the decrease in the validation SSE became negligible compared with the standard error in the validation SSE. To account for this, the best overall model was chosen as the most parsimonious model with a validation SSE not more than one standard error above the minimum SSE (James et al. 2013).

To select an appropriate correlation structure for the error term, we varied the orders p and q and selected the orders that gave the smallest value of the Akaike Information Criterion (AIC). At this stage of model selection, we kept the same input variables as selected from the previous stage, but we re-estimated the regression coefficients β for each value of p and q. To determine whether the inclusion of the R-LINE model predictions improved our model fits, we repeated the entire variable selection and correlation structure selection procedure without the inclusion of the R-LINE predictors and compared the results.

We further examined our model performance by calculating model estimates, $\hat{Y}(t) = X(t)\hat{\beta}$ using $\hat{\beta}$ estimated in the ARMA models for the time periods when measurements at the 10-meter near-road site were not available, but measurements were available from the U.S. EPA/NC DEQ instruments. The U.S. EPA/NC DEQ measurements were first calibrated using the untransformed measurements during the time periods when measurements were available from both sites, to have a slope of 1 and intercept of 0. The U.S. EPA/NC DEQ measurements were log-transformed to correspond with our modeled responses. To avoid undefined log-transformed values for measured concentrations recorded as zero, a small value (0.1) was added to all measurements. The simultaneous transformed measurements were compared, and unadjusted R^2 values were 0.86, 0.83, and 0.30 for NO, NO_x, and BC, respectively.

The low R^2 for the comparison of BC measurements between the NCSU and U.S. EPA sites is mainly because the instruments used different measurement approaches: optical (microAeth) and photoacoustic (PAX). These instruments also have slightly different response times and potential sensitivities (e.g., to humidity or other particle components). Thus, the instruments can give differing readings even if collocated. Thus, the low R^2 value is expected. Because of the low R^2, the BC measurements were not used to test model performance. However, despite using different measurement approaches, the instruments had a similar quantitative response to BC across the range measured, as indicated by a slope very near 1.

Urban Site

At the urban site, statistical models were developed separately for spatiotemporal variability in daily average quadrant air quality data and for spatiotemporal variability in real-time air quality data along the pedestrian transects.

Daily Quadrant Models For the daily quadrant data, O_3, NO_2, NO_x, and $PM_{2.5}$ were considered as the key response variables. The effects of traffic and meteorology variables were investigated using linear regression.

We modeled the daily quadrant responses as:

$$Y_{it} = \mathbf{X}_{it}\boldsymbol{\beta} + \gamma_t + \varepsilon_{it} \qquad (4)$$

where Y_{it} is the concentration at quadrant i on day t, $\mathbf{X}_{it}$ is the row vector of input variables for quadrant i and day t, $\boldsymbol{\beta}$ is a column vector of regression coefficients, γ_t is normal, independent across days t and has variance σ_1^2, and ε_{it} is normal with variance σ^2 and assumed independent across both quadrants and days. The daily random effect is intended to capture daily variation in the background concentrations that affects all quadrants. Input variables included distance-weighted traffic, wind speed, indicator of wind direction from the east (between 60 and 120 degrees), rain, temperature, summer indicator, and interaction between summer indicator and distance-weighted traffic. All input variables were standardized to have mean zero and unit variance to facilitate effect comparison.

Because the number of candidate input variables in the daily quadrant data were small, no variable selection procedure was used to trim the number of input variables. NO_x, NO_2 and $PM_{2.5}$ concentrations were right-skewed and log-transformed before modeling. O_3 concentrations were approximately normal and, thus, were left untransformed.

Pedestrian Transect Models For the pedestrian transect data, UFP PN, O_3, and $PM_{2.5}$ concentrations were treated as response variables; meteorology, traffic, land use, and vehicle emission measurements were used as input variables. UFP PN (particles/cm^3) and $PM_{2.5}$ (μg/m^3) concentrations were recorded at 1-second intervals, while O_3 (ppb) was collected at 10-second intervals. The land use data were used to create a 25-meter grid overlaying the walking route consisting of 52 unique grid cells in which pollutant measurements were collected. For each sampling run, the recorded concentrations were assigned to the nearest grid point based on GPS measurements. Sampling runs typically lasted 30 to 40 minutes. Observations within the same sampling run that were assigned to the same grid points were averaged before analysis, giving at most one observation per grid point per sampling run. Thus, the average of measured values for a given grid cell on a given day is based on approximately one minute or shorter averaging time.

The main purpose of the statistical analysis of the pedestrian transects was to identify factors that help explain spatial variability in observed ambient concentrations. For some runs, many of the $PM_{2.5}$ and O_3 measured concentrations were below the lowest reportable nonzero measured value of 1 μg/m^3 and 1.5 ppb, respectively. Only sampling runs with concentrations above the detection limit for more than 25 grid points (out of 52) were used in the statistical models. Nine of the $PM_{2.5}$ sampling runs, two of the O_3 runs, and one of the UFP PN runs were excluded from the statistical analysis due to lack of observations above the detection level (i.e., measurements in at least 25 of the grid points). For the included sampling runs, approximately 34% of the measurements were below the $PM_{2.5}$ detection level (1 μg/m^3) and were recorded as one-half the detection level (i.e., 0.5 μg/m^3). Approximately 27% of the included measurements were below the O_3 detection level of 1.5 ppb and were similarly recorded as 0.75 ppb. The minimum observed UFP PN concentration was 1,190 particles/cm^3, which was above the minimum detection level of the instrument. For runs for which nearly half, or more, of the grid cells were below detection limit, assigning a constant value of half the detection limit leads to increased spatial homogeneity in the data. Thus, the analysis was constrained to data for which there was observed spatial heterogeneity.

UFP PN and $PM_{2.5}$ distributions were right-skewed, which potentially can lead to skewness in model residuals; therefore, the grid-cell average concentrations were log-transformed before further analysis. O_3 concentrations were approximately normally distributed and, thus, were left untransformed.

A total of 19 input variables were compared. Land use variables included as input variables were distance to the nearest road, distance to the bus stop, average height in the 25-meter grid cell, and percentage of tree cover in a 25-meter grid cell. The traffic sensor on S. Alston Avenue provided vehicle counts within 15-minute intervals. These values were used to derive traffic flows by direction as described above. For each sampling run the mean 15-minute traffic count by direction was calculated. The sum of eastbound and westbound vehicles (E. Lawson Street) and the sum of north-bound and south-bound vehicles (S. Alston Avenue) were used to derive the traffic-weighted R-LINE predictors. The measured traffic counts values were also included as input. Hourly meteorology measurements were taken from a local weather station on the NCCU campus and were used to determine mean temperature, relative humidity, wind speed,

and wind directions by sampling run. Wind from the north was defined as a wind direction between 315 degrees and 45 degrees and wind from the east was defined as a wind direction between 45 and 135 degrees.

Vehicle measurements of VSP, and tailpipe emissions of total HC, CO, and NO_x were averaged by 0.05-mile road segment on either S. Alston Avenue (north–south) or E. Lawson Street (east–west) and traffic direction. Each grid cell was assigned emissions input variables by sampling period and near-side (eastbound/southbound) or far-side (westbound/northbound) direction based on inverse squared distance weighting. The emissions input variables were then summed over the near-side direction and the far-side direction. Walk-along route points greater than 50 meters from the emissions measurements were assigned values equal to the minimum 0.05-mile road segment. Measurements of HC, CO, and NO_x emissions were log-transformed to correspond with the transformed responses.

R-LINE model predictions were made using the grid cells as receptors and assuming unit line sources for S. Alston Avenue and E. Lawson Street. For each pollutant, each grid cell from each sampling run was assigned an R-LINE value for both S. Alston Avenue and E. Lawson Street. Both the sum of these values and the sum of these values multiplied by their corresponding traffic counts were used as input variables in the regression model. R-LINE predictors were log-transformed to correspond with the transformed responses.

Spatial and temporal variation in the measurements was compared using ANOVA. Empirical variograms were used to qualitatively assess the level of spatial dependence. We considered the following model:

$$Y_t(s) = \mathbf{X}_t(s)\boldsymbol{\beta} + \varepsilon_t(s) \qquad (5)$$

where $Y_t(s)$ is the concentration in grid cell s on sampling run t (log(UFP), log (O_3), or log($PM_{2.5}$)). $\mathbf{X}_t(s)$ is a 1-by-k row vector of input variables from grid cell s on sampling run t, $\boldsymbol{\beta}$ is a k-by-1 column vector of regression coefficients, and $\varepsilon_t(s)$ is a normally distributed and spatially correlated error term. We assumed a parametric stationary exponential covariance function with a nugget for the error terms. The errors from different locations within the same sampling run are correlated, and errors from different sampling runs are uncorrelated. The covariance function has the form:

$$\mathrm{Cov}(\varepsilon_t(s_i), \varepsilon_t(s_j)) = \sigma^2 \, exp(-\varphi||s_i - s_j||) + \tau^2 \mathbf{1}\{||s_i - s_j|| = 0\} \qquad (6)$$

$$\mathrm{Cov}(\varepsilon_t(s_i), \varepsilon_{t'}(s_j)) = 0 \qquad (7)$$

where $\mathbf{1}\{A\} = 1$ if A is true and 0 otherwise, φ is the inverse spatial range parameter, σ^2 is the variance of the spatially correlated component of the error, and τ^2 is the variance of the uncorrelated component of the error. Note that this model includes a model with completely uncorrelated errors as a special case when $\sigma^2 = 0$. Distances were scaled so that the maximum distance between route points was equal to 1.

As described above in the description of the freeway models, best subset regression with 50-fold cross validation was used to select the input variables for the model. SSE values of the training data were used to select the best possible model of each size: the best one input variable model, the best two input variable model, and so on. Models of difference sizes were compared using the average SSE of the validation sets and the best model for each pollutant was selected as the one with a validation SSE within one standard error of the minimum SSE. Variable selection was conducted assuming independent errors and the spatial models were fit using only the selected input variables. All input variables were standardized to have a mean zero and unit variance to improve comparisons of the effects. To determine whether the inclusion of the R-LINE model predictions improved our model fits, we repeated the entire variable selection and correlation structure selection procedure without the inclusion of the R-LINE predictors and compared the results.

RESULTS

For two sites, we quantified land use, traffic, vehicle emissions, meteorology, and near-road ambient air quality. The two sites include a freeway and urban site. We developed and tested regression models for temporal variability that include variables for land use, traffic, emissions, and meteorology. We identified the most useful variables based on their contributions to explaining variance in ambient concentrations. We used ANOVA to identify factors that contribute the most to the explainable spatial variation in measured concentrations at the urban site. We used dispersion modeling to evaluate the spatial trend in ambient concentrations measured at the transect perpendicular to the road at the freeway site.

The results include quantification of (1) temporal variability at a fixed monitor 10 meters from a freeway; (2) downwind concentrations perpendicular to the same location; (3) variability in 24-hour average pollutant concentrations at five sites near an urban intersection; and (4) spatiotemporal variability along a walking path near that same intersection. Additional details pertaining to results are given in the following Additional Materials Appendices: A for land use for both sites, B for traffic at the freeway site, C for traffic at the urban site, D for microscale vehicle emissions at both sites, E for air quality at the freeway site, F for air quality at the urban site, G for dispersion modeling pertaining to both sites, and H for additional statistical model results pertaining to both sites.

FREEWAY SITE

Results for the freeway site include quantification of land use characteristics, mesoscale traffic, microscale vehicle emissions, near-road air quality based on measurements and

the R-LINE model, statistical model parameters, and statistical model performance.

Land Use

Comparison of the LIDAR data with our inspection of structures within 2,000 feet of the freeway site identified one new building built since the LIDAR measurements were made in 2007. The main focus of statistical modeling at the freeway site was on a temporal variability. However, spatial variability in ambient air pollutant concentration was quantified based on transects measured along Triple Oaks Drive. Figure 9 shows the 2007 LIDAR imagery analyzed in grid cells of 5 m × 5 m resolution. The EPA monitor is shown with a star. Triple Oaks Drive is the road that emanates from the monitor location toward the northeast. As the figure illustrates, the land use along Triple Oaks Drive is primarily vegetative, with some small residential houses in the close vicinity.

The study area is, on average, 1.8 kilometers from RDU. Although there are nearby arterial roads, the traffic flow on such roads is very low. The terrain elevation varies by approximately 40 meters, but much of this variation is related to a creek bed for Stirrup Iron Creek that runs approximately parallel and to the south of I-40. Thus, the standard deviation of variation in elevation is only 6 meters. Additional details regarding land use at the freeway site are given in Additional Materials Appendix A, including descriptive statistics for selected built environment attributes in Table A.4.

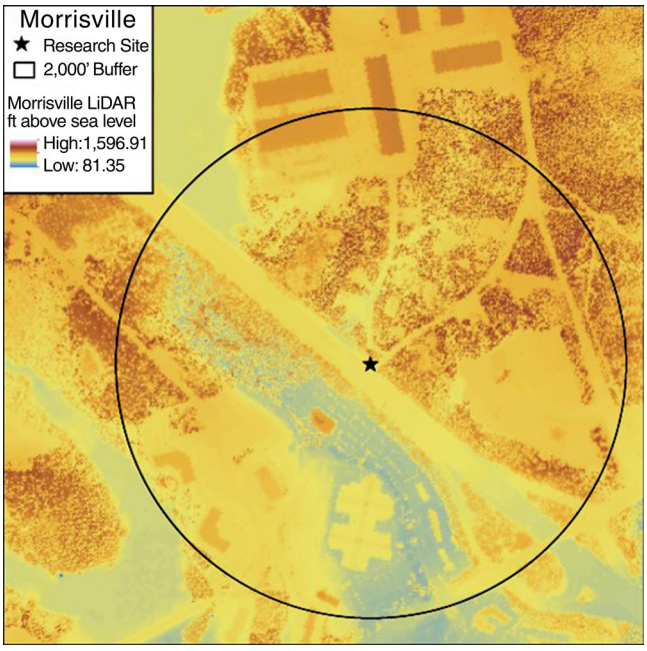

Figure 9. Elevations at the freeway site located on Interstate 40 within 2,000 feet of the fixed-site air quality monitor (shown as a star) Near Triple Oaks Drive, based on 5 m × 5 m grid cells.

Traffic

Figure 10 shows an example of a typical diurnal traffic-activity pattern from an RTMS detector on a sample date (16 March 2015) for the eastbound direction. The primary traffic data are lane-by-lane traffic flow rate, HV flow rate, and vehicle speed. As expected, the rightmost lane carries a higher proportion of traffic than the left lanes. Moreover, a higher fraction of HVs was observed in the rightmost lane. The freeway site experienced both morning and evening peak congestion, with evening operating conditions substantially deteriorated compared with those of the morning. The evening peak congestion results in traffic breakdown exemplified by sudden speed drops between 16:30 and 18:30, as illustrated based on data for a typical day.

Systematic deviation in RTMS counts was observed due to improper calibration of the sensors or having the sensor too close to the westbound lanes. Validation was performed based on recorded videos to assess the accuracy of the RTMS total traffic count and HV counts in each lane (e.g., see Additional Materials Table B.3 for an example). The eastbound total and HV counts for each lane were found to be valid based on comparison of sensor counts and video data. However, there were biases in the westbound data. Figure 11 shows the differences between video and sensor counts for the westbound direction. There was only about a 5% undercount

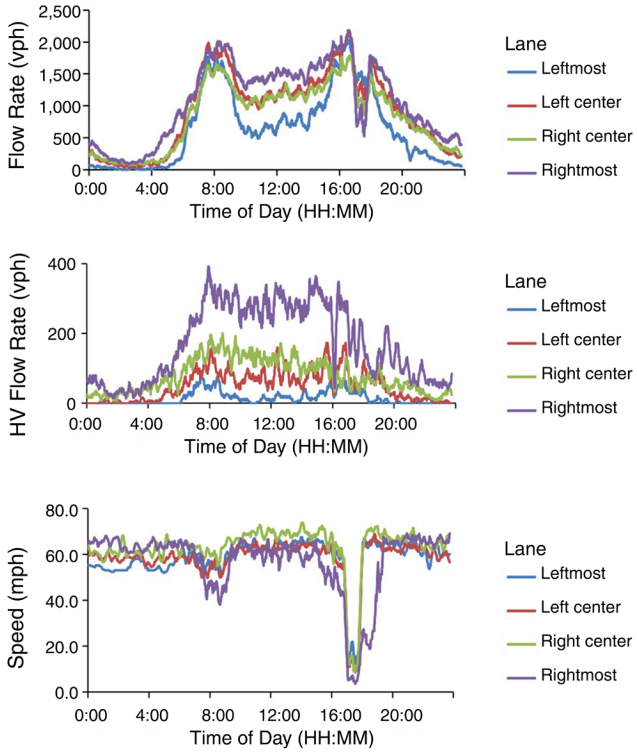

Figure 10. Diurnal lane-by-lane eastbound traffic activities at the freeway site on March 16, 2015: flow rate; HV flow rate; and speed.

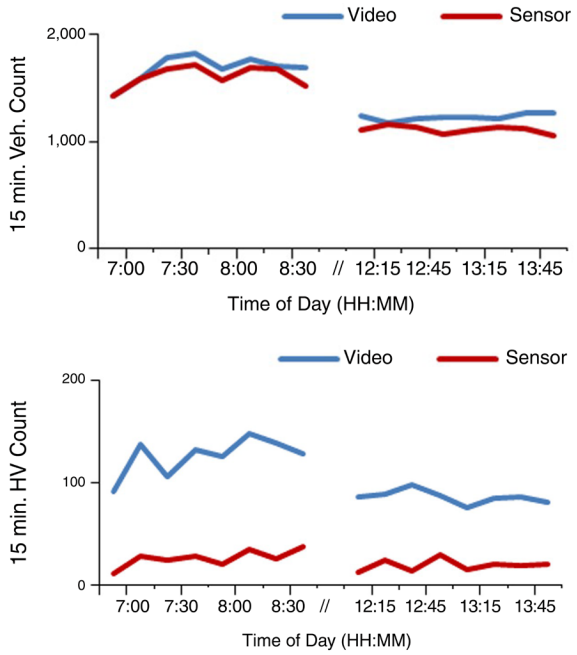

Figure 11. Comparing traffic sensor and video counts at the freeway site for the westbound (nearest to sensor) direction for all vehicles and HVs.

by sensor in total counts summed over all westbound lanes. However, there were compensating errors in the lane-by-lane count. Total vehicle counts in the westbound direction were undercounted by 10% to 16% for the right lane (nearest to the sensor) and over-counted by similar percentages for the left lane (farthest from the sensor). The imbalance in lane assignment in the westbound direction was corrected by applying a lane distribution model for total vehicle counts developed from the eastbound direction and validated with observations from a nearby, far-side sensor (Additional Materials Figure B.2 and Tables B.4 and B.5).

There was about a 70%–90% undercount in the westbound HV counts summed over all lanes. To correct the undercounting of HVs in the westbound direction, a westbound HV lane volume model (% HV by lane) was developed using the lane percentage of HV for the far (eastbound) side. This assumes that the proportion of HV by lane is the same in either travel direction. The model was applied to estimate more accurate lane-by-lane HV counts for the westbound direction. Predicted HV counts for the westbound direction were compared with video data and deviations were within 5% of the observed counts. Detailed examples of corrected data are shown in Additional Materials Figures B.3–B.6 for selected days. Additional information regarding bias correction and traffic results for the freeway site is given in Additional Materials Appendix B.

The diurnal (15 min) profile of the three traffic indices at the freeway site for a winter day (9 February 2016) is plotted in Figure 12. A detailed example of these indices is given in Additional Materials Table B.7. The volume index has a distinctive bimodal pattern with peaks corresponding to the morning and evening rush hours. The HV index peaked during the morning peak, held at approximately a constant moderate level during midday, increased for an evening peak around 17:00, and then decreased gradually into the evening. The density index accentuates the effect of the drop in speed in the evening peak period. During under-saturated traffic conditions, the density remains around 20 vehicles per mile, which corresponds to Level of Service C per the Highway Capacity Manual (TRB 2010). However, during the evening peak period, the speed of the eastbound direction dropped sharply. Consequently, the density index quickly increases to the jam density level (around 180 vehicles per mile).

Emissions

The segment average VSP and mass per distance NO, CO, and HC exhaust emission rates were quantified based on all vehicle runs of the freeway site for off-peak, morning peak,

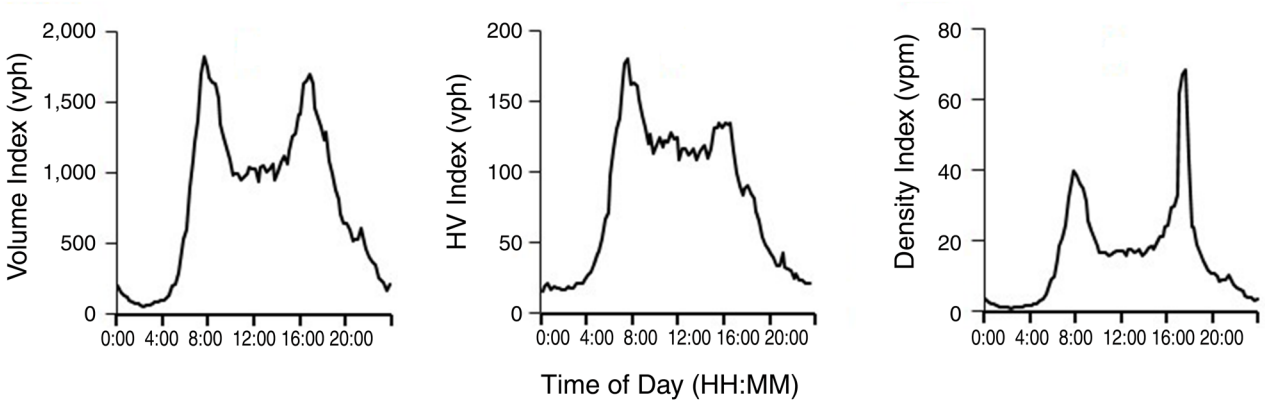

Figure 12. Diurnal variation of traffic flow rate, HV, and density indices at the freeway site on February 9, 2016.

and evening peak periods. As an example, results for the evening peak are given in Figure 13 for NO_x emission rates, which are approximated based on measured NO exhaust concentration. The estimated segment average VSP and mass per distance NO_x emission rates for the combined runs on I-40 site between Airport Boulevard and I-540 (designated as Route 1) during the evening peak are shown. The average VSP ranged from −17 kW/ton to 22 kW/ton over 38 segments on Route 1. Negative values of VSP occurred most typically during deceleration. Negative VSP can also occur if a vehicle is traveling down a hill while coasting. Negative VSP means that the engine is not under load. Based on Frey and colleagues (2003, 2010), emission rates at negative VSP have a constant mean value approximately similar to that for engine idling. Mean emission rates vary monotonically with positive VSP for all measured pollutants. The highest VSP values were located on the ramps onto I-40 associated with acceleration. On the westbound I-40 segment closest to the air quality monitor, there was spatial variability in VSP indicative of transient vehicle operation. Such transients were associated, for example, with weaving between lanes related to the influence of vehicles merging into the through lanes from the nearest on-ramp.

The NO_x emission rates varied from 2.3 mg/mile to 430 mg/mile. The highest values of VSP and mass per distance NO_x emission rates occurred at ramps. Compared with the westbound side of I-40, which is closer to the monitoring site, the NO_x emission rates on the eastbound side tend to be lower. These results indicate that there is spatial variability in engine load and tailpipe exhaust emission rate, especially in the right lane of I-40 westbound during evening rush hour.

Additional details are given in Additional Materials Appendix D regarding results similar to Figure 13 for off-peak and morning peak times of day, as shown in Additional Materials Figures D.6 and D.7, respectively. The spatial patterns in NO_x emission rates for the nearest on ramps at Airport Boulevard to westbound I-40 and I-540 to eastbound I-40 were generally the same regardless of time of day. The emission rates had the highest averages on these ramps. The NO_x emission rates on westbound I-40 immediately in front of the monitoring station were in the range of 36 mg/mile to 64 mg/mile, which is far less than the average rate on the ramps but higher than the rate farther to the west on the westbound side of I-40 and higher than the rates in the eastbound direction on the road segment closest to the monitor. Thus, the general pattern shown in Figure 13 is similar to that for other times of day.

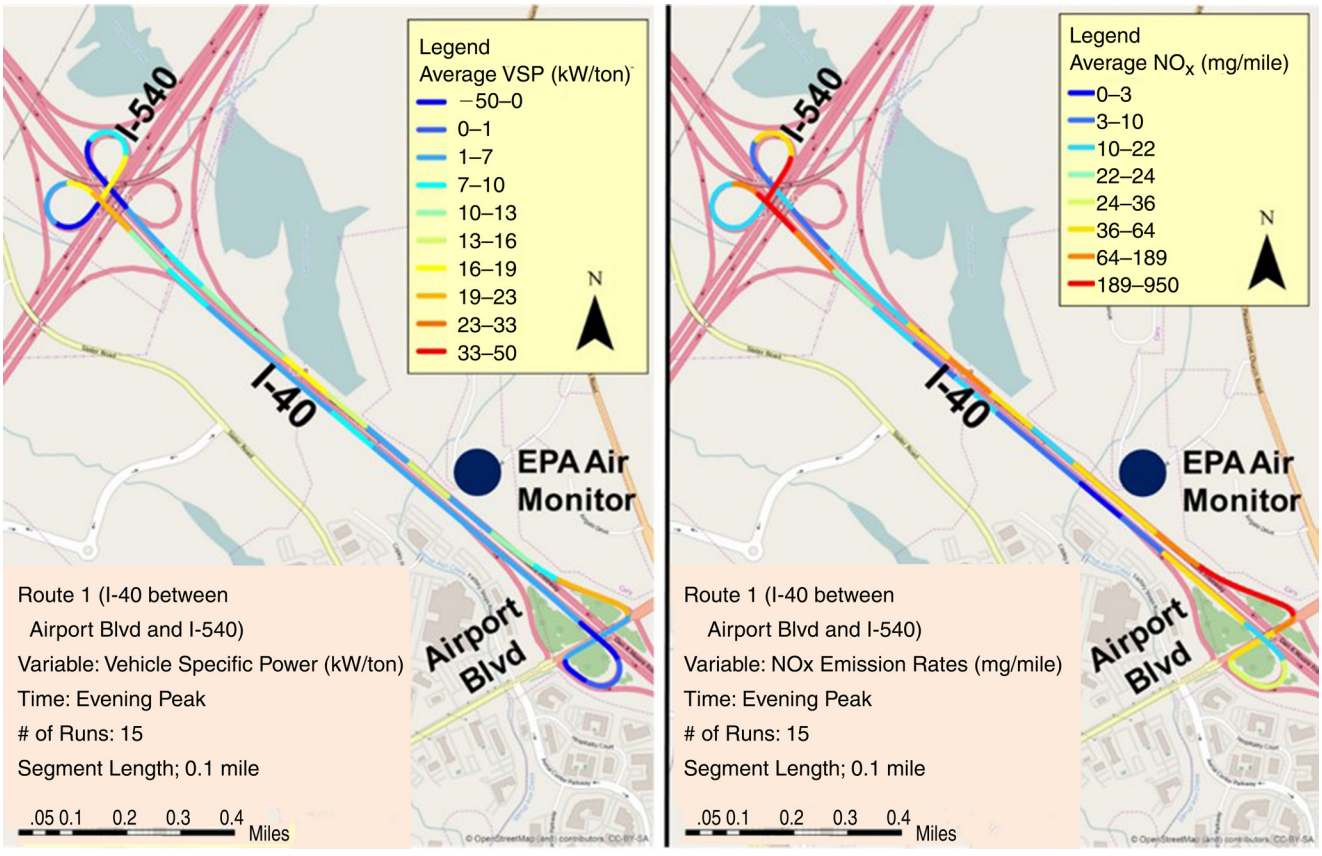

Figure 13. Spatial average VSP and NOx emission rates over 0.1 mile segments of Route 1 for the evening peak. (Map images attributed to OpenStreetMap contributors under Open Database License with cartography licensed as CC BY-SA; *www.openstreetmap.org/copyright*.)

Additional Materials Figure D.4 illustrates lane by lane differences in average VSP and NO_x emission rates in front of the U.S. EPA air monitor at I-40. The result indicates higher VSP and NO_x emission rates in the far-left lane of I-40 westbound, which is consistent with the general expectation that vehicles in the far-left lane are either moving at higher speed or attempting to do so. However, this result is based on a very limited sample of only two runs per lane and thus is illustrative that there can be differences by lane and by segment. The emission rates on I-40 westbound were somewhat higher than on I-40 eastbound across from the monitor, associated with moderate rather than low VSP. The vehicle traffic on the eastbound side near the monitor is farther downstream of the nearest onramp and thus may be less disrupted by weaving associated with vehicles that have recently entered the freeway.

Additional Materials Figures D.3, D.11, and D.12 show the measured NO_x emission rates for 0.1-mile segments of I-40 in both directions for through movements, illustrating the emissions pattern for vehicles that were on the mainline rather than entering at the nearest upstream ramp. For the evening peak, the emission rates were highly variable among the 0.1-mile segments, especially on the westbound side closest to the monitor. There was more variability for off-peak compared with evening peak, and less variability for morning peak compared with evening peak, on the westbound side. The westbound emission rates for segments closest to the monitor tended to be higher in the westbound compared with the eastbound direction for all three time periods. Thus, there was spatial variability in vehicle emissions for through movements as well as for those vehicles that entered the freeway at the ramps nearest to the monitor.

Vehicle emission rates measured on Slater Road, which approximately parallels I-40 upwind, were found to be generally low for the morning and off-peak periods, as shown in Additional Materials Figures D.8, D.9, and D.10 for off-peak, morning peak, and evening peak, respectively. The emission rates tended to be higher in the evening peak than for the other two times of day. However, the vehicle traffic volume is much lower on Slater Road than I-40.

The additional results in Additional Materials Appendix D illustrate that there is lane-by-lane variability, based on data collected for movements upstream and downstream of the nearest ramps, and variation among times of day in VSP and emission rates.

Air Quality Measurements

Air quality results are given regarding the spatial distribution of pollutants near the roadway, downwind transformation of UFPs, and seasonality of inferred vehicle emission factors. No measurements from the I-40 site were below the detection limit for the averaging times presented here. Sensitivities for individual instruments are discussed in Additional Materials Appendix E.

Spatial Distribution of Pollutants The observed downwind concentration profiles of NO_x, BC, integrated UFP PN, and PM mass from summer and winter transect measurements are shown in Figure 14. These measurements were collected with the wind predominantly from the highway. UFP PN and volume concentrations are SMPS measurements integrated over 10 to 400 nanometer particle sizes. The integrated particle volume concentrations are reported as PM mass concentrations (in $\mu g/m^3$) using an estimated overall effective density of 1.5 g/cm^3 (see Additional Materials Appendix E for derivation of estimated PM density and Additional Materials Figure E.11 for evaluation of SMPS-based PM mass estimates). There were strong diurnal and seasonal differences in the spatial distribution of traffic-sourced pollutants (e.g., NO_x, BC, UFP PN). For example, NO_x and UFP PN concentrations were substantially higher in winter. In general, pollutant concentrations were consistently higher during morning rush hours compared with the evening rush hours in both seasons. This trend is consistent with that observed in previous near-road field measurements (Baldauf et al. 2008a; Durant et al. 2010; Gordon et al. 2012). This trend is likely linked with both a lower morning mixing height and high traffic volume during morning rush hour. Diurnal trends in traffic, meteorology, and air pollutant concentrations are discussed in Additional Materials Appendix E and shown in Additional Materials Figures E.3 and E.4.

Consistent with previous measurements (Beckerman et al. 2008; Enroth et al. 2016; Gordon et al. 2012; Karner et al. 2010; Zhu et al. 2002a), downwind concentrations of traffic-related pollutants were observed to decay exponentially with increasing distance from the highway (Figure 14). A strong vehicle emission signature was observed within 100 to 150 meters from the highway edge. Downwind concentrations of species appeared to decay to background levels by 200 to 300 meters from the highway edge, especially in summer. NO_x, BC, and UFP PN approached background conditions closer to the highway in summer in comparison to the winter observations. While half-decay distances (i.e., the distances at which concentrations decay by half of the concentration increase at the road edge) of NO_x, BC, and UFP PN concentrations (relative to 10 m) was observed within 50 to 70 meters in summer, the half-decay distances were approximately 100, 130 and 150 meters for UFP PN, BC, and NO_x, respectively, in winter. Near-road NO_x was dominated by NO in both seasons. With increasing distance from the highway, the NO to NO_x ratio gradually decreased in summer, but remained nearly constant in winter (see Additional Materials Figure E.17). These trends are consistent with reduced photochemical activity and mixing from background air in winter compared with summer. NO_x, BC, and UFP PN levels approached background levels within 200 meters in summer. During winter measurements, 55% to 60% decay was observed for NO_x and BC within 200 meters, whereas approximately 80% decay was observed for UFP PN at this distance. This indicates that the highway-influenced zone is wider during the winter seasons for many pollutants. These trends are likely linked

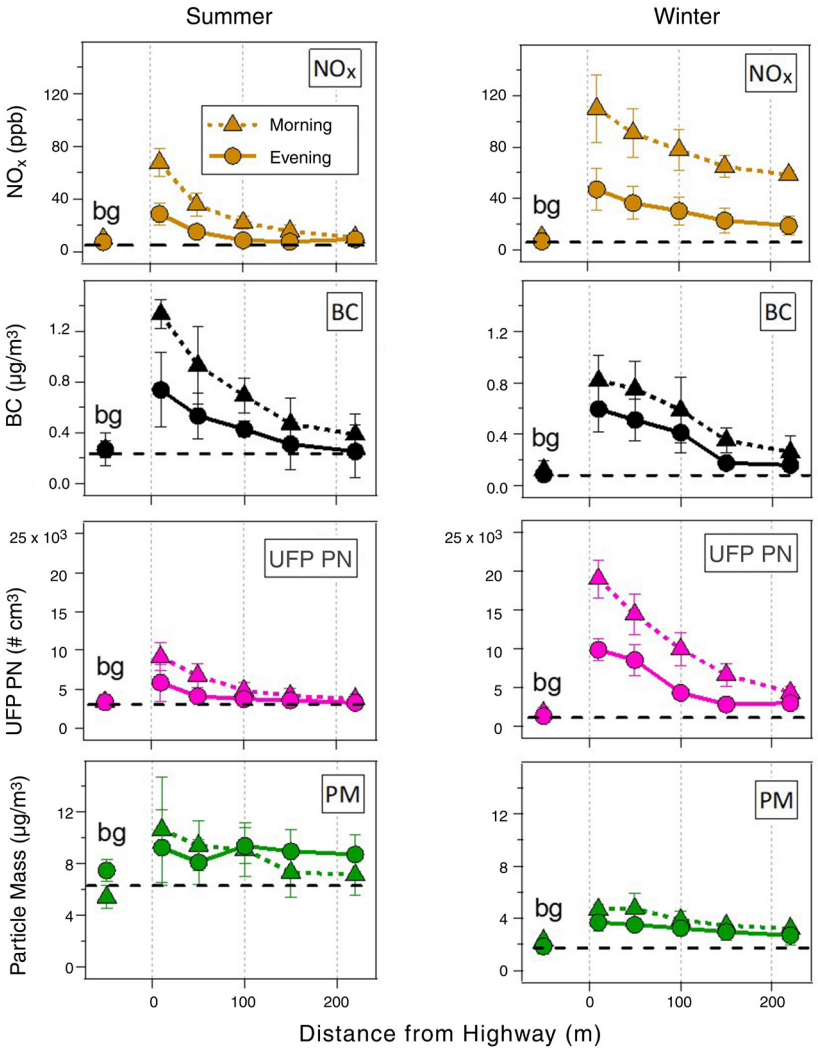

Figure 14. Downwind evolution of NO_x, BC, integrated UFP PN, and particle mass (PM) concentrations (10–400 nm) at the freeway site during summer and winter campaigns. Points shows mean, and error bar shows ±1 standard deviation of measurements from multiple transects runs as listed in Additional Materials Table E.1 (summer $N = 4$; winter $N = 3$). Horizontal black dashed lines are a visual indication of background levels. The background site (bg) location is not shown on horizontal axis; it is approximately 400 m upwind from the main fixed monitor site on the opposite side of I-40. (Reprinted from Saha et al. 2018a, with permission from Elsevier)

to greater atmospheric mixing, and thus dilution, in summer and more stable atmospheric conditions during winter due to lower temperatures.

Concentration gradients of PM mass were observed to be flatter than those of NO_x, BC, and UFP PN in both seasons. Rapid growth of organic aerosol mass downwind of a highway has been reported by Stroud and colleagues (2014) that may counter to some extent the decay of vehicle-emitted primary PM concentration due to dilution, mixing, and evaporation. We observed that the organic aerosol mass decayed more slowly with distance than BC, a conservative traffic tracer. Data supporting these observations are shown in Additional Materials Figure E.18. This could be explained by condensation of semivolatile organic vapors on the existing aerosol surfaces as the air is transported away from the highway. The depositional loss rate of different PM species and sizes could be different than that for BC particles as they travel downwind. However, making a firm conclusion based on these observations is complicated by the fact that the increment in the measured pollutants relative to the background becomes progressively smaller with distance, making these inferences quite uncertain.

Downwind Transformation of Ultrafine Particles The average PN size distributions at different distances from the highway are shown in Figure 15. These measurements were collected during the morning and evening rush-hour transects

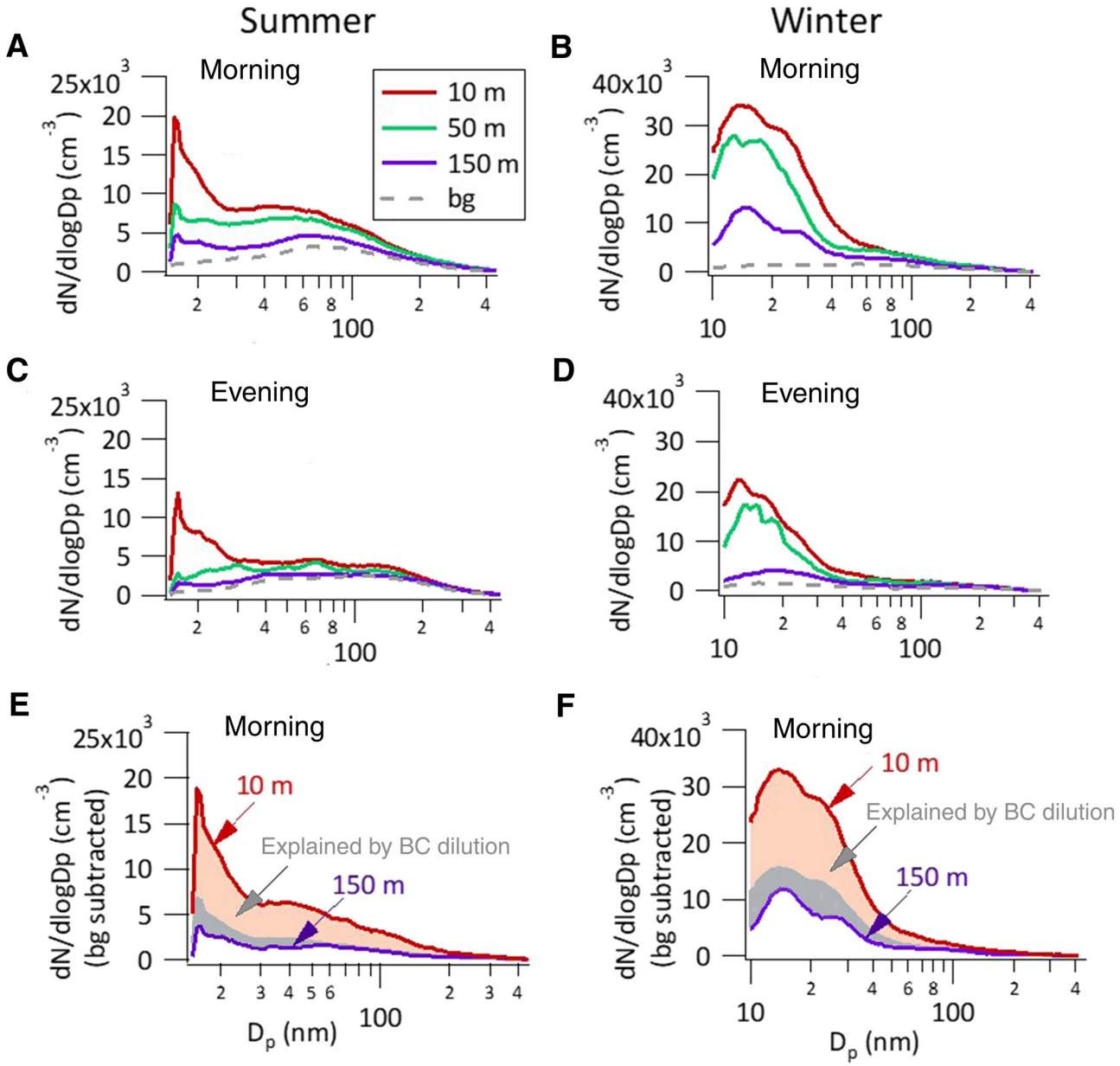

Figure 15. Average particle number size distributions (dN/dlogD_p as a function of particle diameter D_p) at different distances from the edge of the highway at the freeway site. (A–D) Downwind measurements are not background-subtracted; **(E–F)** Background-subtracted average particle number size distributions at 10 m (red) and 150 m (purple) downwind distances. The reddish shaded portion of the measured size distribution at 10 m can be explained by applying the dilution factor at 150 m, determined from the decay profile of background-corrected BC concentrations (Fig. 14). Other processes will be required to explain the gray dotted portion. bg = background; D_p = particle diameter. (Reprinted from Saha et al. 2018a, with permission from Elsevier)

with the wind predominantly from the highway. UFP PN size distributions near the highway were multimodal, with a large peak at <20 nm, while size distributions measured at the background site were similar to those measured at 200 meters from the highway edge (not shown). The dominant ultrafine mode and rapid downwind decay is commonly observed for near-highway particle size distributions (Buonanno et al. 2009; Kozawa et al. 2012; Zhu et al. 2002a, 2006). The downwind evolution of the ultrafine mode varied with time of day and season. In general, higher concentrations and a relatively slower evolution of particle size distribution with distance from the highway were observed during the winter morning. This observed seasonal trend agrees with previous observations (Virtanen et al. 2006; Zhang and Wexler 2004;

Zhu et al. 2004). As discussed above, this is likely due to the less atmospheric dilution and mixing during the winter morning due to a more stable atmospheric condition under colder temperatures.

Dilution is thought to be the dominant process that dictates downwind evolution of the particle size distribution in the near-road environment (Choi and Paulson 2016; Pohjola et al. 2007; Zhang et al. 2004; Zhang and Wexler 2004). Figure 15 (E–F) shows that dilution- and deposition-driven decay, here approximated using the downwind decay profile of BC (an inert particle tracer), cannot explain the observed downwind evolution of the ultrafine mode. Evolution not attributable to dilution alone is more pronounced during the winter season, where a slower decay of BC with distance from the road was measured. This suggests that additional loss processes affect the downwind evolution of the ultrafine mode. A feasible explanation is that a portion of the ultrafine particle is semivolatile and evaporates upon dilution during transport downwind. Another possibility is that the deposition rate of this ultrafine mode is different than that of BC. In particular, a fraction of UFP PN may be produced via homogeneous nucleation and thus be substantially smaller than BC-containing particles. Although the exact reason is yet to be determined, our measurements clearly indicate that while the dilution-driven decay is a dominant loss process for UFPs in the near-road setting, other processes such as evaporation and condensation are required to explain observations. This is consistent with previous modeling studies (Choi and Paulson 2016; Kumar et al. 2011; Zhang et al. 2004; Zhang and Wexler 2004). The volatility of particles in this near-road environment is discussed further by Saha and colleagues (2018b) and may play a role in the evolution of fresh vehicle emissions in the near-road environment.

It has been suggested by Choi and Paulson (2016) that, at distances greater than 60 to 80 meters from the road, evaporation of UFPs is a mechanism affecting the evolution of road-to-ambient particle size distributions. This evaporation process is typically driven by decreases of organic vapor pressure around the particles due to the rapid dilution of the plume (Robinson et al. 2007). Therefore, if some portion of semivolatile species evaporated from the particle-phase to gas-phase, the overall volatility of particles would appear to decrease as they move away from the highway. Therefore, we measured the volatility of particles using a TD system (Huffman et al. 2008; Saha et al. 2015; Saleh et al. 2008; Wehner et al. 2002) at different downwind distances from the highway. Under a fixed set of conditions (e.g., TD temperature and residence time, particle size, loading), the extent of evaporation of particles after heating in a TD can provide insights into their volatility.

We observed that smaller particles evaporated more than larger particles. The extent of evaporation of a particular sized particle (especially within the ultrafine range; ≤100 nm) decreased as the aerosol was transported away from the highway, suggesting that the overall volatility of these particles decreased over time (Saha et al. 2018a). This observation is conceptually consistent with the evaporation of semivolatile species during downwind transport. The contribution of evaporation to the total loss rates will eventually diminish within a few hundred meters from the highway because gas-phase semivolatile species in the plume will reach quasi phase-equilibrium as the plume approaches ambient conditions (Choi and Paulson 2016). Since these TD measurements are not corrected for the contribution of background particles to overall observations, a direct quantitative attribution of the change in volatility of traffic-emitted particles as they move downwind cannot be made based on our observations.

Seasonality of Observed Emission Factors Fleet-average fuel-based emission factors were calculated for various pollutants (i.e., NO, NO_x, BC, UFP PN) using a carbon balance approach (Dallmann et al. 2014; Grieshop et al. 2006; Hudda et al. 2013). See Additional Materials Appendix E, equation E1 and related discussion for more details on this method and its application. Extracted season-specific fuel-based fleet average emission factors for NO, NO_x, BC, and UFP PN are shown in Figure 16. Emission factors for NO, NO_x, and UFP PN were found to be higher in winter in comparison to the summer observations. The study average NO_x emission factor in winter (4.7 ± 2.6 g/kg-fuel) was approximately 20% higher than that during summer (3.8 ± 2.5 g/kg-fuel). A similar level of seasonal variation was observed for the NO emission factor (winter: 3.1 ± 2.0 g/kg-fuel; summer: 2.5 ± 1.7 g/kg-fuel). The study average UFP PN emission factor was a factor of 3 higher in winter ($7.5 \pm 5 \times 10^{14}$/kg-fuel) than in summer ($2.5 \pm 1.7 \times 10^{14}$/kg-fuel). The difference between the study average BC emission factors in winter and summer was not statistically significant (winter: 0.035 ± 0.03 g/kg-fuel; summer: 0.045 ± 0.03 g/kg-fuel).

The observed substantially higher UFP PN emission factors in winter is consistent with greater UFP formation during dilution of vehicle exhaust with colder dilution air (Du and Yu 2006). The study-average emission factors for sub-50 nm and sub-100 nm PM mass (g/kg-fuel; derived from SMPS data assuming density of 1 g/cm^3) were also found to be 3.8 and 2.2 times higher in winter in comparison to the summer, respectively (Additional Materials Figure E.7). A potential explanation for this seasonal change in nanoparticles emissions from motor vehicles is that, under colder conditions, a larger fraction of the semivolatile organic emissions partitions into the particle-phase compared with summer conditions (Grieshop et al. 2006; Lipsky and Robinson 2006; Robinson et al. 2007).

Fleet-average NO_x emission factors derived in our study show reasonable agreement with LDGV emission factors derived from individual passenger cars measured on the I-40 highway by Liu and Frey (2015b) (Additional Materials Figure E.8). The fleet-average emission factors in this study are also similar to those derived from real-world measurements in recent years for LDGV (Ban-Weiss et al. 2008; Bishop and Stedman 2008; Hudda et al. 2013; Liu and Frey 2015b; Park

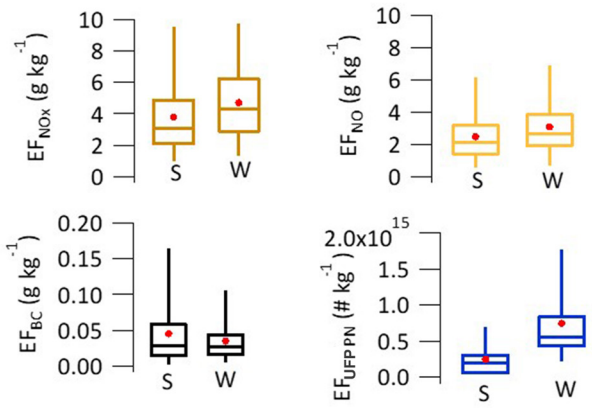

Figure 16. Distribution of fleet-average emission factors extracted at the freeway site. S and W refer to summer and winter measurements, respectively. The ends of the box represent the first and third quartiles, the line inside the box is the median, and the length of the whiskers covers 95% of the data. The red circle represents the mean. EF = emission factor. (Reprinted from Saha et al. 2018a, with permission from Elsevier)

et al. 2011). This is reasonable, since the fraction of HV in the highway I-40 is relatively small (study average 6 ± 3%). This is also makes it difficult to extract HV emission factors from these data. Emission factor values do not have a discernible trend with fleet composition or time of day. Therefore, we do not attempt to report vehicle-class-specific emission factors. Further discussion on emission factor variation and comparison with previous measurements is included in Additional Materials Appendix E (Table E.4, Figures E.9 and E.10).

Dispersion Modeling

Season-average measured and R-LINE modeled concentrations as a function of distance from the highway are compared in Figure 17. The R-LINE configuration is discussed in Additional Materials Appendix G; the model was run with unit emission rates and emission factors measured at the site (Figure 16). R-LINE did a reasonable job of estimating general trends in spatial and temporal patterns in the near-road concentration field. For example, the model predicted higher concentrations in the morning than in the evening in both seasons. However, quantitative discrepancies exist between the measured and modeled concentrations.

The model tended to under-predict the concentrations in the morning and over-predict in the evening, with a few exceptions. Several factors may contribute to this discrepancy, including variability in emission factors, fleet mix, and prediction capability of R-LINE to simulate downwind dispersion. Study-average emission factors and fleet mix are used in this analysis. Emissions factor variability may be influenced by a number of factors, such as variations in the fleet mix and variations in emissions due to temperature changes or underlying stochastic variability within the fleet. The fraction of the HV in the fleet did not vary significantly between morning and evening. Our extracted emission factors did not show any clear temporal pattern, suggesting that if there is consistent diurnal variability in emission factors it is below our ability to detect it. Since the emission factor is a multiplier to the concentration gradient profile, an adjustment in fixed emission factor to make the model match the measurement at a particular location and time (e.g., closer distance to the roadway, morning time in Figure 17) would shift the whole modeled profile and thus the concentrations measured at other locations and times. Therefore, we did not attempt to adjust the emission factors to make the model better match the measured concentration gradients.

The campaign-average diurnal profiles of measured and modeled concentrations are compared in Figure 18 based on long-term measurement data sets from the stationary near-road trailer. The result shows that the R-LINE simulations capture morning peaks and over-predict evening peaks in

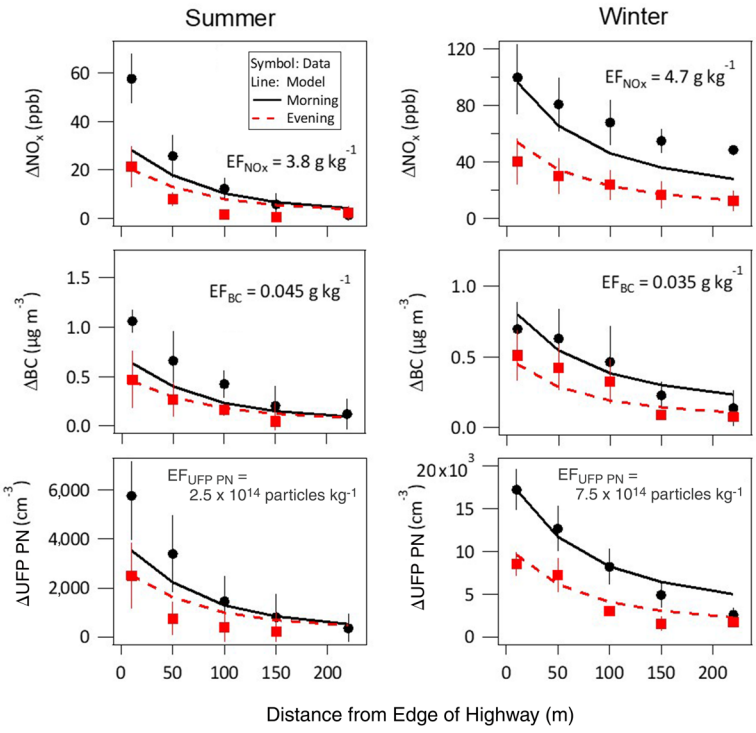

Figure 17. Background-subtracted (Δ) measured and modeled pollutant concentrations as a function of distance from the edge of the highway at the freeway site. Measurements were collected with the wind predominantly from the highway during transect measurements. The symbols show the means with ± one standard deviation. The lines show the average of the modeled concentrations over the corresponding measurement periods. EF = emission factor. (Reprinted from Saha et al. 2018a, with permission from Elsevier)

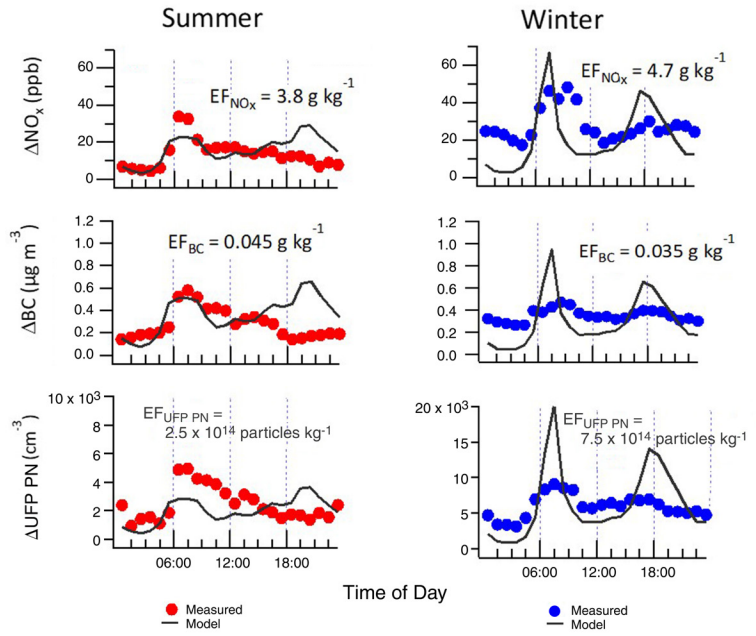

Figure 18. Campaign-average diurnal profiles of background-subtracted (Δ) measured and modeled pollutant concentrations at the freeway site. Pollutant concentrations were collected at the near-road trailer located 10 m away from the highway edge over the I-40 summer and winter campaigns. The line shows an average of the modeled concentrations over the corresponding measurement periods. EF = emission factor.

summer, and over predict both morning and evening peaks in winter. This suggests that R-LINE underestimates dispersion occurring in convective meteorological conditions in the evening, leading to over prediction of roadway impacts in the evening hours. R-LINE predicts greater concentration peaks in the winter morning. The reason for this discrepancy could be due to predicted over-suppression of dispersion by R-LINE under a stable atmosphere in the winter morning. This discrepancy may be influenced by small scale topographical or meteorological variation at the roadside. Further work to assess inputs to R-LINE and model output sensitivity should explore possible contributors to these discrepancies. Including a time-varying emission factor — as is typically done if emissions models (e.g., MOVES) are linked to dispersion models — may address some of this deviation.

Statistical Model

For each of the five responses considered, the input variables selected using best subset selection described above are shown in Table 5. The purpose of quantifying model coefficients is to serve as basis for assessing whether the direction (mathematical sign) and magnitude of these coefficients are consistent with prior scientific knowledge and hypotheses. Thus, evaluation of the model coefficients can help build confidence in the model. The importance of the input variables is further illustrated in Figure 19, which shows the multiple (unadjusted) R^2 for each of the final ordinary least squares (OLS) regression models along with the percentage of response variance explained by each input variable calculated using the method of Lindeman and colleagues (1980).

The dispersion model parameter computed from R-LINE did not contribute to explaining variability in measured ambient BC and PM concentrations and did not have a statistically significant model coefficient. For UFP PN concentration, the R-LINE dispersion parameter, in interaction with the traffic density index (i.e., the RLINE dispersion parameter and traffic density index), contributed only 12% of response variance. The interaction effect of R-LINE with a vehicle volume index was the largest contributor to response variance, at approximately 23% to 24%, for NO and NO_x, respectively. It is not surprising that the combination of the R-LINE dispersion parameter in combination with an index of time-varying emissions does relatively better in estimating near-road NO and NO_x concentrations, compared with BC, PM, and UFP concentrations, since the near-road concentrations of these species are dominated by dispersion rather than physical and chemical transformations and are closely related to emissions source strength that is proportional to the number of vehicles on the road, including both gasoline and diesel vehicles. In contrast, variability in BC concentration is largely related to wind direction favorable to transporting pollutants from the road to the downwind monitor and to HV activity. Variability in PM concentration is dominated by the background concentration, implying that the vehicles on the target road do not contribute substantially to the background. UFP PN concentration variability is sensitive to a variety of factors that represent local primary and precursor emissions (e.g., HV index) and their transport from the road to the monitor (e.g., dispersion represented by an R-LINE variable and wind speed).

Locally measured wind direction from the highway to the monitor was included in the final model for all of the pollutants and observed to have a large positive model coefficient. Temperature was observed to have a negative correlation with the pollutant concentrations but did not explain as much of the variance in the response (Figure 19). HV index was selected as an important input variable for all responses except for PM, for which the volume index had a positive effect. This is an expected finding, as we expect concentrations to be higher when the wind is directed from the roadway toward the monitor and when traffic volumes are higher. The selection of the HV index implicates diesel vehicles as a greater source of PM emissions than other vehicles, which is consistent with prior expectations. The first and second harmonics of time were not selected for any of the responses indicating that there were no temporal trends remaining that were unexplained by other input variables.

Table 5. Regression Parameter Estimates from the ARMA Models for the Freeway Site[a]

Input	BC	NO	NO_x	$PM_{2.5}$	UFP PN
Intercept	−0.779 (0.071)*	2.363 (0.046)*	2.916 (0.045)*	1.161 (0.058)*	8.599 (0.062)*
Background concentration	0.193 (0.026)*	—	—	0.492 (0.018)*	0.383 (0.026)*
Temperature	−0.141 (0.051)*	−0.273 (0.047)*	−0.281 (0.048)*	−0.085 (0.037)*	−0.262 (0.072)*
Summer	—	—	—	—	−0.2 (0.083)*
Weekend	—	—	−0.123 (0.053)*	—	—
sin(2π × time)	—	—	—	—	—
cos(2π × time)	—	—	—	—	—
sin(4π × time)	—	—	—	—	—
cos(4π × time)	—	—	—	—	—
Volume index	—	—	—	0.073 (0.012)*	—
HV index	0.18 (0.019)*	0.367 (0.043)*	0.227 (0.04)*	—	0.198 (0.024)*
Density index	—	—	—	—	—
WS airport	—	—	—	—	—
cos(wd) airport	0.061 (0.025)*	—	—	—	—
WS local	—	—	—	—	—
cos(wd) local	0.118 (0.024)*	0.397 (0.041)*	0.317 (0.038)*	0.069 (0.014)*	0.188 (0.031)*
R-LINE unit source	—	—	—	—	—
R-LINE HV index	—	—	—	—	—
R-LINE volume index	—	0.18 (0.04)*	0.211 (0.037)*	—	—
R-LINE density index	—	—	—	—	0.091 (0.028)*

[a] Input variables not selected by the variable selection procedure indicated with "—"; standard errors of coefficient estimated are in parentheses; * indicates *P* value less than 0.05; time = time of day; wd = wind direction; WS = wind speed.

For the particulate pollutants BC, PM, and UFP PN, R-LINE variables did not substantially improve model fit quantified by a reduction in AIC (Table 6). Additionally, background concentrations were selected for inclusion in the final models of the particulate pollutants and explained a large percentage of the response variance for UFP PN and PM. In contrast, for the gaseous pollutants NO and NO_x, model fits were improved by the R-LINE interaction effects and background concentrations were selected into the models.

Local wind explained variability in NO and NO_x concentration even when considering R-LINE prediction as an input, which suggests that R-LINE, as configured for this application using off-site wind data, while by itself is useful in explaining some variability in measured concentration, does not completely account for the wind dynamics in this scenario. We speculate that that the airport meteorological monitoring site more accurately represents prevailing wind directions, while the local anemometer more accurately represents local wind behavior, both of which explain some of the variability in pollution concentrations.

For all pollutants, the ARMA time-series models resulted in lower AIC values than OLS regression models (Table 6), indicating better fits. The model coefficients for all input variables chosen by the variable selection procedure remained significantly different from 0 ($P < 0.05$) when temporal correlation was accounted for (Table 5). The optimal correlation structure for the particulate pollutants BC, PM, and PN was ARMA(2,1) (in other words, included parameters for AR 1, AR 2, and MA 1), while the gaseous pollutants NO and NO_x had an ARMA(1,0) (in other words, only an AR 1 parameter) optimal correlation structure.

The model selection procedure was run without including R-LINE or local wind variables, and the AICs for the ARMA models were increased to 40, 449, 391, −528, and 305 for BC, NO, NO_x, PM, and UFP PN, respectively, indicating that local wind measurements substantially improve model fits (Additional Materials Tables H.2 and H.3).

Overall, the results in Table 5 and Figure 19 indicate that the dispersion concentration calculated with R-LINE

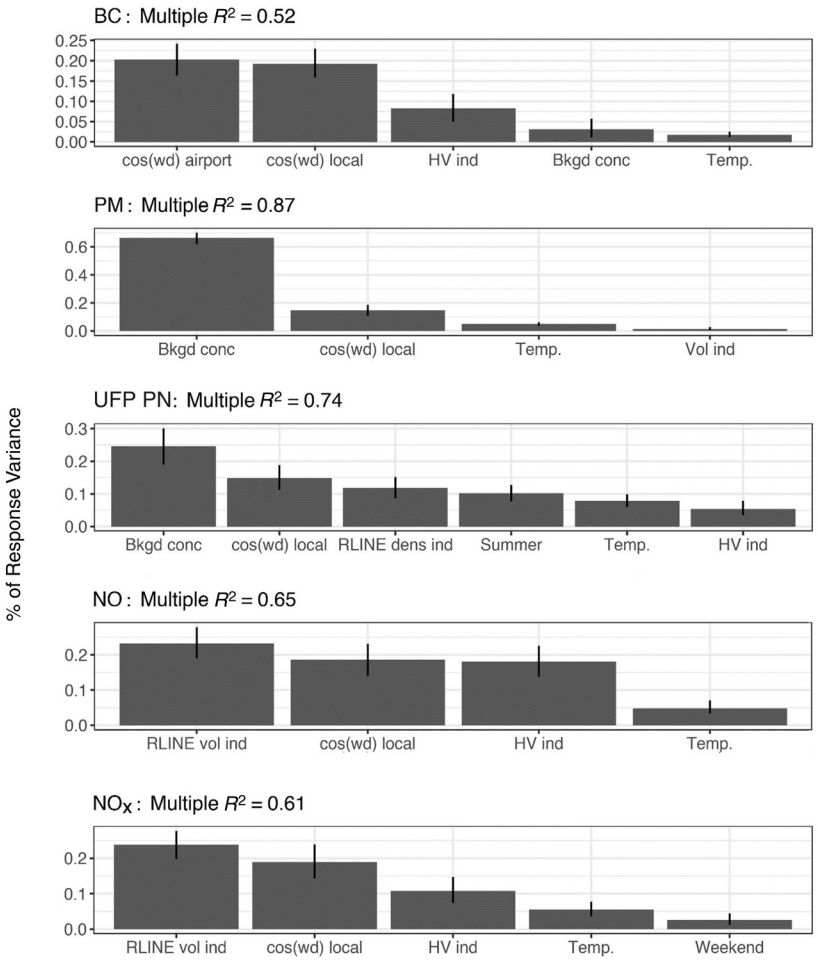

Figure 19. Relative importance of selected input variables in the freeway site statistical models by response variable, including BC, PM, UFP PN, NO, and NO_x concentrations. R^2 values are unadjusted and from the ordinary least squares (OLS) models. wd = wind direction.

explains only a fraction of the variance in observed pollutant concentrations. The importance of other variables, in terms of explaining variability in ambient concentration, was particularly pronounced for particulate species, including BC, PM, and UFPs. Of these, a newly developed HV index contributed to response variance for BC concentration, and a newly developed vehicle density index contributed to an interaction effect that partially explained variability for UFP PN concentration. The HV index also contributed to explanations of variability in NO and NO_x concentrations. A novel finding is that combinations of wind direction data from the local monitor collocated with the air quality monitors and from the more distant meteorological station both explained variability for BC concentration, while the local wind speed (but not the airport wind speed) helped explain variability for all five of the modeled pollutants. Thus, the bottom-line findings with regard to the utility of explanatory variables other than the R-LINE dispersion concentration are that local wind direction, measured near the road, is more important in explaining ambient concentration variability than wind direction measured some distance away, and vehicle-activity metrics directly related to actual real-time traffic are important. These results are specific to the case-study site.

Figure 20 illustrates that, although there is scatter in the comparisons, there is concordance between the values estimated by the model and the in-sample measurements for each of five pollutants, including BC, NO, NO_2, PM, and UFP PN concentrations. In-sample points represent the measurements on which the models were built. The multiple R^2 for the models compared with the in-sample data are given in Figure 19. The result for PM is linear and close to the ideal parity trend line with a slope of one. Of the various pollutants measured, the variability in observed PM near-road concentrations are determined much more by background concentration (as shown in Figure 19) than by factors related to emissions from the road of interest. The pollutants that have more scatter in model estimates compared with the in-sample measurements have a wider distribution of sources of variability among multiple explanatory variables, rather than a dominant contribution from just one variable.

The other comparisons shown in Figure 20 tend to exhibit some bias in the trends, but most notably there is correlation in each case. The BC results were expected to be the noisiest and least correlated because the instruments being compared were based on different detection methods.

There are 242 hours during which we did not collect NO_x or NO measurements at the near-road site. During those hours, we have measurements of all of the input variables. We used the estimated model coefficients in Table 6 to generate model estimates during those hours and compared them to the transformed collocated U.S. EPA NO_x measurements that were available for the same 242 hours. This comparison allows us to evaluate the ability of the model to predict measurements that are out of sample with respect to time and measurement device, since the U.S. EPA NO_x data are collected by a separate instrument. As noted earlier, this comparison was not done for BC because the NCSU and U.S. EPA instruments used different detection methods. The final model was used to estimate concentrations at those hours and was compared with the U.S. EPA measurements, which were not used in the fit of the model, as shown in Figure 20. The resultant models explained 68% of the variability in the

Table 6. Comparisons of Model Akaike Information Criterion (AIC) and Parameter Values for the Freeway Site[a]

	BC	NO	NO_x	$PM_{2.5}$	UFP PN
Number of observations	542	359	359	453	453
With R-LINE Variables					
AIC OLS model	396	491	412	−197	385
AIC ARMA model	31	366	310	−544	266
AR 1 parameter	1.26	0.64	0.60	1.58	1.03
AR 2 parameter	−0.29	—	—	−0.59	−0.08
MA 1 parameter	−0.67	—	—	−0.88	−0.72
Without R-LINE Variables					
AIC OLS model	396	515	474	−197	376
AIC ARMA model	31	377	332	−544	267
AR 1 parameter	1.26	0.64	0.60	1.58	1.03
AR 2 parameter	−0.29	—	—	−0.59	−0.08
MA 1 parameter	−0.67	—	—	−0.88	−0.72

[a] Lower AIC values indicate better models.

AR = autoregressive; MA = moving average; OLS = ordinary least squares.

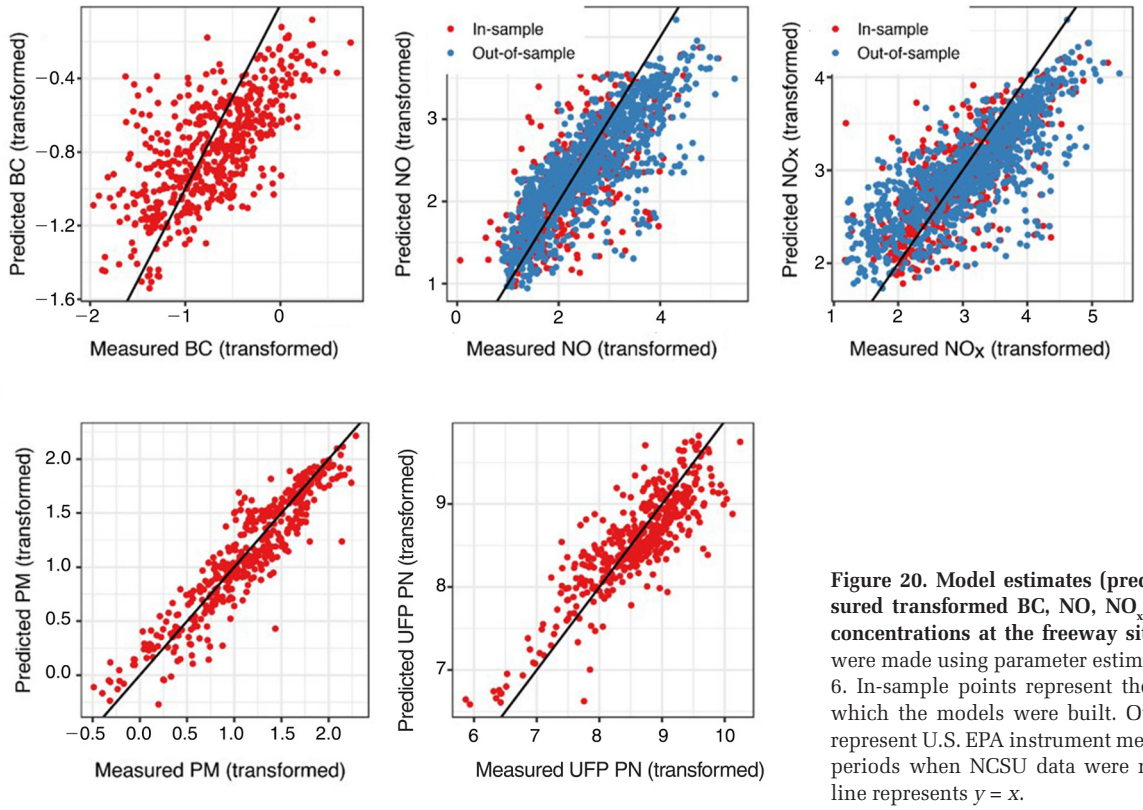

Figure 20. Model estimates (predicted) versus measured transformed BC, NO, NO_x, PM, and UFP PN concentrations at the freeway site. Model estimates were made using parameter estimates shown in Table 6. In-sample points represent the measurements on which the models were built. Out-of-sample points represent U.S. EPA instrument measurements for time periods when NCSU data were not available. Black line represents $y = x$.

U.S. EPA NO measurements and 62% of the variability in the NO_x measurements. The correlation of predictions with out-of-sample measurements increases confidence that the model can explain relative variations in ambient concentrations, even if there is some bias.

URBAN SITE

Results for the urban site include quantification of land-use characteristics, mesoscale traffic, microscale vehicle emissions, near-road air quality based on measurements and the R-LINE model, statistical model parameters, and statistical model performance. These results are specific to the site. Patterns in the data, such as relationships between ambient concentrations and meteorological conditions, are described in the context of these site-specific data.

Land Use

Comparison of the LIDAR data with our inspection of structures within 2,000 feet of the urban site identified five new buildings and six demolitions, which were used to amend the data. Figure 21 shows the amended LIDAR imagery. Additional Materials Table A.5 shows select summary statistics for the 5 m × 5 m grid cells within the urban site using the updated environmental information. There are multiple bus stops, streets, and arterials within the study area. The local area is characterized by rolling hills, with an overall elevation difference of 212 meters, but the standard deviation of the elevation among grid cells is only 5.7 meters. The variation in elevation within a few hundred feet of the intersection of interest is much less than the maximum variation represented by comparing the northern and southern extremes of the study area.

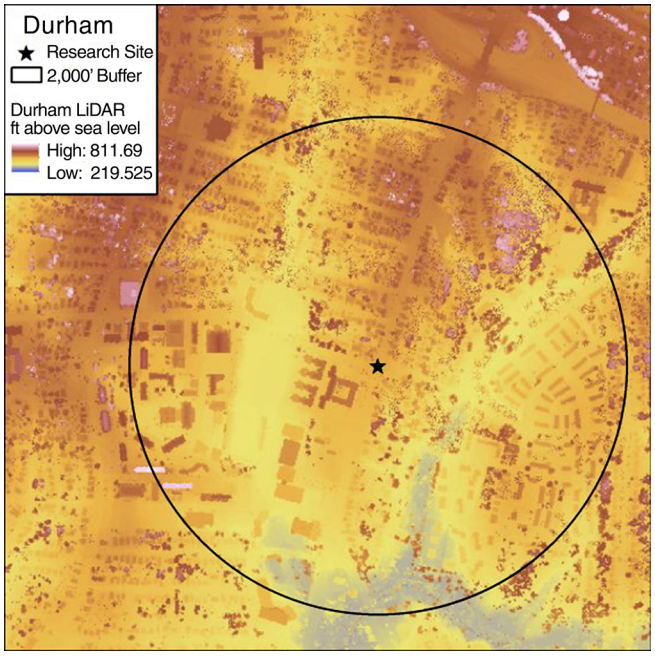

Figure 21. LIDAR measurements of elevation at the urban site located within 2,000 feet of the intersection of Alston Street and Lawson Street in Durham, NC, based on 5 m × 5 m grid cells.

Traffic

Traffic activity includes (a) diurnal traffic counts for each through movement at the intersection of Alston Avenue and Lawson Street; (b) vehicle-volume trends for road segments closest to, and time periods concurrent with, pedestrian transects with portable air monitoring devices; and (c) traffic indices associated with each fixed monitoring device quadrant. Observed total vehicle diurnal patterns at the intersection on an example sample date (25 May 2016) are shown in Figure 22. Video recording was performed during the daytime (06:00–20:00). This site has both morning and evening peaks, with northbound movement heaviest during the morning peak time. Alston Avenue and Lawson Street average about 34 and 12 HV flow rate per hour during daytime, respectively (not shown). Overall, Alston Avenue carries about five times the amount of traffic than does Lawson Street. The estimated weighted indices are given in Additional Material Tables C.3–C.5.

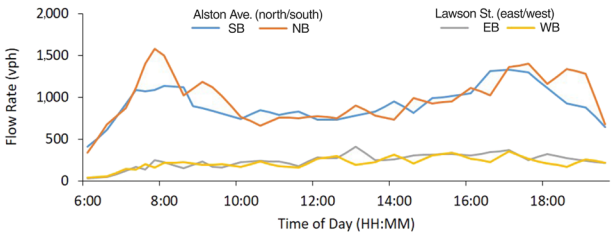

Figure 22. Directional vehicle flow rates at the intersection of Alston Avenue and Lawson Street on May 25, 2016 (Wednesday). EB = eastbound; NB = northbound; SB = southbound; WB = westbound; vph = vehicles per hour.

The flow rates on the west and south legs of the intersection closest to the pedestrian transects at the time periods during which transects were measured had similar patterns as the diurnal traffic trends (Additional Materials Table C.1). The northbound leg serviced more traffic during the morning peak and vice versa in the evening. This is because of the proximity to I-40, north of the intersection. Weekends, as expected near a campus environment, had lower traffic volumes than on weekdays (not shown).

Figure 23 shows the trend in the four traffic indices developed for the fixed-site sensors, based on weekdays of one summer week (May 23–27, 2016). Traffic counts were aggregated daily for traffic indices, to match the daily concentrations generated from the fixed monitors. Q3 and Q5 receptors are located in the same quadrant (southwestern corner of the intersection) with Q5 being closer to the road than Q3. Thus, Q5 had the same values for traffic-volume index and VSP-adjusted traffic-volume index as Q3. Further,

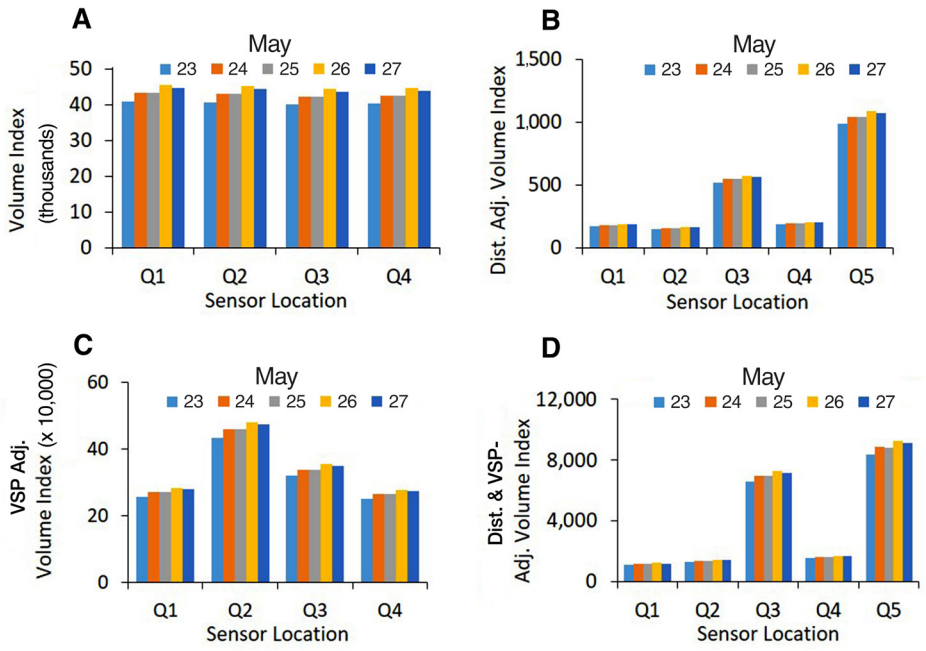

Figure 23. Traffic indices at urban site on May 23–27, 2016: A. volume index; **B.** distance-adjusted volume index; **C.** VSP-adjusted volume index; and **D**. distance- and VSP-adjusted volume index.

both Q3 and Q5 had higher values of the traffic indices than other receptors when adjusting for distance.

Emissions

Figure 24 shows segment average VSP and mass per distance NO_x emission rates for counter-clockwise movements at the Durham site. Results were also obtained for clockwise movements and through movements. Because this is an urban site, the speeds are much lower than at the I-40 site. Therefore, the range of VSP is much lower.

The highest segment average VSP at the Durham site was typically associated with acceleration after making a turn, as shown on Alston Avenue heading north from Cecil Street, and on Alston Avenue heading north from Lawson Street. There was also an engine power demand hot spot on Lawson Street associated with the signalized T-shaped intersection with Lincoln Street For example, in the eastbound direction on Lawson Street, there was often an acceleration after Lincoln Street that was associated with acceleration from the traffic light at this intersection. Although the speed and engine loads at the urban site were relatively low compared with the freeway site, there were some locations that had high segment average NO_x emission rates. Some of these high emission rates were associated with accelerations, such as after making a turn. Others may have been associated with transients in engine operation, as evident on Alston Avenue and on parts of Fayetteville Street south of Lawson Street. Aside from Alston Avenue, the roads at this site are relatively narrow. There can be dithering of the throttle to navigate through narrow lanes. There are some pedestrian crosswalks and other locations at which it may be necessary to let off the throttle before deciding to continue. Overall, the intersection of Lawson Street and Alston Avenue appears to be a NO_x emission hotspot, and NO_x emission rates were typically higher along Alston Avenue between Lawson Street and Cecil Street than for other parts of the site at which pedestrian portable monitoring transects

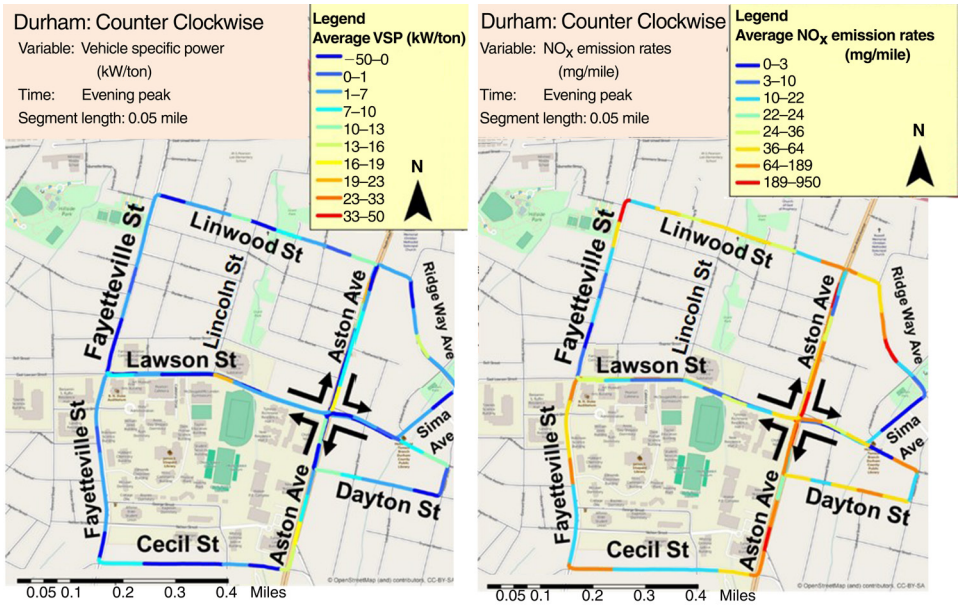

Figure 24. Spatial average VSP and NO_x emission rates (mg/mile) for 0.05 mile segments at the urban site for counter clockwise movement during evening peak. (Map images attributed to OpenStreetMap contributors under Open Database License with cartography licensed as CC BY-SA; *www.openstreetmap.org/copyright*.)

are made. There was also spatial variability in the emissions released along Lawson Street. For example, the NO_x emission rates along Lawson Street between Fayetteville and Alston Avenue were highest near the intersections with these streets, and are also elevated downstream, in either travel direction, with the signalized intersection at Lincoln Street.

In Additional Materials Appendix D, additional figures are given for measured tailpipe NO_x emission rates for all of the clockwise turning movements during the off-peak (Additional Materials Figure D.13) morning peak (Additional Materials Figure D.14), and evening peak periods (Additional Materials Figure D.15). Figures similar to Figure 24 are given for the tailpipe NO_x emission rates for the counter-clockwise turning movements during the off-peak (Additional Materials Figure D.16) and morning peak (Additional Materials Figure D.17) periods. Results are also shown in Additional Materials Figure F.18 for the measured tailpipe NO_x emission rates for the through movements in the evening peak period. The results shown in the appendix for the clockwise movements indicate that there were locations of relatively high NO_x emission rates associated with the following situations:

- Off-peak, clockwise movements: emission hotspots along westbound Lawson Street between Lincoln Street and Fayetteville Street, along the right turn movement from westbound Lawson to northbound Fayetteville, in the southbound direction on Alston north of Lawson and the north bound direction on Alston for vehicles entering from Dayton Street.
- Morning peak, clockwise movements: The emission hotspots were more concentrated at the intersection of Alston Avenue and Lawson Street for all four turning movements.
- Evening peak, clockwise movements: the pattern in this time of day was more similar to that of the off-peak than of the morning peak, with hotspots at the intersection of Alston Avenue and Lawson Street but also at Lawson Street and Fayetteville Street, Alston Avenue and Dayton Street, and Linwood Avenue and Alston Street. There were several segments with moderate to high emissions on Linwood Avenue associated with vehicles entering or exiting Linwood Avenue that interrupt flow for vehicles moving along Lawson Street.

The emission hotspots for these situations were associated with low-speed transients in vehicle operation because the speeds in this area are generally low (below 35 mph) on most of the measured roads.

The emission rates measured for counter-clockwise movements shown in Figure 24 (evening) and in Additional Materials Figures D.16 (off-peak) and D.17 (morning peak) indicate that hotspots can be, but are not always, associated with acceleration immediately after making a turn. For example, for both off-peak and morning peak, the highest emission rate was on Fayetteville Street southbound after a turn from Linwood Street heading westbound. However, after turning from Cecil Street eastbound onto Alston Avenue northbound, the highest emission rate did not occur until the vehicle had cleared the intersection but was still accelerating in the northbound direction. Thus, emissions in the northbound direction on Alston were elevated for about 0.2 miles north of Cecil Street.

Through movements at the intersection of Alston Avenue and Lawson Street typically had lower emission rates than turning movements, based on results for through movements given in Additional Materials Figure D.18. However, northbound through movements on Alston Avenue on approach to the intersection had elevated NO_x emission rates, and eastbound through movements on Lawson Street had elevated emissions after passing Alston Avenue. This is related to the influence of traffic that turns right from northbound Alston Avenue to eastbound Lawson Street that affects vehicles moving through the intersection.

Overall, the comparison of vehicle movements and times of day indicates that emission hotspots were influenced by turning movements as well as by conflicts with other traffic entering or exiting at locations along a measured movement. The location and intensity of hotspots varies with time day.

Air Quality

Measurement results for stationary sites and for pedestrian transects at the urban site are described. Additional details regarding measurement results are given in Additional Materials Appendix F.

Stationary Site Measurements The stationary site measurements were designed to characterize spatial variability in the vicinity of the intersection of interest. Measurements were repeated daily in multiple seasons. Daily average $PM_{2.5}$ levels measured using PEM units installed at four quadrant residential sites (Q1–Q4) and the corner of the intersection (Q5) were 24.5 $\mu g/m^3$ for winter (February 2016) and 25.4 $\mu g/m^3$ for summer (May 2016), as detailed in Additional Materials Tables F.1 and F.2. Meteorological conditions during the measurements are given in Additional Materials Figure F.1. A pilot sampling campaign was attempted in August 2015 but, largely because of human errors, the August 2015 data were set aside. These errors were subsequently avoided by involving senior staff in the field measurements. Furthermore, field blanks were used during the winter 2016 sampling period. More detail is given in Additional Materials Appendix F. The quality-assured values indicate that variation in seasonal average $PM_{2.5}$ concentration was low. These $PM_{2.5}$ seasonal average values were below the 24-hour average level of the NAAQS (35 $\mu g/m^3$). $PM_{2.5}$ measurements from the PEM units were compared with BAM measurements. The PEM units were also cross-checked by deploying them together at the BAM location and at one of the quadrant sampling sites. These validation comparisons took place during February 2016. The hourly $PM_{2.5}$ measurements from the BAM ranged between 8 $\mu g/m^3$ and 21 $\mu g/m^3$ on the

selected measurement day (February 13, 2016; Additional Materials Figure F.2), and averaged 13.5 µg/m³, whereas the 24-hour average $PM_{2.5}$ from the collocated PEM was very similar, at 14.2 µg/m³. Thus, the PEM measurement was consistent with the BAM measurement. The $PM_{2.5}$ measured concentrations from PEM units deployed at three of the quadrant sites (Q1, Q2, and Q3) on the same day ranged from 26 to 60 µg/m³ (Additional Materials Table F.2). Higher $PM_{2.5}$ concentrations at the quadrants compared with the BAM location was expected since the quadrant sites are closer to the intersection.

Day-of-week variation in ambient levels was larger than interseasonal differences (Additional Materials Table F.2). The average ambient $PM_{2.5}$ concentration for summer weekdays (i.e., 5-day average) was 29 µg/m³ compared with 21 µg/m³ for summer weekends (i.e., 2-day average). In the winter season, weekday (5-day average) and weekend concentrations averaged 24 µg/m³ and 26 µg/m³, respectively. Thus, there was more variability by day of week in the summer than in the winter. However, spatial variance among the four quadrants was more pronounced during the winter than the summer season. For example, the average daily $PM_{2.5}$ concentration in the winter ranged from 15 µg/m³ at Q2 to 35 µg/m³ at Q3, which represent the lowest and highest quadrant concentrations, respectively, whereas the $PM_{2.5}$ concentrations varied by less than 2 µg/m³ among the sites in the summer.

Results for the integrated 24-hour NO_2, NO_x O_3, and $PM_{2.5}$ measurements collected at the stationary sites Q1–Q5 are in Figure 25. The highest concentrations of NO_2 and NO_x were observed at Q5, which is located closest to the intersection. The next highest concentrations generally occurred at Q3, which was closer to the road than the other monitors. O_3 and $PM_{2.5}$ did not exhibit as pronounced spatial trends, although for O_3 the highest and lowest measurements were generally observed at Q4 (northwest) and Q3 (southwest), respectively. Details of daily average measurements are given in Additional Materials Table F.3.

In summer 2015, samples were collected on 12 days while in winter 2016, data were collected for 7 days. The average summer season concentrations were 17.3 ppb NO_x, 9.6 ppb NO_2, and 19.1 ppb O_3. The average winter season concentrations were 20.6 ppb NO_x, 11.7 ppb NO_2, and 18.3 ppb O_3 (Additional Materials Table F.3). The levels of NO_x and NO_2 were higher during the winter season while the O_3 levels were slightly higher during the summer season. Higher NO_x and NO_2 levels observed at the urban site in the winter are expected because of more stable atmospheric conditions typical of winter and lower mixing height compared with summer, whereas lower O_3 levels are expected in winter because of lower temperatures and lower actinic irradiance (Seinfeld and Pandis 1998). NO_2 ambient concentrations were higher during weekdays than weekends, in both winter and summer seasons (Additional Materials Table F.4), which is explainable based on higher vehicle counts on weekdays versus weekends. The difference in O_3 concentrations between weekdays and weekends was more pronounced in winter with higher concentrations observed on weekdays in both seasons. There were clear differences in NO_x and NO_2 concentrations at the

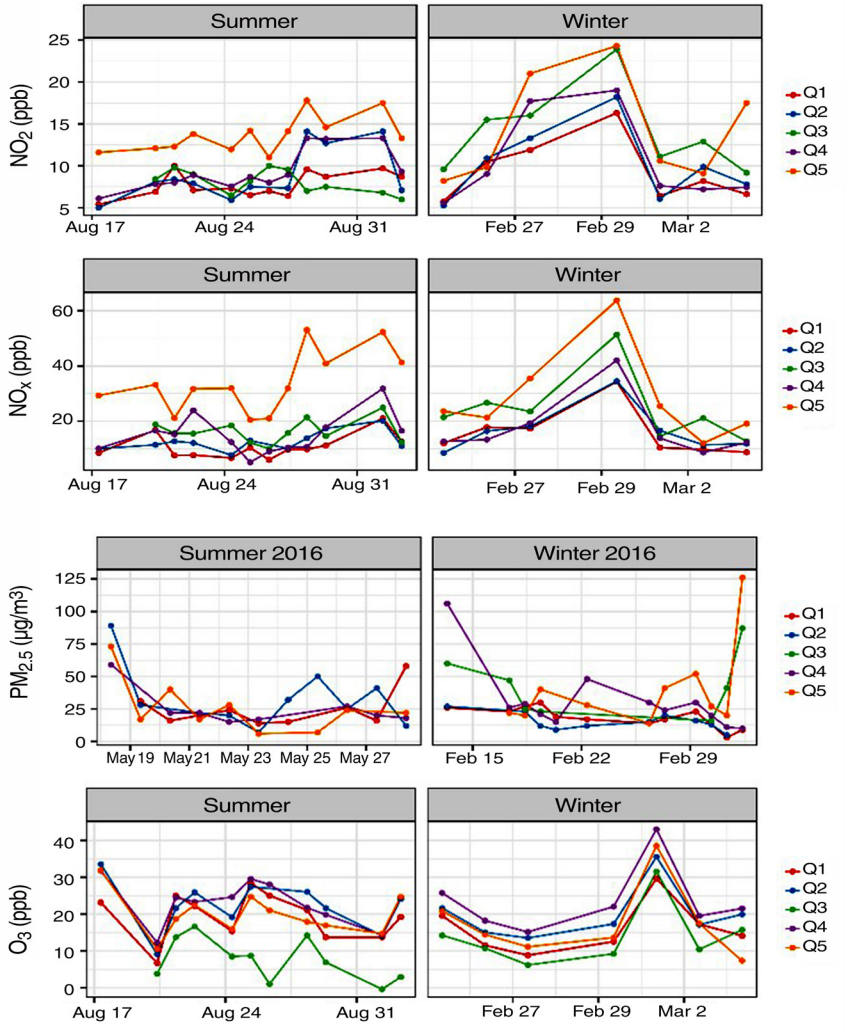

Figure 25. Urban site 24-hour integrated measurements of NO, NO_2, $PM_{2.5}$, and O_3 ambient concentrations at stationary quadrant sites Q1 through Q5 at the urban site.

Table 7. Regression Parameter Estimates from the Random Effects Models of Ambient Concentrations of NO_2, NO_x, O_3, and $PM_{2.5}$ for the Urban Site 24-hr Quadrant Measurements[a]

	NO_2	NO_x	O_3	$PM_{2.5}$
Intercept	2.24 (0.07)*	2.64 (0.09)*	16.13 (1.86)*	3.14 (0.13)*
Distance-adjusted traffic	0.17 (0.02)*	0.33 (0.03)*	−1.35 (0.62)*	0.03 (0.06)
Summer indicator	−0.4 (0.19)	−0.95 (0.23)*	−1.52 (4.49)	0.13 (0.21)
Wind speed	−0.07 (0.07)	−0.2 (0.09)*	2.27 (1.9)	−0.02 (0.14)
Rain	−0.82 (0.32)*	−1.07 (0.39)*	13.58 (7.66)	−0.01 (0.11)
Temperature	0.11 (0.15)	0.55 (0.18)*	7.01 (3.52)	−0.14 (0.2)
Relative humidity	0.22 (0.17)	0.33 (0.21)	−8.75 (4.05)	−0.14 (0.14)
Wind from east	0.07 (0.06)	0.13 (0.07)	0.9 (1.4)	0.25 (0.13)
Distance-adjusted traffic × summer	0.02 (0.02)	0.11 (0.03)*	−0.1 (0.61)	−0.16 (0.06)*

[a] Standard errors of coefficient estimated are in parentheses; * indicates *P* value less than 0.05.

quadrant sites Q2–Q5 with Q1, especially for Q3 and Q5 that were closest to the intersection and had higher concentrations (Figure 25). These differences imply heterogeneity, or spatial variability, in ambient concentrations among the quadrants. NO_x and NO_2 concentrations were inversely correlated with wind speed, as expected, but this effect was significant only for NO_x (Table 7). For O_3, Q3 had the lowest concentrations, which is indicative of O_3 titration by NO near the roadway (e.g., Song et al. 2013), whereas Q2 and Q4 had higher concentrations. These latter two sites are farther from the road and less likely to have been as influenced by NO titration. Limitations of the measurements from the Ogawa samplers include low temporal resolution (daily average) and lack of validation of the ambient measurements using a collocated independent measurement method.

Pedestrian Transect Measurements Student researchers who served as volunteer research assistants carried portable monitors along E. Lawson Street, Alston Avenue, and parts of the NCCU campus during rush hour. Portions of the transect along E. Lawson Street and Alston Avenue were selected because of their proximity to traffic- and vehicle-generated emissions. The portions of the transect in the NCCU campus were selected to obtain spatial variability in ambient concentration measurements as a result of being farther from the vehicle emission sources. $PM_{2.5}$ values measured using the DustTrak had seasonal variance as indicated by higher morning levels during winter (10 μg/m³) than summer (4 μg/m³) and higher evening levels during winter (7 μg/m³) than summer (5 μg/m³). The higher winter concentrations are likely related to lower dispersion because of greater atmospheric stability and lower mixing height. Average $PM_{2.5}$ concentrations were typically higher on weekdays than on weekends, except for winter mornings. As indicated in Figure 26, there was one winter weekend morning measurement, on Saturday, February 13, with a much higher average concentration than those of the other two measured weekend days (February 20 and 27) (33 μg/m³ vs. 1 μg/m³ to 5 μg/m³). The Friday evening on February 12 also had a relatively high $PM_{2.5}$ concentration (37 μg/m³) compared with other weekday evenings (13 μg/m³ or lower). Thus, it appears that there may have been either high regional emissions, stable atmospheric conditions, low mixing height, or combinations of these that were atypical in the evening of February 12 and morning of February 13. If these two large concentrations are omitted, then there is a consistent pattern of higher $PM_{2.5}$ concentration on weekdays than weekends for both times of day. The $PM_{2.5}$ concentration did not have a strong association with meteorological variables such as wind speed or wind direction. Rivas and colleagues (2017) report that problems with measurements of low $PM_{2.5}$ concentrations with DustTrak instruments can be prevented based on frequent zeroing of the instrument. They further note the occurrence of unexplained sudden artefact jumps in measured values. In the

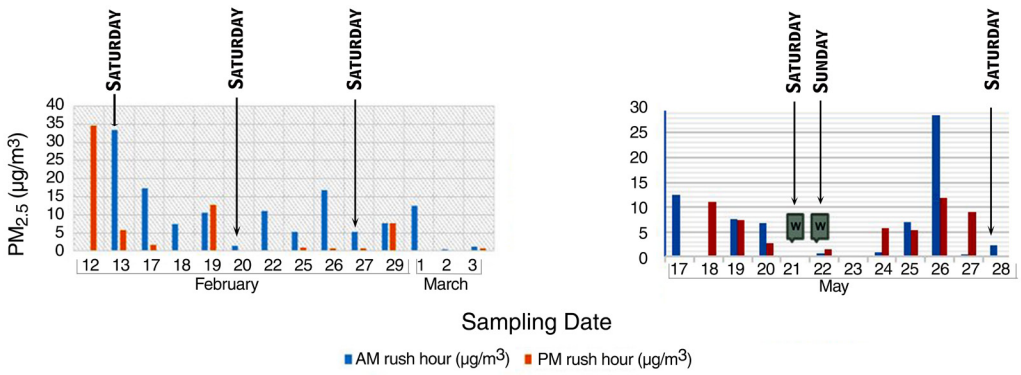

Figure 26. Average $PM_{2.5}$ concentration measured along the pedestrian transect during morning and evening rush hours in winter (February 2016) and summer (May 2016).

current study, zero calibration was done every day before the start of sampling, and we did not observe any unexplained artefacts in measured values.

UFP PN was measured during morning and evening rush hours for winter (February 2016) and summer (May 2016) using P-Trak condensation particle counters. Example time plots of such measurements are given in Additional Materials Figures F.3 and F.4 for winter and summer, respectively. Seasonal and diurnal variations were observed in UFP PN concentration (number of particles per m^3), as indicated in Figure 27. The average UFP PN in winter was almost twice that of summer (12,800/m^3 vs. 6,400/m^3). Diurnal variations in UFP PN were more prominent during winter than summer season. Higher counts were also observed during weekdays than weekends for both winter and summer seasons (14,000/m^3 vs. 8,000/m^3 for winter; 8,000/m^3 vs. 5,000/m^3 for summer). To support spatial statistical analysis of UFP PN data, grid cells were assigned to the pedestrian transect route at approximately 40-meter intervals. UFP PN concentration measurements were assigned to the nearest grid cell on the route, based on GPS coordinates, and averaged by grid cell and sampling run. A model calibration data set with 1,447 complete observations was created, with 300 observations chosen randomly for cross validation. The Durham Area Transit Authority operates both diesel and natural gas buses. Buses that run on diesel were observed a few times during rush-hour pedestrian transect sampling.

O_3 levels were measured for morning and evening rush hours using the POM. O_3 levels were higher in both winter and summer seasons for evening versus morning rush hours (winter weekdays: 34 ppb in the evening vs. 15 ppb in the morning; summer weekdays: 44 ppb in the evening vs. 13 ppb in the morning). O_3 concentrations are expected to be higher in the summer than in the winter because of warmer ambient temperatures and more flux of photons associated with stronger sunlight; concentrations are expected to be higher in the evening than in the morning because O_3 concentrations tend to peak in the mid to late evening associated with diurnal variations in temperature and solar irradiation coupled with lag times for O_3 formation (e.g., Seinfeld and Pandis 1998).

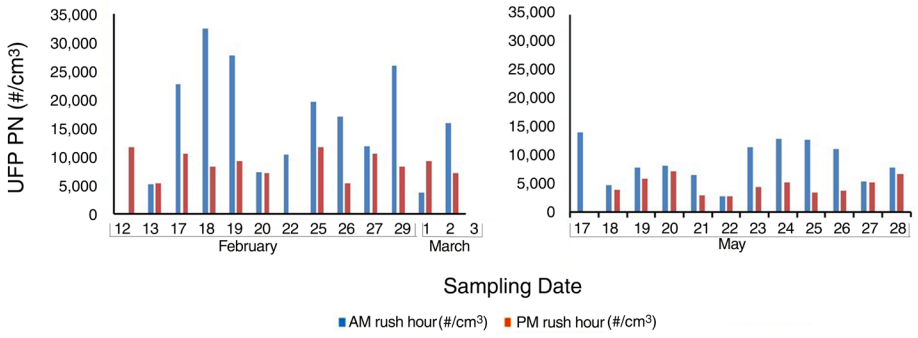

Figure 27. UFP PN measured along the pedestrian transect during morning and evening rush hours in winter and summer.

The spatial variability in measured concentrations of O_3, $PM_{2.5}$, and UFPs along the pedestrian transect is illustrated for summer (May 2016) in Figure 28. For O_3, the highest measured concentrations are farthest from a public road at the interior of the NCCU campus and tend to be lowest at locations are that are close to traffic (e.g., the intersection of Alston Avenue and Lawson Street, several locations along Alston, and several locations along Cecil Street on the southern edge of campus). O_3 levels tend to be suppressed at locations close to fresh emissions of NO_x. This trend is expected because NO reacts with O_3 to form NO_2 and O_2. Over time, concurrent with a distance traveled by the air mass, NO_2 photodissociates in the presence of sunlight to release an oxygen radical that reacts with molecular oxygen to form O_3 (Seinfeld and Pandis 1998). Thus, O_3 levels can be low very close to a roadway but increase with distance from the road.

The relative variation in $PM_{2.5}$ concentration over space is less pronounced than for O_3 or UFPs. The spatial pattern in $PM_{2.5}$ concentration is indicative of concentration hotspots along Alston Avenue and at the intersection of Alston Avenue and Cecil Street. However, the concentration at the intersection of Alston Avenue and Lawson Street does not appear to be very different than for most other locations along either road or for the interior of the NCCU campus.

Compared with $PM_{2.5}$, UFP concentrations had more spatial variability. This is expected since fresh primary PM emissions from passing vehicles are likely to be distributed toward small particle sizes (Frey 2018). Thus, UFPs were selected as a more relevant indicator of local vehicle emissions source strength than $PM_{2.5}$. UFP concentrations have more relative variability than $PM_{2.5}$ concentrations, particularly along Alston Avenue. The UFP concentrations at the intersection of Alston Avenue and Lawson Street tend to be higher than at the campus interior. The relatively high values at the intersection of Alston Avenue and Cecil Street may be partly influenced by cooking emissions from a nearby fast food restaurant.

Average $PM_{2.5}$ concentrations among the spatial grid cells had low (<0.5) positive correlations with UFP PN and low (> −0.5) negative correlations with O_3 concentration (data not shown). Thus, $PM_{2.5}$ concentrations were only weakly correlated with those of UFP PN and O_3. In contrast, UFP PN concentrations had high negative spatial correlation with O_3. This correlation pattern gives further support to an inference that both O_3 and UFP spatial distributions at this site are more sensitive to local emissions sources than is the $PM_{2.5}$ spatial distribution.

Overall, the patterns observed in the measured air quality data at the urban site for both the quadrant and pedestrian transects were con-

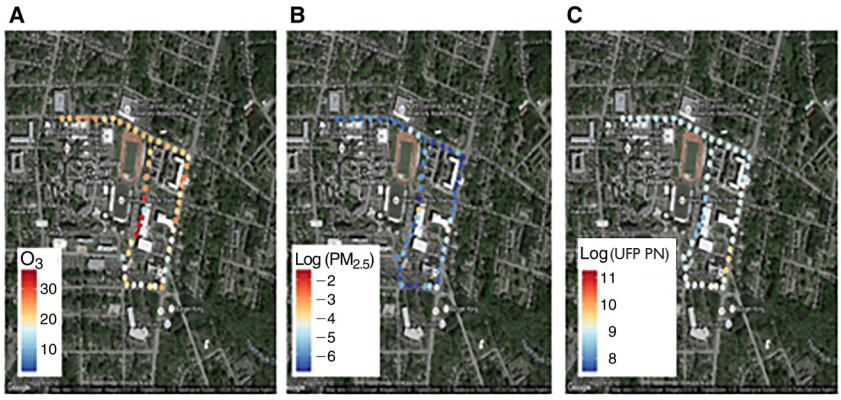

Figure 28. Spatial variation in ambient concentrations of $PM_{2.5}$, UFP PN, and O_3 during summer (May 2016) morning rush hours along the pedestrian transect at the urban site. A. O_3; **B.** $PM_{2.5}$ level (mg/m³) in log scale; and **C.** UFPs (particles/cm³) in log scale. The scale of 500 meters shown in B is the same for A and C.

sistent with expectations. This consistency builds confidence in, but does not prove, the validity of the measurements.

Dispersion Modeling

We used R-LINE to model all hours of the summer 2015 and winter 2015 pedestrian transect measurement periods. Results are illustrated in Figure 29 for CO, which is a tracer of vehicle emissions, for the summer 2015 period. The highest concentrations occur in the morning and evening rush periods when there were high traffic volumes. We also see that the midday and off-peak periods show similar concentration patterns, even though the traffic volumes were significantly different, with nearly six times the traffic volume in the midday as in the off-peak. The effect of vehicle emissions on estimated ambient concentrations is counteracted by the convective midday and stable off-peak atmospheric conditions. Spatially, we see higher estimated concentrations near the top right-hand corner of the walking path graph, which is closest to the intersection of interest. Because of vehicle movements through this intersection, including accelerations that take place at or near the intersection, we expected that the highest measured concentrations would occur in this area for each time period. The results for the winter case are qualitatively similar to those for the summer in terms of trends with respect to time of day and spatially. However, the winter concentrations tend to be higher than in summer related to more stable atmospheric conditions and lower mixing height. Additional details on dispersion modeling are given in Additional Materials Appendix G.

Statistical Models

Statistical models were developed for the urban site based on daily average measurements at the stationary quadrant sites and real-time measurements along the pedestrian transect. Additional statistical modeling results are given in Additional Materials Table H.4, for a spatial model for the pedestrian transect without R-LINE predictors.

Stationary Quadrant Sites Table 8 gives the estimated variance components for each of the pollutant models. The term σ^2 represents the estimated error variance, while σ_1^2 represents the estimated variance of the random effect of day. For NO_2 and NO_x the estimated error variance is approximately equal to the variance of the random effect of day, while it is greater for O_3 and $PM_{2.5}$.

As shown in Table 7, the distance-adjusted traffic-volume index was positively associated with NO_x and NO_2, and negatively associated with O_3 measurements, with a greater effect on NO_x in the summer season. None of the input variables, except the interaction between distance-adjusted traffic and summer, is significant with respect to variation in $PM_{2.5}$ concentration. In contrast to the freeway site, the effect of temperature on NO_x within

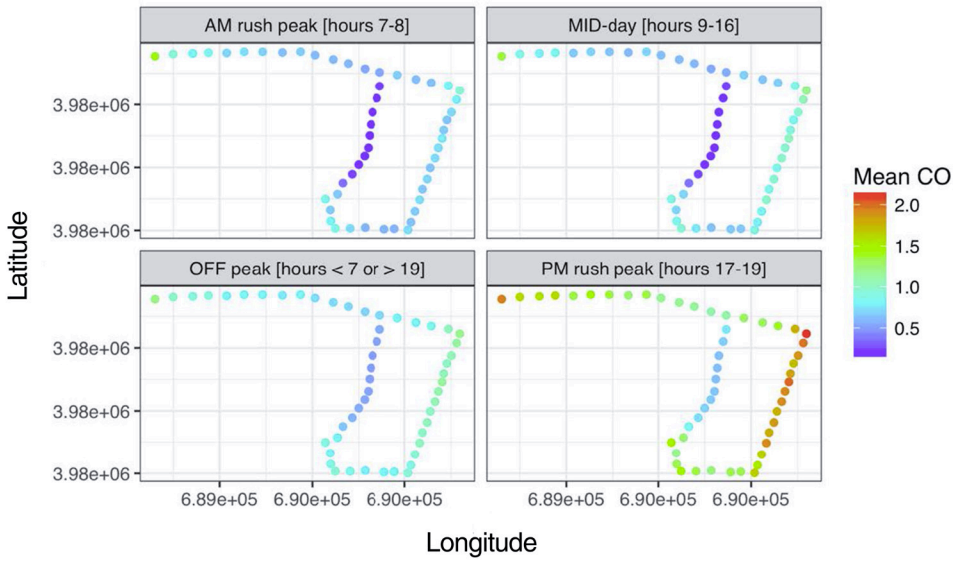

Figure 29. Mean R-LINE modeled grid cell average CO concentrations for summer 2015 by time period for the urban site.

Table 8. Estimated Variance Components for NO_2, NO_x, O_3, and $PM_{2.5}$ 24-Hour Average Ambient Concentrations Measured at Quadrants of the Urban Site

	NO_2	NO_x	O_3	$PM_{2.5}$
Number of observations	88	88	82	86
Variance components[a]				
σ_1^2	0.04	0.06	18.	0.11
σ^2	0.05	0.06	31.92	0.30

[a] σ_1^2 = estimated variance of the random effect of day; σ^2 represents the estimated error variance.

seasons is positive. Rain was negatively associated with NO_2 and NO_x concentrations. The maximum rainfall during the study was 0.84 inches in a day. The other days with positive rainfall were all less than 0.15 inches, so the magnitude of the effect indicated for rain may not be valid for larger amounts of rain. Relative humidity and indicator of wind from the east were not significant inputs for of any of the pollutants. The lack of significant association with wind direction and speed may be due to the variability in wind throughout the 24-hour sample.

The meaning of the statistical models of Table 7 is inferred, not just based on the statistical results, but also by taking into account the plausibility of the indicated relationship. For example, it is plausible that NO_2, NO_x, and $PM_{2.5}$ concentrations near the intersection are directly proportional to distance-adjusted traffic, the latter of which is a surrogate indicator of emissions source strength. Furthermore, it is plausible that O_3 concentrations near the intersection are inversely proportional to distance-adjusted traffic, because O_3 is titrated by locally emitted NO.

Pedestrian Transect We present results for three pollutants measured during both winter and summer sampling sessions: UFP PN (measured with a P-Trak), $PM_{2.5}$ (DustTrak) and O_3 (POM). In Figure 30, we mapped the transformed concentrations averaged over time and by grid cell. UFP PN concentrations were highest along Alston Avenue, which has high traffic volumes, and lowest along the path taken through the interior of the NCCU campus. The route passes by two bus stops along Alston Avenue and one on Lawson Street. O_3 was inversely correlated with UFP PN, with the highest values observed in the interior of the NCCU campus. $PM_{2.5}$ was elevated in some spots along Lawson Street and Alston Avenue, but the spatial distribution was not smooth.

ANOVA was used to test the importance of spatial versus temporal variation, with spatial variation represented by the grid cell id and temporal variation represented by both date and sampling period (morning vs. evening). The *F*-ratio is generally used to evaluate the significance of the output response to variation in the inputs. Furthermore, a larger *F*-ratio indicates that the variance between treatments is greater than the variance within a treatment. A treatment is a specific combination of factor levels. A factor is a potential explanatory variable. The results shown in Table 9 indicate that the sampling period, which has the largest *F*-ratio, is the largest

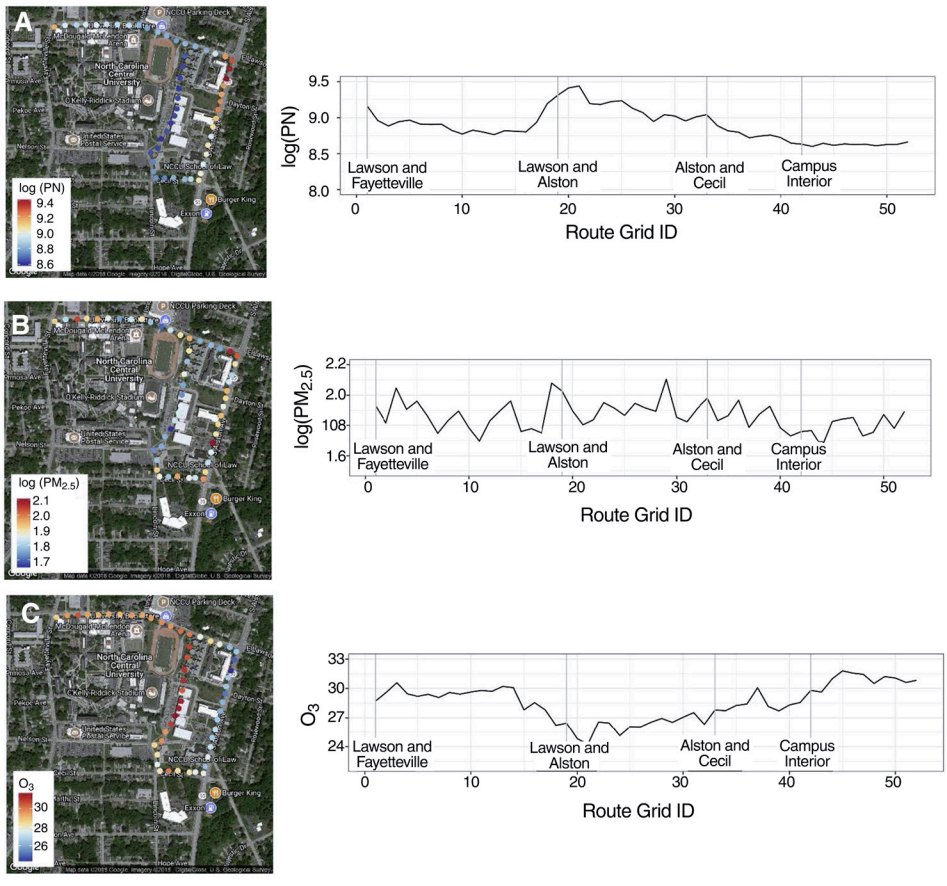

Figure 30. Mean transformed measured concentrations averaged over season, day, and period for the urban site, including maps and line plots of spatial variability. A. logarithm of total PN measured in #/cm^3, **B.** logarithm of $PM_{2.5}$ mass concentration measured in µg/m^3, and **C.** O_3 mixing ratio measured in ppb. The averaging time for each grid cell is approximately 1 minute.

Table 9. ANOVA Tests of Spatial Versus Temporal Variation for the UFP PN, $PM_{2.5}$, and O_3 Concentrations at the Urban Site Based on Pedestrian Transects (Walk-Along Route)[a]

	df	SSE	MSE	*F*-ratio[b]
UFP PN				
Period	1	130	130.0	438.9*
Day	23	575	25.0	84.4*
Grid point	51	109	2.1	7.2*
Residuals	2,172	643	0.3	
$PM_{2.5}$				
Period	1	46	46.5	66.7*
Day	21	1,823	86.8	124.5*
Grid point	51	14	0.3	0.4
Residuals	1,849	1,289	0.7	
O_3				
Period	1	270,635	270,635	5,419.2*
Day	23	121,982	5,303.5	106.2*
Grid point	51	6,380	125.1	2.5*
Residuals	1,930	96,385	49.9	

[a] Each measurement for one pedestrian transect, one time period, and one grid point represents approximately a one-minute average.

[b] * indicates *F*-ratio is significant.

df = degrees of freedom; SSE = sum of squared error; MSE = mean squared error.

source of variance in UFP PN and O_3 concentrations among the factors considered, followed by date (day) and grid cell. For $PM_{2.5}$, the date contributed more to variance in concentration than any other factor, followed in relative importance by sampling period. For UFP PN and O_3, the spatial location (grid point) along the transect was statistically significant, but with small *F*-ratios is indicated to contribute less to spatial variability in ambient concentrations than other factors. In Additional Materials Table H.4, an alternative version of Table 9 is given based on excluding grid-cell data below the detection limit. Both Tables 9 and Additional Materials Table H.4 are based on the same data completeness criteria for each run. The relative ranking of key sources of variance based on Additional Materials Table H.4 is the same as that in Table 9, although there are quantitative differences in numerical values. Thus, the key findings are robust to whether grid-cell concentrations below the detection limit for complete runs are included or excluded from the analysis.

The input variables selected using the cross-validation method described above, along with the percentage of response variance explained by each input variable calculated using the method of Lindeman and colleagues (1980), are shown in Figure 31. The morning indicator explained the greatest percentage of the variance in both UFP PN and O_3. Wind speed, measurements of traffic on Alston Avenue, and measured NO_x tailpipe emissions each explained at least 5% of the variance in UFP PN, while the variance in PM was best explained by wind speed and measurements of traffic on Alston.

The spatial models had substantially lower AIC values than the OLS regression models for all of the responses (Table 10). Inclusion of the R-LINE variables in the model very slightly improved the fit of the UFP PN and O_3 models (lower spatial AIC) but did not affect the $PM_{2.5}$ model. These findings were similar to those based on the exclusion of all grid-cell concentrations below the detection limit, as shown and discussed in Additional Materials Table H.5. Thus, the key qualitative findings are robust to treatment of values below the detection limit. The R^2 for the spatial models are similar for UFP PN and O_3 with or without values below the detection limit, but lower for $PM_{2.5}$ (0.22 with values below the detection limit included [Table 10] versus 0.30 with values below the detection limit excluded [Additional Materials Table H.5]). The number of observations below the detection limit for $PM_{2.5}$ is 297 out of the 1,849 indicated in Table 10. Assigning such data, one half of the detection limit leads to more uniformity in the spatial distribution of $PM_{2.5}$ concentrations among grid cells, which is consistent with the lower R^2.

Coefficient estimates with the R-LINE predictors are given in Table 11, and coefficient estimates without the R-LINE predictors are given in Additional Materials Table H.4. Among the pollutants, a larger share of variability in O_3 concentrations was explained by the model inputs (unadjusted $R^2 = 0.83$)

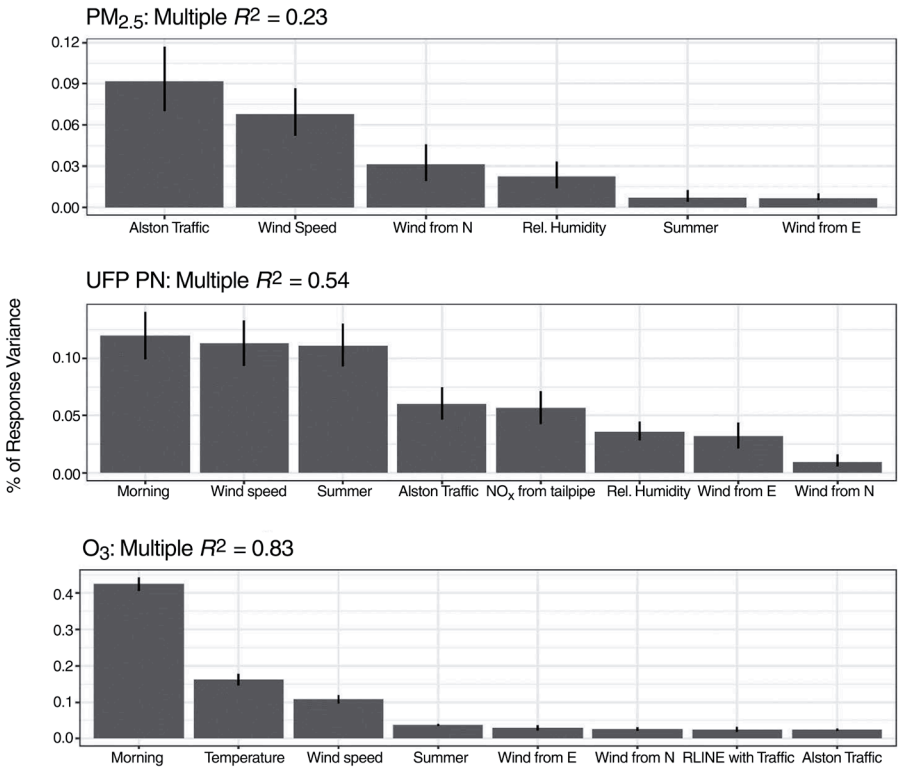

Figure 31. Percentage of response variance in measured concentrations of PM, UFP PN, and O_3 for the pedestrian transect (walk-along route) explained by each input and the unadjusted R^2 from the ordinary least squares (OLS) model.

compared with $PM_{2.5}$ concentrations, for which variability was relatively poorly explained by the model inputs (unadjusted R^2 = 0.22) (Table 10). This is also apparent in the estimated versus observed scatter plots (Figure 32). There is considerable scatter in each of these figures because each data point represents a very short averaging time of typically one minute or less for a given transect, day, and grid point. The poor fit of the $PM_{2.5}$ model is consistent with the previous finding that the variation in $PM_{2.5}$ concentrations at this site is driven more by temporal than spatial variability, likely due to temporal variation in regional sources. The estimated spatial range of O_3 and PM at this site was higher than that of UFP PN, indicating that spatial correlation in UFP PN decreases more quickly with distance. For UFP PN the variance of the spatially correlated component of the error (σ^2) was much larger than the variance of the uncorrelated component of the error (τ^2), while for PM the values were more similar indicating greater variability in measurements taken under the same conditions.

The estimated regression coefficients from the spatial model are given in Table 11. For PM, none of the spatially varying inputs — such as distance to the intersection, distance from the nearest street, proportion of tree cover, distance to bus stop, averaging building height, the tailpipe emissions from the vehicles on the nearest road segment, or average VSP on the nearest road segment — explained the variation in observed ambient concentration along the transect. As noted earlier, $PM_{2.5}$ concentrations tend to be more spatially homogenous than for UFP PN. Thus, it is not surprising that variations in $PM_{2.5}$ concentrations along the transect would not be explained by spatially varying inputs. However, $PM_{2.5}$ concentrations along the transect were related to the variation in traffic count on Alston Avenue, which is an indicator of general trends in traffic flow along the various roads that influence ambient concentration along the pedestrian transect. As expected, near-road $PM_{2.5}$ concentrations were inversely proportional to wind speed. $PM_{2.5}$ concentrations along the transect were mitigated by winds from the north that ventilate the site. Although the model results are suggestive of possible relationships between $PM_{2.5}$ concentration and relative humidity, wind from the east indicator, and summer indicator, the coefficients for these three inputs are not statistically significant.

The results for $PM_{2.5}$ given in Table 11 are similar to results obtained when grid-cell concentrations below the detection limit were excluded, as given in Additional Materials Table H.6 and discussed in detail in Additional Materials Appendix H. The two models agree in terms of the identification of significant inputs, which are the traffic count on Alston Avenue, the wind speed, and the indicator for wind from the north. The sign and magnitude of the coefficients for these inputs are similar between the two models. Thus, focusing on the inputs for which the coefficients are statistically significant, the two models are very similar, indicating that the model is robust to whether data below the detection limit are included or excluded.

Likewise, for UFP PN, the selection of input variables and the coefficient estimates are robust to whether grid-cell concentrations below detection limits for complete runs are included or excluded. Unlike PM, however, there is a spatially varying input, NO_x tailpipe emissions, that helps explain variability in ambient concentration. The regression parameter estimates are consistent with expectations that UFP PN is proportional to traffic count, higher in the morning (related to meteorology), inversely proportional to windspeed (because of increased dilution), and inversely related to relative humidity (because of increased agglomeration to larger particles).

Table 10. Comparisons of Model Fit for the Urban Pedestrian Transect Models, Including Data Below the Detection Limit, With and Without R-LINE Variates for Measured Concentrations of PM, UFP PN, and O_3[a]

	PM	UFP PN	O_3
Number of observations	1,849	2,160	1,923
With R-LINE Variables			
AIC OLS model	5,716	3,564	12,633
AIC spatial model	2,886	2,127	11,426
σ^2	1.06	0.27	31.96
τ^2	0.16	0.03	10.19
$1/\varphi$	2.23	0.17	0.792
R^2	0.22	0.53	0.830
Without R-LINE Variables			
AIC OLS model	5,716	3,620	1,2645
AIC spatial model	2,886	2,130	1,1420
σ^2	1.06	0.27	32.2
τ^2	0.16	0.03	10.51
$1/\varphi$	2.23	0.18	0.898
R^2	0.22	0.52	0.829

[a] Smaller AIC values indicate better fit.

σ^2 = variance of the spatially correlated component of the error; τ^2 = variance of the uncorrelated component of error; $1/\varphi$ = spatial range parameter; R^2 = coeffecient of determination.

Table 11. Regression Parameter Estimates from the Spatial (Pedestrian Walk-Along) Models for the Urban Site[a]

Input	$PM_{2.5}$ (SE)	UFP PN (SE)	O_3 (SE)
Intercept	1.19 (0.15)*	8.89 (0.1)*	26.69 (0.17)*
Distance to intersection	—	—	—
Distance from nearest street	—	—	—
Proportion tree cover	—	—	—
Distance to bus stop	—	—	—
Avg. height	—	—	—
CO tailpipe emissions	—	—	—
NO_x tailpipe emissions	—	0.12 (0.04)*	—
HC tailpipe emissions	—	—	—
Measured VSP	—	—	—
Traffic count Alston Ave.	0.66 (0.19)*	0.25 (0.1)*	−4.34 (0.2)*
Wind speed	−0.52 (0.17)*	−0.42 (0.08)*	5.73 (0.2)*
Temperature	—	—	7.5 (0.45)*
Relative humidity	0.27 (0.21)	−0.33 (0.15)*	—
Wind from the north	−0.43 (0.2)*	−0.08 (0.1)	3.31 (0.2)*
Wind from the east	−0.18 (0.17)	0.16 (0.12)	−0.98 (0.25)*
Morning indicator	—	0.42 (0.14)*	−9.7 (0.27)*
Summer indicator	−0.2 (0.17)	−0.26 (0.16)	−2.29 (0.4)*
R-LINE unit emissions	—	—	—
R-LINE traffic-weighted	—	—	−1.8 (0.29)*

[a] Input variables not selected by the variable selection procedure indicated with "—"; standard errors (SE) of coefficient estimated are in parentheses; * indicates *P* value less than 0.05.

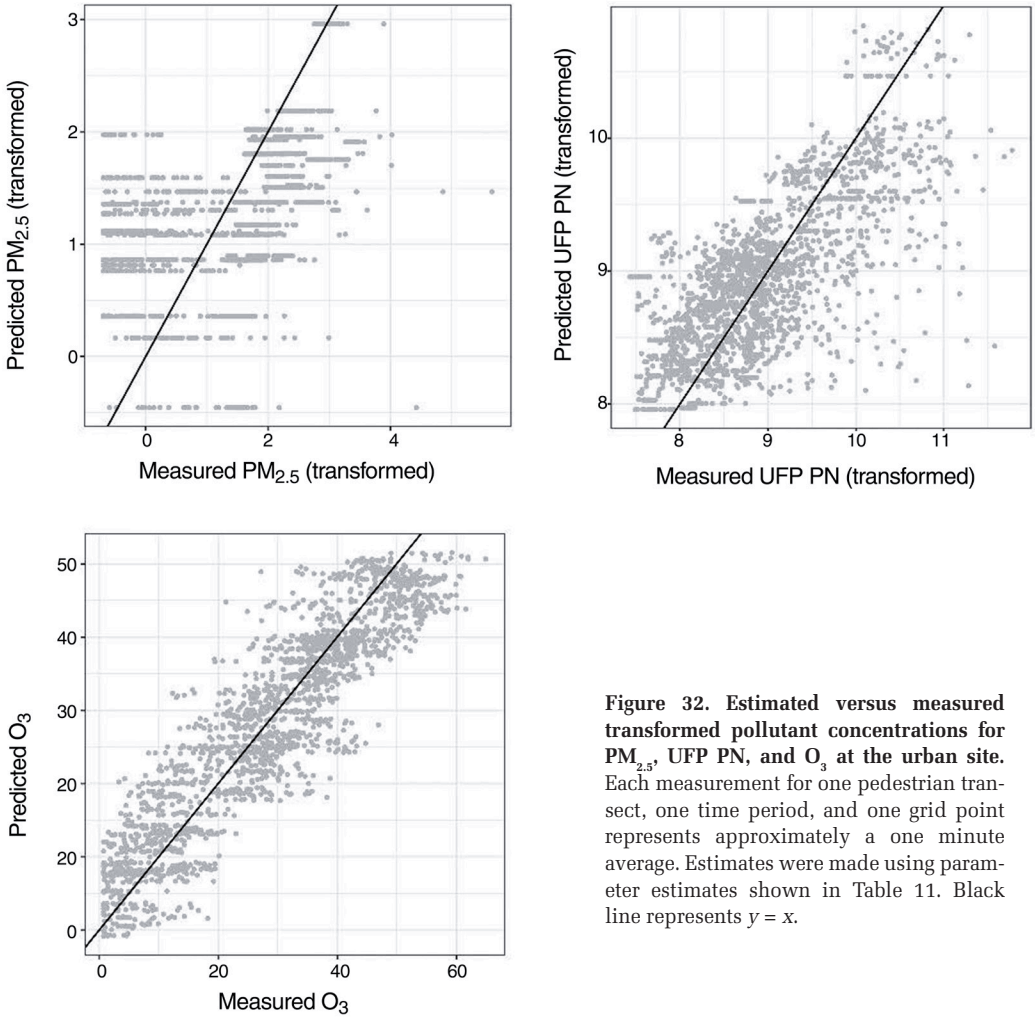

Figure 32. Estimated versus measured transformed pollutant concentrations for $PM_{2.5}$, UFP PN, and O_3 at the urban site. Each measurement for one pedestrian transect, one time period, and one grid point represents approximately a one minute average. Estimates were made using parameter estimates shown in Table 11. Black line represents $y = x$.

For O_3, the urban pedestrian transect model includes negative coefficients for traffic count on Alston Avenue and for the R-LINE traffic-weighted input. Both of these inputs are indicators of primary emissions source strength. The primary emissions that most affect O_3 concentrations near roadways are NO_x emissions. In particular, as described earlier, NO tends to oxidize to NO_2. Primary NO_2 emitted from the tailpipe, and secondary NO_2 formed from oxidation of NO, react with O_3 to convert it to O_2. Thus, these negative signs are expected. Higher ambient temperature typically causes higher O_3 concentrations (Seinfeld and Pandis 1998). Lower O_3 concentrations in the morning are expected, since O_3 generation typically reaches a peak in the evening. Lower O_3 concentrations in the summer are contrary to what is typically observed on an areawide basis in urban areas but is consistent with the effect of local vehicle emissions on titrating O_3 near roadways. Areawide O_3 concentrations tend to be higher in the summer than in other seasons; thus, a larger magnitude of reduction in O_3 concentration from titration by NO_x is possible in the summer. Likewise, the inferred trend of increasing wind speed leading to an increase in near-road O_3 concentration is reasonable. Higher wind speed more rapidly disperses primary tailpipe exhaust emissions, including NO_x, leading to a greater spatial scale over which O_3 titration occurs, such that titration may not happen as extensively at locations very close to the road. Given that UFP PN is expected to be highly influenced by primary vehicle emissions, and that O_3 near the road is inversely influenced by primary vehicle emissions, it is consistent that the signs for the indicators for wind from the north and from the east are opposite for O_3 compared with UFP PN. As discussed in detail in Additional Materials Appendix H, despite some numerical differences, the key qualitative findings for O_3 are similar whether grid-cell concentrations below detection limit are excluded or not.

Overall, the statistical modeling results for the urban site indicate that the dispersion variable contributes relatively little toward explaining variability in observed concentrations for multiple pollutants. In contrast, the spatial variability explained by the statistical models of the transects is more sensitive to variables related to real-time traffic metrics, meteorology, time of day, season, and real-world vehicle tailpipe emissions, depending on the pollutant.

DISCUSSION AND CONCLUSIONS

A relatively large set of potential explanatory variables were quantified based on site-specific data from an intensive study of two field sites. We found that a relatively small number of input variables were useful in explaining variability in ambient concentrations, with a focus on temporal variability at the freeway site and both temporal and spatial variability at the urban site. We also found that many of our candidate input variables did not help explain variability in ambient concentrations at our measured sites. This section is based on the literature review in the Introduction, literature cited

in the Methods and Results sections, and upon the results of this work.

KEY RESULTS AND IMPLICATIONS

For the freeway site, we found that relatively simple linear statistical models could be developed, with unadjusted R^2 ranging from 0.52 for BC to 0.87 for PM, that explain temporal variability in the hourly roadside concentration of five pollutants. These models were based on only four to six input variables. Ambient temperature and locally measured wind direction were selected for all models; however, wind direction typically explained more variance in ambient concentration than did temperature. For BC, UFPs, NO, and NO_2, the HV index significantly explained temporal variability; however, its relative importance compared with other explanatory variables differed by pollutant. Although HVs comprise a small fraction of the vehicle count at the measured site, they contribute a disproportionate share of NO_x and primary PM emissions. Since HVs are typically diesel, and diesel PM is primarily BC, it is not surprising that near-road BC concentrations are proportional to the HV index. NO and NO_2 are emitted from HVs. HVs with post-combustion controls, such as diesel particle filters, emit a smaller mass of particles than those without, but have substantial UFP emissions (Frey 2018). Thus, the fitted model is plausible in terms of the relationship between HV index and temporal variability in near-road ambient concentrations. The lack of selection of the HV index as an input variable for variability in total particle mass in the fine particle size range is not surprising. Diesel truck primary emissions are in the smaller end of the fine particle size range for which BC and UFP ambient concentrations are more sensitive. The dispersion variable computed using R-LINE explained 25% or less of the variability in observed ambient concentrations.

At the urban site, there were no inputs that explained variability in the observed 24-hour average concentrations of NO, NO_x, O_3, and $PM_{2.5}$ surrounding the intersection of interest. Thus, there was heterogeneity in the input variable selection for the best fitted statistical models. However, the distance-adjusted traffic-volume index was useful in explaining a portion of the variability in ambient concentrations for three of the four pollutants.

Spatial variability in the pedestrian transect grid-cell ambient concentrations, with a typical averaging time of about one minute, was related to traffic count on Alston Avenue and to wind speed for all three measured pollutants ($PM_{2.5}$, UFPs, O_3). Wind direction indicators explained some variability for PM and O_3 concentrations. Time-of-day indicators were explanatory for spatial variability in UFP PN and O_3 concentrations. Spatial variability in measured vehicle emissions contributed to variability in UFP concentrations. Spatial variability in O_3 concentration was related to spatial variability in R-LINE predictors. The latter is somewhat surprising because O_3 is a secondary pollutant. R-LINE does not account for the chemistry of secondary pollutant formation. However, O_3 concentrations near roadways are inversely related to near-road NO_2 concentrations, the latter of which are predicted to some extent by R-LINE. Generally, the estimated trends between input variables and observed concentrations were plausible and consistent with expectations.

Conversely, several input variables were not selected for the spatial variability in pedestrian transect concentrations, including the proportion of tree cover, the distance to the nearest bus stop, the average height of the local environment, distance to the intersection, spatial and time of day variation in measured CO and HC tailpipe emissions, and spatial and time of day variation in VSP for nearby road segments.

Thus, based on both the freeway and urban site statistical models, the findings indicate that relatively simple models based on a relatively small number of input variables were generally adequate to explain more than 50% of the temporal variability in ambient concentrations at both sites and the spatial variability at the urban site. The exception was PM at the urban site, for which only 23% of variance could be explained. However, as with any statistical model, the results are conditional on the site conditions, the study boundaries, and the range of variation in the input variables and the range of variation in the dependent variables. The results indicate that, even with intensive measurement of site-specific explanatory variables, it is challenging to fully explain variability in one-hour average measured concentrations. The unexplained variation in ambient concentration could be related to several factors, including random errors in measurements, stochastic spatial variability in meteorological conditions, and short (one-hour) averaging time. The first of these was addressed to the extent practicable based on study design, instrument selection, and the QA and QC of the measurements. R^2 is expected to increase as averaging time increases.

For example, the freeway site measurements focused on fixed site and transect measurements closest to a particular location on I-40 that was a sufficient distance from the nearest ramps, such that the emission source strength appears to be proportional to traffic volume. However, if multiple near-road measurement locations had been selected, with some near ramps, some near merge areas, and so on, it is more likely that spatial variability in emissions intensity related to transients in vehicle operations would have been found to explain spatial variability in ambient concentration. Similarly, had the urban site included a larger study area, with perhaps more spatial variability in pedestrian concentrations along larger stretches of roadway, coupled with more spatial variation in emissions source strength, the relationship between tailpipe emissions and ambient concentration might have been stronger. Furthermore, we did not sample any particularly strong emissions episodes or adverse meteorological conditions (e.g., very stable atmosphere) that could have led to higher concentrations and perhaps more temporal variability or differences in the pattern of spatial variability. Thus, one should be careful not to over-generalize that candidate input variables

not selected in the models developed here would not need to be considered as appropriate under other conditions.

A few other observations from this study are listed here. Some are not novel, but there is still value to confirming findings from prior studies based on a new set of sites that were not previously measured. These observations include the following:

- Near-road air quality was typically proportional to traffic flow, weighted by vehicle mix and proximity to the monitoring site, and influenced by wind speed, wind direction, and mixing height.
- Pollutant air quality concentrations decreased inversely with distance from the roadway. The observed gradients were influenced by mixing (dilution), season and time of day (which is related to variation in atmospheric stability and mixing height). Furthermore, the gradient was different for conservative (nonreactive) pollutants versus others, such as UFPs, for which transformations (e.g., evaporation, condensation, or coagulation) took place near the roadway. Furthermore, some PM near the roadway was from the formation of SOA.
- Partitioning of fresh particles, especially UFPs, varied with downwind distance (e.g., smaller particles evaporated as they travel downwind). Traffic emissions contributed large numbers of UFPs, superimposed on the areawide concentration of larger particles. The local contribution of vehicle emissions diluted with distance from the source.

Some detailed discussions are provided with regard to each of the major groups of input variables that were quantified.

LAND USE

At the I-40 site, there was not a statistically significant impact of variations in land use within the near-road air quality influence area. A priori, we chose a 2,000-foot (609-m) buffer around the monitoring site, but the results of air quality measurements imply that the impact of vehicle traffic on I-40 likely does not extend beyond 200 to 300 meters. Although there is variability in terrain elevation just south of I-40 because of a creek bed, and there are trees on either side of Triple Oak Drive on which transects perpendicular to I-40 in the downwind direction were measured, these did not appear to have a substantial impact on our results. For example, downwind concentrations reached background levels in many cases within 200 meters of I-40, indicating that TRAP emissions dispersed and, in some cases, transformed, to background levels well within the land use buffer. As other studies have noted, however, there can be variability in results between sites (e.g., Patton et al. 2014). For example, if we could have replicated this study at other locations along I-40, or at other freeway sites, we may have found more substantial influences from variability in the built and natural environments.

At the urban site, air quality concentrations at the interior of the NCCU campus were typically lower for $PM_{2.5}$ and UFPs, and higher for O_3, than on sidewalks near roadways. Daily average air quality NO_x and NO_2 concentrations at residential quadrants were typically lower, and O_3 levels were typically higher, than at roadside. Some of this spatial variation can be attributed to dilution and to O_3 titration. Some of it may be related to the effect of vegetation and housing in the quadrants.

MESOSCALE TRAFFIC

The distance-adjusted HV index, which includes only HV volume on the freeway, helps to explain variability in near-road concentrations at the freeway site. This is plausible because HVs are primarily diesel and thus tend to have higher emissions of oxides of nitrogen and primary particles than LDGVs (Frey 2018). Similarly, the distance-adjusted total volume by quadrant helped explain variability in concentrations at the urban site. The level of HVs at the urban site was low, which could explain why an HV index did not appear in the model for the urban site.

Real-time high-resolution traffic sensors can be used to develop metrics that explain temporal variability in near-road air quality. HV counts in each lane, weighted by the inverse of distance from each lane to the monitor, were found to help explain variability in near-road air quality at the freeway site. RTMS sensors, which are widely deployed along many freeways, enable length-based HV classification. Distance-weighted indices had a higher correlation with the difference between near site concentration and background concentration than did indices that are unweighted by distance.

Traffic counts for all vehicles and HVs at the freeway site were clearly diurnal and varied by lane. Vehicle mix varied by lane, with a higher proportion of HVs in the right lane in either travel direction, with a more even lane volume distribution during the peaks. The diurnal pattern (especially on weekdays) included morning and evening peak congestion, with evening peak congestion typically being the worse of the two.

Single loop detectors, such as those available at the urban site, are commonly used throughout the United States, but are not available on all roads. These detectors measure upstream traffic counts in a single lane and may not represent all movements through an intersection. The traffic count data from such detectors is accurate, but typically cannot be resolved by vehicle type or turning movement. Double loop detectors can provide additional data regarding vehicle classification and speed but are less common.

At the urban site, distance-adjusted traffic counts helped explain variability in daily average NO_2, NO, and O_3 concentration among the Q1 to Q5 locations. Although detailed traffic counts were quantified by each of 12 movements through the intersection at Alston Avenue and Lawson Street, the aggregated counts were more useful in discriminating between traffic flows on the intersection streets. Alston Ave-

nue carries, on average, five times more traffic than Lawson Street. Furthermore, the ratio of traffic counts on Alston downstream versus upstream of the intersection ranges within approximately 0.9 and 1.1 (Additional Materials Figure C.4), indicating that there is not much effect of turning movements on the vehicle flow at this intersection. Thus, in some cases, the use of traffic count for a predominately higher traffic road at an intersection might be a simplified surrogate for the data-intensive distance-adjusted traffic count.

Although the statistical models developed here were based on hourly average input data, traffic data can be quantified at a higher temporal resolution, if needed.

MICROSCALE VEHICLE EMISSIONS

Measurements at the freeway site demonstrate that vehicle emissions are not uniformly distributed along a link of roadway, even for the segment of I-40 between Airport Boulevard and I-540 at which the U.S. EPA/NC DEQ fixed-site monitor is located. Emissions vary with time of day, lane, proximity to ramps and, therefore, among specific locations on the roadway. Some of this variation can be explained by VSP. Tailpipe exhaust emission rates of CO, NO, and HC typically increase monotonically with increasing positive VSP, and these emissions are correlated with each other. Thus, either VSP or measured exhaust emissions of one or more of these pollutants, distributed over the road network, could be indicators of emission source strength. However, none of these were selected in the final freeway site model. There are possible reasons for this, such as (a) near-road air quality impacts are strongest when the wind is perpendicular to the roadway, which limits the effective segment length of roadway over which local emissions influence measured air quality; (b) air quality measurements were limited to one freeway site and thus did not capture as much variability in microscale vehicle operations and emissions as might be found based on comparisons of multiple sites.

In contrast to the freeway site, microscale vehicle emissions were found to be useful in explaining a small portion of variability in UFP concentration at the urban site. Thus, the urban site results illustrate that variability in microscale vehicle emissions over multiple segments of a road can be a source of spatial variability in near-road air quality.

AIR QUALITY MEASUREMENTS

Given the day-to-day variability observed at the freeway and urban sites, multiple days of measurements are needed to obtain stable estimates of mean concentrations that enable comparison between seasons, among locations, and among different times of day. A methodology for determination of minimum sample sizes is a need for further work.

At the freeway site, measurements for multiple pollutants, including NO_x, BC, UFP PN, and PM mass, indicate strong spatial gradients with exponential decay of NO_x, BC, and UFP PN concentrations with increasing distance from the roadway, and a lower relative rate of decay for PM. NO_x and BC are approximately conservative species in that they have little reactivity during the time and distance of transport from the roadway within the observed 200 meters. The spatial gradient in the concentration of these species is indicative of the roles of the mixing and dilution processes. The dynamics of UFP PN are more complex than can be explained simply based on decay alone. NO_x, BC, and UFP PN approached background concentrations within 200 meters of the freeway in the summer. For winter mornings, the concentrations of NO_x, BC, UFP PN, and PM were higher than background, indicating that under very stable atmospheric conditions the buffer downwind of a roadway influenced by traffic emissions can extend beyond 200 meters.

UFP PN concentrations were more variable with distance than PM mass concentrations. Although primary PM emissions are diluted, and some primary PM may evaporate, there is a counter-acting effect of the formation of secondary particles downwind of traffic, most likely related to SVOC emitted from vehicles. There is some possibility that the location of the transect downwind of the freeway may have affected particle dilution, since the transect was measured on a road surrounded on either side by trees. However, there was not much of a vegetation barrier between the freeway and along Triple Oaks Drive during periods when the wind was blowing perpendicular to the roadway, and the road itself cuts a path between the trees through which air can be transported.

Dilution alone (as indicated by BC decay) cannot explain the UFP concentration gradient versus downwind distance, especially at distances between 10 and 150 meters from the road. Most likely, SVOC components of UFPs evaporate during transport, the particle deposition rate is higher than for BC particles, or for combinations of these two factors. Our measurements also indicate that smaller particles evaporate more rapidly than do larger particles, which may be related in part to variations in specific organic species that comprise particles of different sizes. Evaporation as a loss process diminishes in effect within a few hundred meters of the road. UFP PN concentrations and emission factors were substantially higher in winter than summer, which indicates that a larger fraction of SVOC emissions partition to the particle phase with colder air.

At the urban site, air pollutant concentrations were variable from day to day, between seasons, and spatially, based on the fixed-site measurements. $PM_{2.5}$ and NO_x concentrations were highest near the intersection of interest, whereas O_3 concentrations were the lowest. The measured concentrations generally followed expected patterns with regard to day of week (weekday, weekend), season, and distance from the intersection.

For the urban transects, the UFP measurements had more spatial variability than the $PM_{2.5}$ measurements. O_3 levels

were low near the intersection and highest in the interior of the NCCU farthest from a roadway, which is indicative of the near-road O_3 titration effect based on interaction with vehicle-exhaust NO_x emissions. Thus, from an air quality perspective, there is a trade-off in the near-road environment between higher ambient concentrations for primary pollutants from vehicles and lower ambient concentration of O_3.

DISPERSION MODELING

Measured spatial-and-temporal distribution of pollutant concentrations were compared with modeled concentrations from R-LINE. The model was capable of capturing the general trends in diurnal cycle and downwind decay profile of different pollutants. However, the model tended to underestimate morning concentrations and overestimate evening concentrations. R-LINE also appears to be underestimating dispersion occurring during convective meteorological conditions in the late afternoon and may be oversuppressing dispersion during morning stable conditions. An area for possible future work is to conduct additional evaluations of R-LINE compared with measurement data and to develop bias correction factors. However, based on the results of the statistical analysis, the dispersion concentrations calculated based on the current incarnation of R-LINE were useful in explaining some of the observed variability in near-road air quality for several of the site-specific pollutant-specific models.

STATISTICAL MODELING

At the freeway site, input variables that took extra effort to measure or quantify, such as upwind background concentration at the freeway site and HV index at the freeway site, resulted in improved quantification of temporal variability in roadside ambient concentration. At the urban intersection site, distance-adjusted traffic was a useful input. For the spatial model of pedestrian transect concentrations at the urban site, variables that improved the model included (a) local traffic count on the major thoroughfare for $PM_{2.5}$, UFP PN, and O_3; and (b) NO_x tailpipe emissions for UFP PN. The latter is likely a surrogate either for primary (directly emitted) particle number emissions, emissions of particle precursors such as organic compounds, or both.

IMPLICATIONS OF FINDINGS

For freeway sites, data from existing state-of-practice sensors can be used to generate high resolution traffic indices that can help explain variability in near-road pollutant concentrations. Freeway RTMS sensors that are not properly calibrated can still produce accurate total vehicle counts but cannot be relied upon to generate accurate vehicle classification, especially when the sensor is not optimally positioned. This bias can be corrected. Urban sites generally have fewer usable traffic sensors, except for system detectors used to control traffic. These are typically single loop detectors that can provide vehicle count for an individual lane.

An implication of the high spatial and temporal resolution of near-road impacts of vehicle emissions is that there are likely to be additional sources of variability that were not measured in this study. For example, to assess the effect of land use — including built and natural environment — at higher resolution would require either a more intensive and extensive microscale measurement campaign, measurement of more sites, or combinations of both. For example, more intensive microscale measurements would be similar in nature to the transects conducted at both the freeway and urban sites, to assess spatial variation at higher resolution, and to do so for different seasons and times of day that would represent different conditions of atmospheric stability, mixing height, wind speed, and wind direction. Concurrent with air quality measurements, measurements should also be made of spatial and temporal variability in traffic activity, vehicle emissions source strength, and meteorology.

Further work is merited to assess the role of microscale emissions. For example, NCSU has collected data on tailpipe exhaust emissions measured with portable emissions measurement systems for over 200 LDGVs, each operated on a set of predetermined routes between the NCSU campus, north Raleigh, and Research Triangle Park. These routes entail 110 miles of round trip driving that includes a variety of road types and land uses. These unique data could be used to quantify microscale vehicle emissions, based on empirical measurement, over a large number of potential near-road monitoring sites. The empirical measurements could be used to identify locations with substantial spatial variability in emissions among road segments and, therefore, as the basis for targeting additional air quality measurement studies. Differences in land use patterns and mesoscale traffic could also be incorporated into development of a study design to assess the role of variability more thoroughly in land use, traffic, and emissions on near-road air quality.

Another avenue for future work is to evaluate the potential role of traffic and emissions simulation modeling as a predictor of near-road air quality. Traffic simulation models predict the movement of individual vehicles on a road network and can be used to estimate 1–10 Hz speed trajectories for individual vehicles. Although these models are subject to errors and have prediction uncertainties, the models are typically improving with time. Microscale emissions estimators have been developed and coupled with traffic simulation models to allow predictions of on-road emissions at high spatial and temporal resolution (e.g., Zhou et al. 2015).

Air quality measurement with reference method or research grade instrumentation can be expensive. There is growing interest in the role of so-called low-cost sensors as a means to be able to deploy more sensors to characterize spatial variability, and to be able to do so for long periods of time to better quantify temporal variability (e.g., Jiao et al.

2015). Given concerns about accuracy, interference, and other data quality limitations, it is unlikely that such sensors can completely replace reference methods. For example, available lower-cost PM sensors cannot detect UFPs, so will be of limited use in measurement of these critical species. However, a hybrid measurement approach in which high quality sensors are deployed strategically, supplemented by low-cost sensors for enhanced spatial coverage, could produce data from which a myriad of hypothesized factors that might affect near-road air quality could be tested.

We developed and tested regression models that included variables for land use, traffic, emissions, and meteorology and that explain most of the temporal variability in traffic-related near-road air pollutant concentrations at both sites and most of the spatial variability at the urban site. Except for PM at the urban site, we found that models with only four to six inputs could explain the majority of variability in ambient concentration representing temporal variability, spatial variability, or a combination of both. The variables that were the most useful in explaining variability in ambient concentrations at the two sites were site-specific indicators of traffic and meteorology.

ACKNOWLEDGMENTS

We thank Sue Kimbrough, Rich Baldauf and Richard Snow of the U.S. EPA Office of Research and Development, Research Triangle Park, NC, for help and support with establishing the roadside trailer facility for this study, for sharing NO_x, BC, CO, O_3, and meteorological data from the existing U.S. EPA/NC DEQ monitoring site, and for the loan of a NO_x analyzer for this study. We thank Steve Weiandt (Atlantic Investment Management) for providing access to and support for establishing the background site for this study. Six undergraduate and graduate students at NCCU, especially Ms. Corliss Johnson and Mr. Kshitij Kumar, assisted with field sampling throughout the project.

REFERENCES

Aggarwal S, Jain R, Marshall JD. 2011. Real-time prediction of size-resolved ultrafine particulate matter on freeways. Environ Sci Technol 46:2234–2241; doi:10.1021/es203290p.

Alam A, Ghafghazi G, Hatzopoulou M. 2014. Traffic emissions and air quality near roads in dense urban neighborhood: Using microscopic simulation for evaluating effects of vehicle fleet, travel demand, and road network changes. Transp Res Rec 2427:83–92; doi:10.3141/2427-09.

Ahangar FE, Heist D, Perry S, Venkatram A. 2017. Reduction of air pollution levels downwind of a road with an upwind noise barrier. Atmos Environ 155:1–10; doi:10.1016/j.atmosenv.2017.02.001.

Baldauf R, Thoma E, Hays M, Shores R, Kinsey J, Gullett B, et al. 2008a. Traffic and meteorological impacts on near-road air quality: Summary of methods and trends from the Raleigh Near-Road Study. J Air Waste Manag Assoc. 58:865–878; doi:10.3155/1047-3289.58.7.865.

Baldauf RW, Heist D, Isakov V, Perry S, Hagler GSW, Kimbrough S, et al. 2013. Air quality variability near a highway in a complex urban environment. Atmos Environ 64:169–178; doi/10.1016/j.atmosenv.2012.09.054.

Baldauf R, Thoma E, Khlystov A, Isakov V, Bowker G, Long T, et al. 2008b. Impacts of noise barriers on near-road air quality. Atmos Environ 42:7502–7507; doi:10.1016/j.atmosenv.2008.05.051.

Ban-Weiss GA, McLaughlin JP, Harley RA, Lunden MM, Kirchstetter TW, Kean AJ, et al. 2008. Long-term changes in emissions of nitrogen oxides and particulate matter from on-road gasoline and diesel vehicles. Atmos Environ 42:220–232; doi:10.1016/j.atmosenv.2007.09.049.

Barcelo MA, Varga D, Tobias A, Diaz J, Linares C, Saez M. 2016. Long term effects of traffic noise on mortality in the city of Barcelona 2004–2007. Environ Res 147:193–206.

Batterman S, Burke J, Isakov V, Lewis T, Mukherjee B, Robins T. 2014. A comparison of exposure metrics for traffic-related air pollutants: Application to epidemiology studies in Detroit, Michigan. Int J Environ Res Public Health Basel 11:9553–9577.

Batterman S, Cook R, Justin T. 2015a. Temporal variation of traffic on highways and the development of accurate temporal allocation factors for air pollution analyses. Atmos Environ 107:351–363; doi:10.1016/j.atmosenv.2015.02.047.

Batterman S, Ganguly R, Harbin P. 2015b. High resolution spatial and temporal mapping of traffic-related air pollutants. Int J Environ Res Public Health 12:3646–3666.

Batterman SA, Zhang K, Kononowech R. 2010. Prediction and analysis of near-road concentrations using a reduced-form emission/dispersion model. Environ Health 9:29. Available: *https://doi.org/10.1186/1476-069X-9-29*.

Beckerman B, Jerrett M, Brook JR, Verma DK, Arain MA, Finkelstein MM. 2008. Correlation of nitrogen dioxide with other traffic pollutants near a major expressway. Atmos Environ 42:275–290; doi:10.1016/j.atmosenv.2007.09.042.

Beckett KP, Freer-Smith PH, Taylor G. 1998. Urban woodlands: Their role in reducing the effects of particulate pollution. Environ Pollut 99:347–360; doi:10.1016/s0269-7491(98)00016-5.

Beckett KP, Freer-Smith PH, Taylor G. 2000. Particulate pollution capture by urban trees: Effect of species and windspeed. Glob Change Biol 6:995–1003; doi:10.1046/j.1365-2486.2000.00376.x.

Bergen S, Sheppard LA, Kaufman JD, Szpiro AA. 2016. Multipollutant measurement error in air pollution epidemiology studies arising from predicting exposures with penalized regression splines. Appl Statist 65:731–753.

Bishop GA, Stedman DH. 2008. A decade of on-road emissions measurements. Environ Sci Technol 42:1651–1656; doi:10.1021/es702413b.

Biswas S, Ntziachristos L, Moore KF, Sioutas C. 2007. Particle volatility in the vicinity of a freeway with heavy-duty diesel traffic. Atmos Environ 41:3479–3493; doi:10.1016/j.atmosenv.2006.11.059.

Bowker GE, Baldauf R, Isakov V, Khlystov A, Petersen W. 2007. The effects of roadside structures on the transport and dispersion of ultrafine particles from highways. Atmos Environ 41:8128–8139; doi:10.1016/j.atmosenv.2007.06.064.

BTS (Bureau of Transportation Statistics). 2017. Table 1-11: Number of U.S. Aircraft, Vehicles, Vessels, and Other Conveyances. Bureau of Transportation Statistics. United States Department of Transportation. Available: *https://www.rita.dot.gov/bts/sites/rita.dot.gov.bts/files/publications/national_transportation_statistics/html/table_01_11.html* [accessed 26 December 2017].

Buccolieri R, Gromke C, Di Sabatino S, Ruck B. 2009. Aerodynamic effects of trees on pollutant concentration in street canyons. Sci Total Environ 407:5247–5256; doi:10.1016/j.scitotenv.2009.06.016.

Buonanno G, Lall AA, Stabile L. 2009. Temporal size distribution and concentration of particles near a major highway. Atmos Environ 43:1100–1105; doi:10.1016/j.atmosenv.2008.11.011.

Burke JM, Zufall MJ, Özkaynak H. 2001. A population exposure model for particulate matter: Case study results for $PM_{2.5}$ in Philadelphia, PA. J Expos Anal Environ Epidemiol 11:470–89; doi:10.1038/sj.jea.7500188.

Chambers M, Schmitt R. 2015. Diesel-powered Passenger Cars and Light Trucks, Fact Sheet, Bureau of Transportation Statistics, U.S. Department of Transportation. Available: *www.bts.gov/sites/bts.dot.gov/files/legacy/Diesel FactSheet.pdf*.

Chang HH, Fuentes M, Frey HC. 2012. Time series analysis of personal exposure to ambient air pollution and mortality using an exposure simulator. J Expos Sci Environ Epidemiol 22:483–488; doi:10.1038/jes.2012.53.

Chang SY, Vizuete W, Valencia A, Naess B, Isakov V, Palma T, et al. 2015. A modeling framework for characterizing near-road air pollutant concentration at community scales. Sci Total Environ 538:905–921; doi:10.1016/j.scitotenv.2015.06.139.

Charron A, Harrison RM. 2003. Primary particle formation from vehicle emissions during exhaust dilution in the roadside atmosphere. Atmos Environ 37:4109–4119; doi:10.1016/s1352-2310(03)00510-7.

Choi H-W, Frey HC. 2009. Light duty gasoline vehicle emission factors at high transient and constant speeds for short road segments. Transp Res Part D: Transp Environ 14: 610–614. Available: *https://doi.org/10.1016/j.trd.2009.09.001*.

Choi W, Paulson SE. 2016. Closing the ultrafine particle number concentration budget at road-to-ambient scale: Implications for particle dynamics. Aerosol Sci Technol 50:448–461; doi:10.1080/02786826.2016.1155104.

Choi W, Ranasinghe D, Bunavage K, DeShazo JR, Wu L, Seguel R, et al. 2016. The effects of the built environment, traffic patterns, and micrometeorology on street level ultrafine particle concentrations at a block scale: Results from multiple urban sites. Sci Total Environ 553:474–485; doi:10.1016/j.scitotenv.2016.02.083

Choi W, Ranasinghe D, DeShazo JR, Kim JJ, Paulson SE. 2018. Where to locate transit stops: Cross-intersection profiles of ultrafine particles and implications for pedestrian exposure. Environ Pollut 233:235–245; doi:10.1016/j.envpol.2017.10.055.

Cimorelli AJ, Perry SG, Venkatram A, Weil JC, Paine RJ, Wilson RB, et al. 2005. AERMOD: A dispersion model for industrial source applications. Part I: General model formulation and boundary layer characterization. J Appl Meteorol Climatol 44:682–693.

Clements AL, Jia Y, Denbleyker A, McDonald-Buller E, Fraser MP, Allen DT, et al. 2009. Air pollutant concentrations near three Texas roadways, Part II: Chemical characterization and transformation of pollutants. Atmos Environ 43:4523–4534; doi:10.1016/j.atmosenv.2009.06.044.

Clifford S, Mazaheri M, Salimi F, Ezz WN, Yeganeh B, Low-Choy S, et al. 2018. Effects of exposure to ambient ultrafine particles on respiratory health and systemic inflammation in children. Environ Intern 114:167–180.

Coifman B. 2006. Vehicle level evaluation of loop detectors and the remote traffic microwave sensor. J Transport Engr 132:213–226.

Dallmann TR, Onasch TB, Kirchstetter TW, Worton DR, Fortner EC, Herndon SC, et al. 2014. Characterization of particulate matter emissions from on-road gasoline and diesel vehicles using a soot particle aerosol mass spectrometer. Atmos Chem Phys 14:7585–7599; doi:10.5194/acp-14-7585-2014.

de Nazelle A, Bode O, Orjuela JP. 2017. Comparison of air pollution exposures in active vs passive travel modes in European cities: A quantitative review. Environ Int 99:151–160; doi:10.1016/j.envint.2016.12.023.

Devlin RB, Smith CB, Schmitt MT, Rappold AG, Hinderliter A, Graff D, et al. 2014. Controlled exposure of humans with metabolic syndrome to concentrated ultrafine ambient particulate matter causes cardiovascular effects. Toxicol Sci 140:61–72; doi:10.1093/toxsci/kfu063.

Di Q, Koutrakis P, Schwartz J. 2016. A hybrid prediction model for $PM_{2.5}$ mass and components using a chemical transport model and land use regression. Atmos Environ 131:390–399; doi:10.1016/j.atmosenv.2016.02.002.

Dionisio KL, Baxter LK, Burke J, Özkaynak H. 2016. The importance of the exposure Metric in air pollution epidemiology studies: When does it matter, and why? Air Qual Atmos Health 9:495–502; doi:10.1007/s11869-015-0356-1.

Dons E, Int Panis L, Van Poppel M, Theunis J, Wets G. 2012. Personal exposure to black carbon in transport microenvironments. Atmos Environ 55:392–398; doi:10.1016/j.atmosenv.2012.03.020.

Du H, Yu F. 2006. Role of the binary H_2SO_4–H_2O homogeneous nucleation in the formation of volatile nanoparticles in the vehicular exhaust. Atmos Environ 40:7579–7588; doi:10.1016/j.atmosenv.2006.07.012.

Durant JL, Ash CA, Wood EC, Herndon SC, Jayne JT, Knighton WB, et al. 2010. Short-term variation in near-highway air pollutant gradients on a winter morning. Atmos Chem Phys 10:8341–8352; doi:10.5194/acp-10-8341-2010.

Enroth J, Saarikoski S, Niemi J, Kousa A, Ježek I, Močnik G, et al. 2016. Chemical and physical characterization of traffic particles in four different highway environments in the Helsinki metropolitan area. Atmos Chem Phys 16:5497–5512; doi:10.5194/acp-16-5497-2016.

Ewing R., Cervero R. 2010. Travel and the built environment: A meta-analysis. J Amer Plan Assoc 76:265–294.

FHWA Federal Highway Administration. 2016. Updated Interim Guidance on Mobile Source Air Toxic Analysis in NEPA Documents. Available: *https://www.fhwa.dot.gov/ENVIRonment/air_quality/air_toxics/policy_and_guidance/msat/2016msat.pdf* [accessed 26 December 2017].

Finn D, Clawson KL, Carter RG, Rich JD, Eckman RM, Perry SG, et al. 2010. Tracer studies to characterize the effects of roadside noise barriers on near-road pollutant dispersion under varying atmospheric stability conditions. Atmos Environ 44:204–214; doi:10.1016/j.atmosenv.2009.10.012.

Franklin M, Vora H, Avol E, McConnell R, Lurmann F, Liu F, et al. 2012. Predictors of intra-community variation in air quality. J Expo Sci Environ Epidemiol 22:35–147.

Frey HC. 2018. Trends in onroad transportation energy and emissions. J Air Waste Manage Assoc 68:514–563; doi:10.1080/10962247.2018.1454357.

Frey HC, Unal A, Rouphail NM, Colyar JD. 2003. On-road measurement of vehicle tailpipe emissions using a portable instrument. J Air Waste Manage Asso 53:992–1002.

Frey HC, Zhang K, Rouphail NM. 2008. Fuel use and emissions comparisons for alternative routes, time of day, road grade, and vehicles based on in-use measurements. Environ Sci Technol 42:2483–2489. Available: *https://doi.org/10.1021/es702493v*.

Frey HC, Zhang K, Rouphail NM. 2010. Vehicle-specific emissions modeling based upon on-road measurements. Environ Sci Technol 44:3594–3600; doi:10.1021/es902835h.

Friberg MD, Zhai X, Holmes HA, Chang HH, Strickland MJ, Sarnat SE, et al. 2016. Method for fusing observational data and chemical transport model simulations to estimate spatiotemporally resolved ambient air pollution. Environ Sci Technol 50:3695–3705; doi:10.1021/acs.est.5b05134.

Gamba P, Houshmand B. 2000. Digital surface models and building extraction: A comparison of IFSAR and LIDAR data. Geosci Remote Sens 38:1959–1968.

Gentner DR, Jathar SH, Gordon TD, Bahreini R, Day DA, El Haddad I, et al. 2017. Review of urban secondary organic aerosol formation from gasoline and diesel motor vehicle emissions. Environ Sci Technol 51:1074–1093; doi:10.1021/acs.est.6b04509.

Ghasemian M, Amini S, Princevac M. 2017. The influence of roadside solid and vegetation barriers on near-road air quality. Atmos Environ 170:108–117; doi:10.1016/j.atmosenv.2017.09.028.

Ginzburg H, Liu X, Baker M, Shreeve R, Jayanty RKM, Campbell D, et al. 2015. Monitoring study of the near-road $PM_{2.5}$ concentrations in Maryland. J Air Waste Manag Assoc 65:1062–1071; doi:10.1080/10962247.2015.1056887.

Gordon M, Staebler RM, Liggio J, Li S-M, Wentzell J, Lu G, et al. 2012. Measured and modeled variation in pollutant concentration near roadways. Atmos Environ 57:138–145; doi:10.1016/j.atmosenv.2012.04.022.

Grana M, Toschi N, Vicentini L, Pietroiusti A, Magrini A. 2017. Exposure to ultrafine particles in different transport modes in the city of Rome. Environ Pollut 228:201–210; doi:10.1016/j.envpol.2017.05.032

Grieshop AP, Lipsky EM, Pekney NJ, Takahama S, Robinson AL. 2006. Fine particle emission factors from vehicles in a highway tunnel: Effects of fleet composition and season. Atmos Environ 40, Supplement 2:287–298; doi:10.1016/j.atmosenv.2006.03.064.

Hagler GSW, Lin MY, Khlystov A, Baldauf RW, Isakov V, Faircloth J, et al. 2012. Field investigation of roadside vegetative and structural barrier impact on near-road ultrafine particle concentrations under a variety of wind conditions. Sci Total Environ 419:7–15; doi:10.1016/j.scitotenv.2011.12.002.

Hagler GSW, Thoma ED, Baldauf RW. 2010. High-resolution mobile monitoring of carbon monoxide and ultrafine particle concentrations in a near-road environment. J Air Waste Manag Assoc 60:328–336; doi:10.3155/1047-3289.60.3.328.

Hanigan IC, Williamson GJ, Knibbs LD, Horsley J, Rolfe MI, Cope M, et al. 2017. Blending multiple nitrogen dioxide data sources for neighborhood estimates of long-term exposure for health research. Environ Sci Technol 51:12473–12480; doi:10.1021/acs.est.7b03035.

Heist D, Isakov V, Perry S, Snyder M, Venkatram A, Hood C, et al. 2013. Estimating near-road pollutant dispersion: A model inter-comparison. Transp Res Part D: Transp Environ 25:93–105; doi:10.1016/j.trd.2013.09.003.

Heist DK, Perry SG, Brixey LA. 2009. A wind tunnel study of the effect of roadway configurations on the dispersion of traffic-related pollution. Atmos Environ 43:5101–5111; doi:10.1016/j.atmosenv.2009.06.034.

Henderson SB, Beckerman B, Jerrett M, Brauer M. 2007. Application of land use regression to estimate long-term concentrations of traffic-related nitrogen oxides and fine particulate matter. 41:2422–2428; doi:10.1021/es0606780.

Hudda N, Fruin S, Delfino RJ, Sioutas C. 2013. Efficient determination of vehicle emission factors by fuel use category using on-road measurements: Downward trends on Los Angeles freight corridor I-710. Atmos Chem Phys 13:347–357; doi:10.5194/acp-13-347-2013.

Huffman JA, Ziemann PJ, Jayne JT, Worsnop DR, Jimenez JL. 2008. Development and characterization of a fast-stepping/scanning thermodenuder for chemically resolved aerosol volatility measurements. Aerosol Sci Technol 42:395–407; doi:10.1080/02786820802104981.

Isakov V, Arunachalam S, Batterman S, Bereznicki S, Burke J, Dionisio K, et al. 2014. Air quality modeling in support of the Near-Road Exposures and Effects of Urban Air Pollutants Study (NEXUS). Int J Environ Res Public Health 11:8777–8793.

James G, Witten D, Hastie T, Tibshirani R. 2013. An Introduction to Statistical Learning. Vol 112. New York: Springer.

Jamriska M, Morawska L, Mergersen K. 2008. The effect of temperature and humidity on size segregated traffic exhaust particle emissions. Atmos Environ 42:2369–2382; doi:10.1016/j.atmosenv.2007.12.038.

Jandarov RA, Sheppard LA, Sampson PD, Szpiro AA. 2017. A novel principal component analysis for spatially misaligned multivariate air pollution data. Appl Stat 66:3–28.

Jeong C-H, Evans GJ, Healy RM, Jadidian P, Wentzell J, Liggio J, et al. 2015. Rapid physical and chemical transformation of traffic-related atmospheric particles near a highway. Atmos Pollut Res 6:662–672; doi:10.5094/APR.2015.075.

Jiao W, Hagler GSW, Williams RW, Sharpe RN, Weinstock L, Rice J. 2015. Field assessment of the Village Green Project: An autonomous community air quality monitoring system. Environ Sci Technol 49:6085–6092; doi:10.1021/acs.est.5b01245.

Karner AA, Eisinger DS, Niemeier DA. 2010. Near-roadway air quality: Synthesizing the findings from real-world data. Environ Sci Technol 44:5334–5344; doi:10.1021/es100008x.

Karottki DG, Bekö G, Clausen G, Madsen AM, Andersen ZJ, Massling A, et al. 2014. Cardiovascular and lung function in relation to outdoor and indoor exposure to fine and ultrafine particulate matter in middle-aged subjects. Environ Int 73:372–381; doi:10.1016/j.envint.2014.08.019.

Kastner-Klein P, Plate EJ. 1999. Wind-tunnel study of concentration fields in street canyons. Atmos Environ 33:3973–3979; doi:10.1016/s1352-2310(99)00139-9.

Kendrick CM, Koonce P, George LA. 2015. Diurnal and seasonal variations of NO, NO_2 and $PM_{2.5}$ mass as a function of traffic volumes alongside an urban arterial. Atmos Environ 122:133–141; doi:10.1016/j.atmosenv.2015.09.019.

Khan T, Frey HC, Rastogi N, Wei T. 2020. Geospatial variation of real-world tailpipe emission rates for light-duty gasoline vehicles. Environ Sci 54:8968–8979; doi:10.1021/acs.est.0c00489.

Kimbrough S, Baldauf RW, Hagler GSW, Shores RC, Mitchell W, Whitaker DA, et al. 2013. Long-term continuous measurement of near-road air pollution in Las Vegas: Seasonal variability in traffic emissions impact on local air quality. Air Qual Atmos Health 6:295–305; doi:10.1007/s11869-012-0171-x.

Kozawa KH, Winer AM, Fruin SA. 2012. Ultrafine particle size distributions near freeways: Effects of differing wind directions on exposure. Atmos Environ 63:250–260.

Kuhn T, Biswas S, Fine PM, Geller M, Sioutas C. 2005. Physical and chemical characteristics and volatility of PM in the proximity of a light-duty vehicle freeway. Aerosol Sci Tech 39:347–357.

Kumar P, Ketzel M, Vardoulakis S, Pirjola L, Britter R. 2011. Dynamics and dispersion modelling of nanoparticles from road traffic in the urban atmospheric environment — A review. J Aerosol Sci 42:580–603; doi:10.1016/j.jaerosci.2011.06.001.

Kumar P, Morawska L, Birmili W, Paasonen P, Hu M, Kulmala M, et al. 2014. Ultrafine particles in cities. Environ Int 66:1–10; doi:10.1016/j.envint.2014.01.013.

Kweon B-S, Mohai P, Lee S, Sametshaw AM. 2018. Proximity of public schools to major highways and industrial facilities, and students' school performance and health hazards. Environ Planning B: Urban Anal City Sci 45:312–329; doi:10.1177/0265813516673060.

Lambe AT, Logue JM, Kreisberg NM, Hering SV, Worton DR, Goldstein AH, et al. 2009. Apportioning black carbon to sources using highly time-resolved ambient measurements of organic molecular markers in Pittsburgh. Atmos Environ 43:3941–3950; doi:10.1016/j.atmosenv.2009.04.057.

Landkocz Y, Ledoux F, André V, Cazier F, Genevray P, Dewaele D, et al. 2017. Fine and ultrafine atmospheric particulate matter at a multi-influenced urban site: Physicochemical characterization, mutagenicity and cytotoxicity. Environ Pollut 221:130–140; doi:10.1016/j.envpol.2016.11.054.

Lanzinger S, Schneider A, Breitner S, Stafoggia M, Erzen I, Dostal M, et al. 2016. Associations between ultrafine and fine particles and mortality in five central European cities — Results from the UFIREG study. Environ In 88:44–52; doi:10.1016/j.envint.2015.12.006.

Lee D, Sarran C. 2015. Controlling for unmeasured confounding and spatial misalignment in long-term air pollution and health studies. Environmetrics 26:477–487.

Lin MY, Khlystov A. 2012. Investigation of ultrafine particle deposition to vegetation branches in a wind tunnel. Aerosol Sci Technol 46:465–472; doi:10.1080/02786826.2011.638346.

Lindeman RH, Merenda PF, Gold RZ. 1980. Introduction to Bivariate and Multivariate Analysis. Glenview, IL:Scott Foresman.

Lipsky EM, Robinson AL. 2006. Effects of dilution on fine particle mass and partitioning of semivolatile organics in diesel exhaust and wood smoke. Environ Sci Technol 40:155–162; doi:10.1021/es050319p.

Liu B, Frey HC. 2015a. Quantification and application of real-world light duty vehicle performance envelope for speed and acceleration. Transportation Research Record. 2503:128–136; doi: 10.3141/2503-14.

Liu B, Frey HC. 2015b. Variability in light-duty gasoline vehicle emission factors from trip-based real-world measurements. Environ Sci Technol 49:12525–12534; doi:10.1021/acs.est.5b00553.

Liu, Y, Shaddick G, Zidek JV. 2017. Incorporating high-dimensional exposure modelling into studies of air pollution and health. Stat Biosci 9:559–581.

Luben TJ, Nichols JL, Dutton SJ, Kirrane E, Owens EO, Datko-Williams L, et al. 2017. A systematic review of cardiovascular emergency department visits, hospital admissions and mortality associated with ambient black carbon. Environ Int 107:154–162; doi:10.1016/j.envint.2017.07.005.

Lumley T based on Fortran code by Alan Miller. 2017. Leaps: Regression Subset Selection. Available: *https://CRAN.R-project.org/package=leaps*.

Marshall JD, Nethery E, Brauer M. 2008. Within-urban variability in ambient air pollution: Comparison of estimation methods. Atmos Environ 42:1359–1369. Available: *https://doi.org/10.1016/j.atmosenv.2007.08.012*.

Massoli P, Fortner EC, Canagaratna MR, Williams LR, Zhang Q, Sun Y, et al. 2012. Pollution gradients and chemical characterization of particulate matter from vehicular traffic near major roadways: Results from the 2009 Queens College Air Quality Study in NYC. Aerosol Sci Technol 46:1201–1218; doi:10.1080/02786826.2012.701784.

Merbitz H, Fritz S, Schneider C, 2012. Mobile measurements and regression modeling of the spatial particulate matter variability in an urban area. Sci Tot Environ 438:389–403. Available: *https://doi.org/10.1016/j.scitotenv.2012.08.049*

Michanowicz DR, Shmool JLC, Cambal L, Tunno BJ, Gillooly S, Olson Hunt MJ, et al. 2016. A hybrid land use regression/line-source dispersion model for predicting intra-urban NO_2. Transp Res Part D: Transp Environ 43:181–191; doi:10.1016/j.trd.2015.12.007.

Milando CW, Batterman SA. 2018. Operational evaluation of the R-LINE dispersion model for studies of traffic-related air pollutants. Atmos Environ 182:213–224; doi:10.1016/j.atmosenv.2018.03.030.

Ning Z, Hudda N, Daher N, Kam W, Herner J, Kozawa K, et al. 2010. Impact of roadside noise barriers on particle size distributions and pollutants concentrations near freeways. Atmos Environ 44:3118–3127; doi:10.1016/j.atmosenv.2010.05.033.

Özkaynak H, Frey HC, Burke J, Pinder RW. 2009. Analysis of coupled model uncertainties in source-to-dose modeling of human exposures to ambient air pollution: A $PM_{2.5}$ case study. Atmos Environ 43:1641–1649; doi:10.1016/j.atmosenv.2008.12.008.

Park SS, Kozawa K, Fruin S, Mara S, Hsu Y-K, Jakober C, et al. 2011. Emission factors for high-emitting vehicles based on on-road measurements of individual vehicle exhaust with a mobile measurement platform. J Air Waste Manag Assoc 61:1046–1056.

Patterson RF, Harley RA. 2019. Evaluating near-roadway concentrations of diesel-related air pollution using RLINE. Atmos Environ 199:244–251; doi:10.1016/j.atmosenv.2018.11.016.

Patton AP, Milando C, Durant JL, Kumar P. 2017. Assessing the suitability of multiple dispersion and land use regression models for urban traffic-related ultrafine particles. Environ Sci Technol 51:384–392; doi:10.1021/acs.est.6b04633.

Patton AP, Perkins J, Zamore W, Levy JI, Brugge D, Durant JL. 2014. Spatial and temporal differences in traffic-related air pollution in three urban neighborhoods near an interstate highway. Atmos Environ 99:309–321; doi:10.1016/j.atmosenv.2014.09.072.

Pohjola MA, Pirjola L, Karppinen A, Härkönen J, Korhonen H, Hussein T, et al. 2007. Evaluation and modelling of the size fractionated aerosol particle number concentration measurements nearby a major road in Helsinki — Part I: Modelling results within the LIPIKA project. Atmos Chem Phys 7:4065–4080; doi:10.5194/acp-7-4065-2007.

Rich DQ, Utell MJ, Croft DP, Thurston SW, Thevenet-Morrison K, Evans KA, et al. 2018. Daily land use regression estimated woodsmoke and traffic pollution concentrations and the triggering of ST-elevation myocardial infarction: A case-crossover study. Air Qual Atmos Health 11:239–244; doi:10.1007/s11869-017-0537-1.

Richmond-Bryant J, Owen RC, Graham S, Snyder M, McDow S, Oakes M, et al. 2017. Estimation of on-road NO_2 concentrations, NO_2/NO_x ratios, and related roadway gradients from near-road monitoring data. Air Qual Atmos Health 10:611–625; doi:10.1007/s11869-016-0455-7.

Ritner M, Westerlund KK, Cooper CD, Claggett M. 2013. Accounting for acceleration and deceleration emissions in intersection dispersion modeling using MOVES and CAL3QHC. J Air Waste Manag Assoc 63:724–736; doi:10.1080/10962247.2013.778220.

Rivas I, Mandana M, Viana M, Moreno T, Clifford S, He C, et al. 2017. Identification of technical problems affecting performance of DustTrak DRX aerosol monitors. Sci Total Environ 584-585:849–855.

Rizza V, Stabile L, Vistocco D, Russi A, Pardi S, Buonanno G. 2019. Effects of the exposure to ultrafine particles on heart rate in a healthy population. Sci Total Environ 650: 2403–2410.

Robinson AL, Donahue NM, Shrivastava MK, Weitkamp EA, Sage AM, Grieshop AP, et al. 2007. Rethinking organic aerosols: Semivolatile emissions and photochemical aging. Science 315:1259–1262; doi:10.1126/science.1133061.

Rowangould GM. 2013. A census of the U.S. near-roadway population: Public health and environmental justice considerations. Transport Res Part D 25:59–67; doi:10.1016/j.trd.2013.08.003.

Saha PK, Khlystov A, Grieshop AP. 2015. Determining aerosol volatility parameters using a "dual thermodenuder" system: Application to laboratory-generated organic aerosols. Aerosol Sci Technol 49:620–632; doi:10.1080/02786826.2015.1056769.

Saha PK, Khlystov A, Grieshop AP. 2018a. Downwind evolution of the volatility and mixing state of near-road aerosols near a U.S. interstate highway. Atmos Chem Phys 18:2139–2154.

Saha PK, Khlystov A, Snyder MG, Grieshop AP. 2018b. Characterization of air pollutant concentrations, emission factors, and dispersion near a North Carolina interstate freeway across two seasons. Atmos Environ 177:143–153; doi:10.1016/j.atmosenv.2018.01.019.

Saleh R, Walker J, Khlystov A. 2008. Determination of saturation pressure and enthalpy of vaporization of semi-volatile aerosols: The integrated volume method. J Aerosol Sci 39:876–887; doi:10.1016/j.jaerosci.2008.06.004.

Saliba G, Saleh R, Zhao Y, Presto AA, Lambe AT, Frodin B, et al. 2017. Comparison of gasoline direct-injection (GDI) and port fuel injection (PFI) vehicle emissions: Emission certification standards, cold-start, secondary organic aerosol formation potential, and potential climate impacts. Environ Sci Technol 5:6542–6552; doi:10.1021/acs.est.6b06509.

Sandhu GS, Frey HC. 2012. Real-world measurement and evaluation of duty cycles, fuels, and emission control technologies of heavy-duty trucks. Transp Res Rec 2270:180–187; doi:10.3141/2270-21.

Sandhu GS, Frey HC, Bartelt-Hunt S, Jones E. 2016. Real-world activity, fuel use, and emissions of diesel side-loader refuse trucks. Atmos Environ 129:98–104; doi:10.1016/j.atmosenv.2016.01.014.

Seinfeld JH, Pandis SN. 1998. Atmospheric Chemistry and Physics: From Air Pollution to Climate Change. New York: John Wiley & Sons.

Singh A, Rajput P, Sharma D, Sarin MM, Singh D. 2014. Black carbon and elemental carbon from postharvest agricultural-waste burning emissions in the Indo-Gangetic Plain. Adv Meteorol; doi:10.1155/2014/179301.

Snyder M, Arunachalam S, Isakov V, Talgo K, Naess B, Valencia A, et al. 2014. Creating locally resolved mobile-source emissions inputs for air quality modeling in support of an exposure study in Detroit, Michigan, USA. Int J Environ Res Public Health 11:12739–12766.

Snyder MG, Venkatram A, Heist DK, Perry SG, Petersen WB, Isakov V. 2013. R-LINE: A line source dispersion model for near-surface releases. Atmos Environ 77:748–756; doi:10.1016/j.atmosenv.2013.05.074.

Song S-K, Shon Z-H, Kim Y-K, Kang Y-H, Jeong J-H. 2013. Influence of an enhanced traffic volume around beaches in the short period of summer on ozone. Atmos Environ 71:376–388; doi:10.1016/j.atmosenv.2013.02.003.

Stroud CA, Liggio J, Zhang J, Gordon M, Staebler RM, Makar PA, et al. 2014. Rapid organic aerosol formation downwind of a highway: Measured and model results from the FEVER study. J Geophys Res Atmos 119:1663–1679; doi:10.1002/2013JD020223

Sun YL, Zhang Q, Schwab JJ, Chen W-N, Bae M-S, Hung H-M, et al. 2012. Characterization of near-highway submicron aerosols in New York City with a high-resolution aerosol mass spectrometer. Atmos Chem Phys 12:2215–2227; doi:10.5194/acp-12-2215-2012.

Tobias A, Rivas I, Reche C, Alastuey A, Rodriguez S, Fernandez-Camacho, et al. 2018. Short-term effects of ultrafine particles on daily mortality by primary vehicle exhaust versus secondary origin in three Spanish cities. Environ Int 111:144–151; doi:10.1016/j.envint.2017.11.015

TRB (Transportation Research Board of the National Academies). 2010. Highway Capacity Manual. Washington, DC:Transportation Research Board of the National Academies.

Unal A, Frey HC, Rouphail NM. 2004. Quantification of highway vehicle emissions hot spots based upon on-board measurements. J Air Waste Manag Assoc 54:130–140; doi:10.1080/10473289.2004.10470888.

Unal A, Rouphail NM, Frey HC. 2003. Effect of arterial signalization and level of service on measured vehicle emissions. Trans Res Rec 1842:47–56.

U.S. DOT (U.S. Department of Transportation). 2012. National Transportation Statistics. United States Department of Transportation. Available: *https://www.rita.dot.gov/bts/sites/rita.dot.gov.bts/files/publications/transportation_statistics_annual_report/2012/index.html* [accessed 23 December 2017].

U.S. EPA (U.S. Environmental Protection Agency). 2007. Control of Hazardous Air Pollutants from Mobile Sources: Regulatory Impact Analysis. EPA420-R-07-002. Ann Arbor, MI:U.S. Environmental Protection Agency.

U.S. EPA (U.S. Environmental Protection Agency). 2010. Integrated Science Assessment for Carbon Monoxide. EPA/600/R-09/019F. Research Triangle Park, NC:U.S. Environmental Protection Agency.

U.S. EPA (U.S. Environmental Protection Agency). 2016. Integrated Science Assessment for Oxides of Nitrogen – Health Criteria. EPA/600/R-15/068. Research Triangle Park, NC:U.S. Environmental Protection Agency.

U.S. EPA (U.S. Environmental Protection Agency). 2017a. Air Emissions Inventories: Air Emissions Sources. U.S. Environmental Protection Agency. Available: *https://www.epa.gov/air-emissions-inventories*. [accessed 26 June 2021].

U.S. EPA (U.S. Environmental Protection Agency). 2017b. Regulations for Greenhouse Gas Emissions from Passenger Cars and Trucks. U.S. Environmental Protection Agency. Available: *https://www.epa.gov/regulations-emissions vehicles-and-engines/regulations-greenhouse-gas-emissions passenger-cars-and*. [accessed 26 December 2017].

U.S. EPA (U.S. Environmental Protection Agency). 2019. Integrated Science Assessment for Particulate Matter. EPA/600/R-19/188F. Research Triangle Park, NC:U.S. Environmental Protection Agency.

U.S. EPA (U.S. Environmental Protection Agency). 2020. Integrated Science Assessment for Ozone and Related Photochemical Oxidants. EPA/600/R-20/012. Research Triangle Park, NC:U.S. Environmental Protection Agency.

Verma V, Pakbin P, Cheung KL, Cho AK, Schauer JJ, Shafer MM, et al. 2011. Physicochemical and oxidative characteristics of semi-volatile components of quasi-ultrafine particles in an urban atmosphere. Atmos Environ 45:1025–1033; doi:10.1016/j.atmosenv.2010.10.044.

Virtanen A, Rönkkö T, Kannosto J, Ristimäki J, Mäkelä JM, Keskinen J, et al. 2006. Winter and summer time size distributions and densities of traffic-related aerosol particles at a busy highway in Helsinki. Atmos Chem Phys 6:2411–2421; doi:10.5194/acp-6-2411-2006.

Wehner B, Philippin S, Wiedensohler A. 2002. Design and calibration of a thermodenuder with an improved heating unit to measure the size-dependent volatile fraction of aerosol particles. J Aerosol Sci 33:1087–1093; doi:10.1016/S0021-8502(02)00056-3.

Weichenthal S, Van Ryswyk K, Goldstein A, Bagg S, Shekkarizfard M, Hatzopoulou M. 2016. A land use regression model for ambient ultrafine particles in Montreal, Canada: A comparison of linear regression and a machine learning approach. Environ Res 146:65–72; doi:10.1016/j.envres.2015.12.016.

Wolf K, Schneider A, Breitner S, Meisinger C, Heier M, Cyrys J, et al. 2015. Associations between short-term exposure to particulate matter and ultrafine particles and myocardial infarction in Augsburg, Germany. Int J Hyg Environ Health 218:535–542; doi:10.1016/j.ijheh.2015.05.002.

Xu J, Wang A, Hatzopoulou M. 2016. Investigating near-road particle number concentrations along a busy urban corridor with varying built environment characteristics. Atmos Environ 142:171–180; doi:10.1016/j.atmosenv.2016.07.041

Yli-Pelkonen V, Setälä H, Viippola V. 2017. Urban forests near roads do not reduce gaseous air pollutant concentrations but have an impact on particles levels. Landsc. Urban Plan. 158:39–47; doi:10.1016/j.landurbplan.2016.09.014.

Yuchi W, Sbihi H, Davies H, Tamburic L, Brauer M. 2020. Road proximity, air pollution, noise, green space and neurologic disease incidence: A population-based cohort study. Environ Health 19:8; doi:10.1186/s12940-020-0565-4.

Zhang K, Batterman S. 2013. Air pollution and health risks due to vehicle traffic. Sci Total Environ 450–451:307–316; doi:10.1016/j.scitotenv.2013.01.074.

Zhang KM, Wexler AS. 2004. Evolution of particle number distribution near roadways — Part I: analysis of aerosol dynamics and its implications for engine emission measurement. Atmos Environ 38:6643–6653; doi:10.1016/j.atmosenv.2004.06.043.

Zhang KM, Wexler AS, Zhu YF, Hinds WC, Sioutas C. 2004. Evolution of particle number distribution near roadways. Part II: the "Road-to-Ambient" process. Atmos Environ 38:6655–6665; doi:10.1016/j.atmosenv.2004.06.044.

Zhou X, Tanvir S, Lei H, Taylor J, Liu B, Rouphail NM, et al. 2015. Integrating a simplified emission estimation model and mesoscopic dynamic traffic simulator to efficiently evaluate emission impacts of traffic management strategies. Transport Res — Part D 37:123–136.

Zhu Y, Hinds WC, Kim S, Shen S, Sioutas C. 2002a. Study of ultrafine particles near a major highway with heavy-duty diesel traffic. Atmos Environ 36:4323–4335; doi:10.1016/S1352-2310(02)00354-0.

Zhu Y, Hinds WC, Kim S, Sioutas C. 2002b. Concentration and size distribution of ultrafine particles near a major highway. J Air Waste Manag Assoc 52:1032–1042; doi:10.1080/10473289.2002.10470842.

Zhu Y, Hinds WC, Shen S, Sioutas C. 2004. Seasonal trends of concentration and size distribution of ultrafine particles near major highways in Los Angeles: Special Issue of Aerosol Science and Technology on findings from the Fine Particulate Matter Supersites Program. Aerosol Sci Technol 38:5–13; doi:10.1080/02786820390229156.

Zhu Y, Kuhn T, Mayo P, Hinds WC. 2006. Comparison of daytime and nighttime concentration profiles and size distributions of ultrafine particles near a major highway. Environ Sci Technol 40:2531–2536; doi:10.1021/es0516514.

MATERIALS AVAILABLE ON THE HEI WEBSITE

The Additional Materials contain supplemental material not included in the printed report. They are available on the HEI website, *www.healtheffects.org/publications.*

Appendix A. Land Use

Appendix B. Traffic Data — Freeway Site

Appendix C. Traffic Data — Urban Site

Appendix D. Microscale Vehicle Emissions

Appendix E. Freeway Site Air Quality Measurements

Appendix F. Urban Site Air Quality Measurements

Appendix G. Dispersion Modeling

Appendix H. Statistical Modeling

ABOUT THE AUTHORS

H. Christopher Frey is the Glenn E. Futrell Distinguished University Professor in the Department of Civil, Construction, and Environmental Engineering at North Carolina State University. Frey served as the principal investigator of this project and led the aspects of the study related to measurement and modeling of microscale vehicle emissions at both the freeway and urban sites. His research focuses on the source-to-outcome continuum including air pollutant emissions, air quality, human exposure to air pollution, and risk assessment of adverse effects from such exposures. He has chaired the U.S. EPA's Clean Air Scientific Advisory Committee, serves on the U.S. EPA Science Advisory Board, and was a lead author for the IPCC 2006 Good Practice Guidance on uncertainty in greenhouse gas inventories. Frey has served on National Research Council study committees regarding air pollution and on the NRC's Board of Environmental Studies and Toxicology. He is a fellow of the Air & Waste Management Association and of the Society for Risk Analysis, served on the Board of Directors of A&WMA, and was president of the Society for Risk Analysis in 2006. He has a BS in mechanical engineering from the University of Virginia, an MS in engineering in mechanical engineering from Carnegie Mellon University, and a PhD in engineering and public policy from Carnegie Mellon.

Andrew P. Grieshop is an associate professor of environmental engineering at North Carolina State University, where he directs the Grieshop Atmosphere and Environment Lab. For this project, he participated as a coprincipal investigator, established the I-40 measurement site, and coordinated the near-road measurements of traffic-related pollutants, with a focus on fine PM properties, in cooperation with Dr. Khlystov. He also participated in data synthesis and analysis efforts across the project components. His research program addresses sources and evolution of atmospheric aerosols, characterization of in-use emissions from mobile and stationary combustion sources, linkages between air pollution emissions and climate change, air pollution exposure assessment, technical policy analysis of the environmental impacts of energy systems, and energy and environment in developing countries. Grieshop received his BS in mechanical engineering from University of California, Berkeley and his MS in mechanical engineering and PhD in mechanical engineering and engineering and public policy from Carnegie Mellon University. He was a Postdoctoral Research Fellow at the University of British Columbia.

Andrey Khlystov participated in this project as a coprincipal investigator and contributed to measurement and analysis of air quality data at the freeway site. He is director of the Organic Analytical Laboratory at the Desert Research Institute, where he also serves as an associate research professor. Khlystov has over 20 years of experience in air quality studies. He has been involved in the development and testing of sampling techniques for organic and inorganic air pollutants, the study of spatial and temporal variability of air pollutants, and aerosol thermodynamics. He has a PhD from Wageningen University in the Netherlands, and bachelor's and master's degrees in physical chemistry from Novosibirsk State University, Russia.

John J. Bang is the director of the Environmental Health Program and is the chair and an associate professor in the Department of Environmental, Earth, and Geospatial Sciences at North Carolina Central University, Durham. He participated in this project as a coprincipal investigator and led the measurement of air quality at the urban site. His research interests include exposure and risk assessment related to environmental health. He has a BS in biochemistry from the University of Illinois at Urbana-Champaign, an MD from the University of Illinois at Chicago, and a PhD in environmental sciences and engineering from the University of Texas at El Paso.

Nagui M. Rouphail served as director of the Institute for Transportation Research and Education at North Carolina State University, from January 2002 through August 2016. Rouphail also held the rank of chair and professor (now professor emeritus) in the Department of Civil, Construction, and Environmental Engineering at North Carolina State University. He participated in this project as coprincipal investigator and led the measurement and modeling of traffic activity. Rouphail is an internationally recognized scholar in the areas of highway capacity and operations, traffic simulation and intelligent transport systems, and the interface of traffic flow and air quality. He has published over 160 refereed journal articles and has won ten best paper awards from Transportation Research Board of the National Academies, American Society of Civil Engineers, and Institute for Transportation Engineers. He served as associate editor for several transportation journals including *Transportation Science*, *Transportation Research Part B*: *Methodological*, and the *Journal of Intelligent Transportation Systems*. He received his BS in civil engineering from Cairo University, and his MS and PhD from the Ohio State University, Columbus.

Joseph Guinness received his bachelor's in math and physics from Washington University in St. Louis and his PhD in statistics from the University of Chicago. He is currently visiting assistant professor of statistics at Cornell University, on leave from his position as assistant professor of statistics at North Carolina State University. Guinness provides statistical expertise for analyzing spatiotemporal data in environmental sciences and has research interests in health, soil chemistry, weather, and climate. He participated in this project as coprincipal investigator and led the statistical methods and data analysis aspects of this project in succession to Dr. Fuentes.

Daniel Rodríguez is chancellor's professor in the Department of City and Regional Planning and associate director of the Institute for Transportation Studies at The University of California, Berkeley. His research focuses on the reciprocal relationship between the built environment and transportation and its effects on the environment and health. Prior to this he was distinguished professor of sustainable community design at University of North Carolina, Chapel Hill, where he participated in this project as a coprincipal investigator. He led the characterization of the built environment and land-use patterns for the project's two study sites.

Montse Fuentes participated in this project as a coprincipal investigator and led the statistical methods and data analysis aspects of the work. Fuentes performed these functions while she served as the head of the Department of Statistics and James M. Goodnight Distinguished Professor of Statistics at North Carolina State University. Her research has applications in such areas as weather forecasting, oceanography, climate, ecology, air pollution and human health effects from pollution. Fuentes transitioned from North Carolina State to Virginia Commonwealth University (VCU) during the course of the project. At VCU, she is dean of the College of Humanities and Sciences. She received a dual bachelor's degree in mathematics and music (piano) from the University of Valladolid in Spain and a PhD in statistics from the University of Chicago.

Provat Saha conducted field measurements of air quality at the urban site, including preparation of instruments, deployment of instruments, QA, data analysis, data interpretation, and reporting. He participated in this project as a graduate research assistant as part of his PhD in civil engineering at North Carolina State University. Upon completing his degree, he joined Carnegie Mellon University as a postdoctoral researcher in the Department of Mechanical Engineering.

Halley Brantley is a graduate student working on her PhD in statistics at North Carolina State University. She conducted statistical analyses for the project as a research assistant under the guidance of Joe Guinness and Montse Fuentes. She is currently an ORISE fellow at the U.S. EPA with interests in the application of spatiotemporal methods to next-generation air quality measurements. She has a BS in chemistry from Davidson College and a master's in environmental management from Duke University.

Michelle Snyder led the applications of the R-LINE near-road dispersion model as a research associate in the Institute for the Environment at the University of North Carolina, Chapel Hill. Snyder was the lead developer of R-LINE as a postdoctoral researcher at the U.S. EPA. She has a BS in physics and mathematics from Elon University, and master's and doctoral degrees in physics from North Carolina State University. She is currently a senior scientist with AMEC Foster Wheeler Environment and Infrastructure UK Limited.

Shams Tanvir contributed to the collection, QC, and analysis of traffic data, and development of statistical models for the freeway and urban sites. He participated in this project as a graduate research assistant as part of his PhD in civil engineering at North Carolina State University. Currently, he is working as a research associate in the Institute for Transportation Research and Education. His research interests are sustainable mobility, driver behavior analysis, cyber physical systems, and transportation system modeling.

Kwanpyo Ko contributed to measurement and analysis of traffic activity for the freeway and urban sites. He participated in this project as a graduate research assistant as part of his PhD in civil engineering at North Carolina State University.

Theophraste Noussi contributed to the measurement of air quality at the urban site. He participated in this project as a master's student in the Department of Environmental, Earth and Geospatial Sciences at North Carolina Central University.

Maryam Delavarrafiee contributed to the analysis of vehicle-activity and emissions data for the freeway and urban sites. She participated in this project as a graduate research assistant as part of her PhD in civil engineering at North Carolina State University. Upon completing her degree, she joined the California Air Resources Board in El Monte, CA.

Sanjam Singh contributed to measurement and analysis of vehicle-activity and emissions data for the freeway and urban sites. He participated in this project as a graduate research assistant as part of his MS in environmental engineering at North Carolina State University. Upon completing his degree, he joined Geosyntec Consultants in South Carolina.

OTHER PUBLICATIONS RESULTING FROM THIS RESEARCH

Frey HC, Delavarrafiee M, Singh S. 2017. Real-world freeway and ramp activity and emissions for light-duty gasoline vehicles. Transportation Research Record 2627:17–25; doi:10.3141/2627-03.

Saha PK, Khlystov A, Grieshop AP. 2018. Downwind evolution of the volatility and mixing state of near-road aerosols near a U.S. interstate highway, Atmospheric Chemistry and Physics 18:2139–2154; doi:10.5194/acp-18-2139-2018.

Saha PK, Khlystov A, Snyder MG, Grieshop AP. 2018. Characterization of air pollutant concentrations, emission factors, and dispersion near a North Carolina interstate freeway across two seasons. Atmospheric Environment 177:143–153; doi:10.1016/j.atmosenv.2018.01.019.

Saha PK, Reece SM, Grieshop AP. 2018. Seasonally varying secondary organic aerosol formation from in-situ oxidation of near-highway air. Environ Sci Technol 52:7192–7202; doi:10.1021/acs.est.8b01134.

Research Report 207, *Characterizing Determinants of Near-Road Ambient Air Quality for an Urban Intersection and a Freeway Site*, H.C. Frey et al.

INTRODUCTION

Traffic emissions are an important source of urban air pollution, and exposure to traffic-related air pollution has been associated with various adverse health effects. In 2010, HEI published Special Report 17, *Traffic-Related Air Pollution: A Critical Review of the Literature on Emissions, Exposure, and Health Effects,* which summarized and synthesized research related to the health effects from exposure to traffic emissions. The report concluded that the evidence was sufficient to support a causal relationship between short- and long-term exposure to traffic-related air pollution and exacerbation of asthma in children. It found suggestive evidence of a causal relationship between exposure to traffic-related air pollution and other outcomes, including all-cause and cardiovascular mortality, and limited evidence of associations for some other outcomes (HEI 2010). Because many additional studies have been published since the earlier review, HEI has recently published a new systematic review of the epidemiological literature on the health effects of long-term exposure to traffic-related air pollution (HEI 2022), which supports and strengthens earlier findings on associations between health effects and exposure to this type of air pollution.

Because traffic-related air pollution exposure is of public health interest, it is important to understand where and at what levels people are exposed to air pollution from traffic emissions. However, exposure assessment is challenging because traffic-related air pollution is a complex mixture of many particulate and gaseous pollutants and is highly variable across locations and time (HEI 2010). The highest concentrations of traffic-related air pollutants occur within a few hundred meters of major roads, with the extent of the impact zone depending on the pollutant, geography, land use characteristics, and meteorological conditions (Karner et al. 2010; Zhou and Levy 2007).

Researchers often estimate exposure to traffic-related air pollution by developing and evaluating statistical models that rely on detailed measurement campaigns that have adequate design and instrumentation to identify concentrations and variations in air pollutants within and between neighborhoods. Approaches to assess exposure to traffic-related air pollution have included measurement campaigns using fixed sites or mobile platforms at various distances from busy roads and models such as land use regression and dispersion models (e.g., Beelen et al. 2013; Hoek 2017; Patton et al. 2020). In some cases, infiltration of air pollutants to the indoor environment and time–activity patterns have been included for more accurate estimates of personal exposure to air pollution from traffic and other outdoor sources (e.g., Dons et al. 2012; Goldstein et al. 2021; Wallace 2000; Wheeler et al. 2011). These exposure estimation approaches often rely on statistical models where many potential parameters are considered for inclusion, with the implicit assumption that more detailed parameters used as input for these models will result in models with greater explanatory power (i.e., higher R^2) (HEI 2010).

In 2013, following the recommendation of the 2010 Special Report to improve exposure assessment of traffic-related air pollution for use in health studies, HEI issued Request for Applications (RFA*) 13-1, *Improving Assessment of Near-Road Exposure to Traffic Related Pollution.* HEI funded five studies under RFA 13-1 and an additional nine other studies related to exposure assessment or health effects of traffic-related air pollution under other RFAs (see Preface). In response to RFA 13-1, Dr. H. Christopher Frey and colleagues from North Carolina State University and other institutions proposed a 2.5-year study, "Characterizing the Determinants of Vehicle Traffic Emissions Exposure: Measurement and Modeling of Land-Use, Traffic, Emissions, Transformation, and Transport." They proposed to explore how traffic activity metrics, land use parameters, and transport of pollutants influence spatial and temporal variability in air pollutant concentrations within several hundred meters of roads in the Raleigh–Durham area. The HEI Research Committee recommended Dr. Frey's application for funding because it included measurement of ultrafine particles (UFPs), characterization and modeling of pollutant transport, and transformation of pollutants from the source to the near-road environment.

This Critique provides the HEI Review Committee's evaluation of the study. It is intended to aid the sponsors of HEI and the public by highlighting both the strengths and limitations of the study and by placing the Investigators' Report in scientific and regulatory context.

Dr. H. Christopher Frey's 3-year study was funded under RFA 13-1, "Improving Assessment of Near-road Exposure to Traffic-Related Pollution," and began in July 2014. Total expenditures were $886,446. Frey and colleagues submitted a draft Investigators' Report for review in December 2017. Following several revisions, a final revised report was submitted in October 2021 and accepted for publication. During the review process, the HEI Review Committee and the investigators had the opportunity to exchange comments and to clarify issues in both the Investigators' Report and the Review Committee's Critique. No potential conflict of interest was reported by the authors. This report was completed before Dr. Frey took a position with the U.S. Environmental Protection Agency.

* A list of abbreviations and other terms appears at the end of this volume.

SUMMARY OF THE STUDY

SPECIFIC AIMS

Dr. Frey and colleagues explored how traffic activity metrics, land use parameters, and transport of pollutants influence near-road air pollutant concentrations at a freeway site and an urban intersection site in the Raleigh–Durham area. The specific aims were to

1. explain spatial and temporal variability in traffic-related air pollutant ambient concentrations at two near-roadway locations
2. develop and test refined parameters to represent land use, traffic, emissions, and dispersion
3. prioritize modeling inputs according to their ability to explain variability in ambient concentrations to help focus efforts for future data collection and model development.

The study incorporated key concepts from various fields related to roads and air pollution, including transportation, mobile source emissions, traffic operations, and meteorology (Critique Figure 1).

STUDY DESIGN AND APPROACH

The study included two sites that represented a heavily traveled freeway and a busy urban intersection (Critique Figure 2). Both sites were located in the Research Triangle Park area of North Carolina, and measurements were conducted between July 2015 and May 2016. An overview of the measurement campaigns and models developed at the two sites is provided in the Critique Table. The freeway site was adjacent to an eight-lane freeway with 140,000-145,000 vehicles per day (I-40) in Raleigh, NC, and the urban site was centered on an intersection with about 1,000 vehicles per day in Durham, NC. At each site, the investigators compiled extensive data on land use (i.e., road density, surface elevation, and other features listed in Critique Table 1) and traffic activity from databases maintained by state agencies. Vehicle specific power – a measure of instantaneous engine load – and tailpipe exhaust emissions from investigator-driven cars were measured by devices mounted on the cars while the investigators repeatedly drove through both study sites.

Near-road air pollutant measurements were made using a variety of intense monitoring approaches. Stationary monitoring was used at both sites: at two locations 10 meters from each side of the freeway and at five sites surrounding the urban intersection. Additionally, a mobile laboratory in a vehicle was used to take measurements downwind of the freeway, and mobile monitoring by pedestrians was used to take measurements along sidewalks near the urban intersection. Quality control included field blanks, confirmation that all mobile monitors read zero concentrations when the inlet air was filtered, and siting the instruments used for mobile monitoring alongside regulatory monitors to confirm that both sets of instruments measured the same concentrations before and after the measurement campaigns.

The investigators developed dispersion and statistical models of the measured air pollutants at both sites to better understand which parameters explained the highest fraction of the variability in concentrations as measured by their contributions to model R^2. They ran the U.S. Environmental Protection Agency's experimental Research LINE-source dispersion model (R-LINE; Snyder et al. 2013) with unit emissions, season-specific surface meteorology from Raleigh–Durham International Airport, and upper air soundings (vertical distribution of meteorological properties) from Greensboro airport. As is typical for R-LINE, the investigators later scaled the R-LINE output based on fleet-average emissions factors to include the time-varying traffic contributions to air pollutant concentrations.

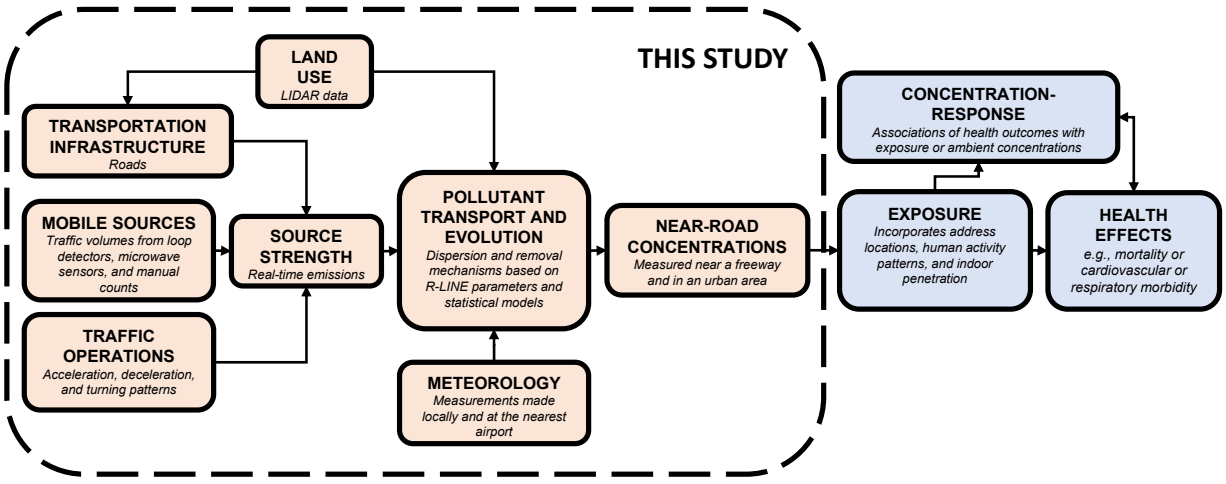

Critique Figure 1. Schematic of the various components of near-road exposure modeling in this study. R-LINE is a line source dispersion model and LIDAR is Light Detection and Ranging, a method of measuring elevation and identifying land surface features. Adapted from Investigators' Report Figure 2.

Critique Table. Measurements Performed and Models Developed at the Freeway and Urban Sites

		Freeway Site in Raleigh, NC	Urban Intersection in Durham, NC
Measurements	**Land Use**	Distance to fixed monitor, distance to bus stops and service frequency, distance to I-40; presence of commercial, industrial, public service, and recreational uses or residential buildings; tree canopy; and LIDAR elevation	Distance to bus stops and service frequency, distance to intersection; presence of commercial, industrial, public service, and recreational uses or residential buildings; tree canopy; employment types with low or high trip generation or attraction; and LIDAR elevation
	Traffic	Remote Traffic Microwave Sensor (routine, continuous) measurements with vehicle length used to classify heavy or light vehicles, and three traffic indices derived from those measurements for total and individual freeway lanes	Inductive single loop detector (routine, continuous) measurements embedded in the road surface for traffic count of vehicles entering the intersection via the main travel lanes, supplemented by video and four traffic indices derived from the measurements to provide total and heavy vehicle traffic counts by lane and turning movement
	Emissions	Vehicle specific power from onboard diagnostics scanner and NO, CO, and HC emissions from PEMS on four probe cars of different models each driven up and down the freeway on 5 days during off peak, morning peak, and evening peak hours between March 7, 2016, and May 26, 2016	Vehicle specific power from onboard diagnostics scanner and NO, CO, and HC emissions from PEMS on four probe cars of different models each driven on loops through the intersection on 5 days during off peak, morning peak, and evening peak hours between March 7, 2016, and May 26, 2016
	Air Quality Measurements	Hourly NO_x, NO, NO_2 UFPs, BC, $PM_{2.5}$, and PM composition and volatility from June 1 to July 2, 2015, and January 18 to February 20, 2016, at a long-term fixed site 10 m downwind of the freeway, paired with a monitor 10 m upwind of the freeway NO_x, UFPs, BC, and $PM_{2.5}$ on 4 days in June 2015 and 3 days in February 2016 at 15–20 stops (20 min each) per day by a mobile platform along a line perpendicularly downwind of the freeway	24-hour average $PM_{2.5}$, NO_2, NO_x, and O_3 at five fixed sites surrounding an intersection on 12 days in February to March 2016 and 11 days in May 2016 Real-time short-term (typically 1-min average) measurements of $PM_{2.5}$, UFPs, and O_3 along a pedestrian sidewalk near the intersection 14 days in February to March 2016 and 10 days in May 2016
Models	**Dispersion Model**	R-LINE predictions based on freeway emissions, generated for all pollutants and measurement locations	R-LINE predictions based on emissions from all nearby roads, generated for all pollutants and measurement locations
	Statistical Models	Temporal model of pollutant concentrations at the fixed site by the freeway	Separate spatial–temporal models of pollutant concentrations at the sites surrounding the intersection and along the pedestrian sidewalk

BC = black carbon; CO = carbon monoxide; HC = hydrocarbons; LIDAR = light detection and ranging; NO = nitrogen oxide; NO_2 = nitrogen dioxide; NO_x = nitrogen oxides including NO, nitrogen dioxide, and other oxides of nitrogen; O_3 = ozone; PEMS = portable emissions measurement system; $PM_{2.5}$ = particulate matter ≤ 2.5 µm in aerodynamic diameter and measured as mass concentration; R-LINE = U.S. Environmental Protection Agency's Research LINE-source dispersion model; UFPs = ultrafine particles measured as number concentration.

Critique Figure 2. Aerial photography of the freeway (left) and urban intersection (right) sites. Yellow dots show locations of fixed-site air quality monitors, which were complemented by mobile monitoring and emissions measurements (locations not shown). Imagery source: OpenStreetMap.

The statistical models were of the type known as predictive models or spatial-temporal land use regression models in epidemiology and explanatory models in engineering. Potential input parameters to statistical models were developed from the detailed site characterizations, including common parameters like distance to roads or land use, and a new detailed assessment of land surface features from light detection and ranging (LIDAR) data validated with field observations. Other inputs included continuous traffic on the streets closest to the measurement sites, vehicle emissions measured near the monitoring sites, parameters based on the R-LINE output, and local wind data. The R-LINE parameters were developed as statistical interactions of the R-LINE model output (not adjusted for traffic volumes) with measured or standardized traffic volume or density. Statistical models were tested with and without parameters for spatial autocorrelation and with and without parameters based on the R-LINE output.

The investigators selected as their final statistical models the linear regressions that maximized the fit to measurements (measured as lower Akaike Information Criterion and higher adjusted R^2 in 50-fold cross validation) while using the fewest parameters possible. Performance of the models was reflected in the coefficient of determination (adjusted R^2), with models explaining more than half of the variability in measured air pollutant concentrations (adjusted R^2 > 0.50) – a value considered by the investigators to reflect satisfactory model performance. The contribution of each parameter to the adjusted R^2 of the final statistical models was also reported.

KEY RESULTS

This study contributes a rich set of results on traffic activity, emissions, and air quality that can inform the discussion of whether more detailed measurements in space and time help with the development of better near-road air quality models.

Traffic Activity, Emissions, and Air Quality Measurements

- Generally, vehicle specific power and emissions of NO_x from the probe cars driven by the investigators increased with the traffic speed, but they also depended on the freeway lane, turning movements, conflicts with other vehicles, and time of day.
- Air pollutant concentrations varied generally as expected. For example, there was apparent exponential decay of traffic-related air pollutants (NO_x, UFPs, and black carbon [BC]) with distance from the freeway but less change in concentrations of particulate matter ≤ 2.5 µm in aerodynamic diameter ($PM_{2.5}$) with distance. At the urban intersection site, concentrations of the pollutants measured at both sites ($PM_{2.5}$, NO_x, and UFPs) were lower than at the freeway site and followed similar spatial patterns with distance from traffic.

Air Quality Models

- At the freeway site, the adjusted R^2 of statistical models ranged from moderate for black carbon (adjusted R^2 = 0.52) to good for $PM_{2.5}$ (adjusted R^2 = 0.87), and the UFP model had moderate-to-good performance (adjusted R^2 = 0.74; Critique Figure 3, top panel). At least one real-time *vehicle activity* metric and local wind direction were included in the statistical models of all five pollutants. The investigators reported that parameters that contributed most strongly to the model adjusted R^2 at the fixed sites adjacent to the freeway varied by pollutant and that depending on the pollutant other parameters such as temperature, background concentrations, and weekend versus weekday also contributed to higher adjusted R^2 in the statistical models.

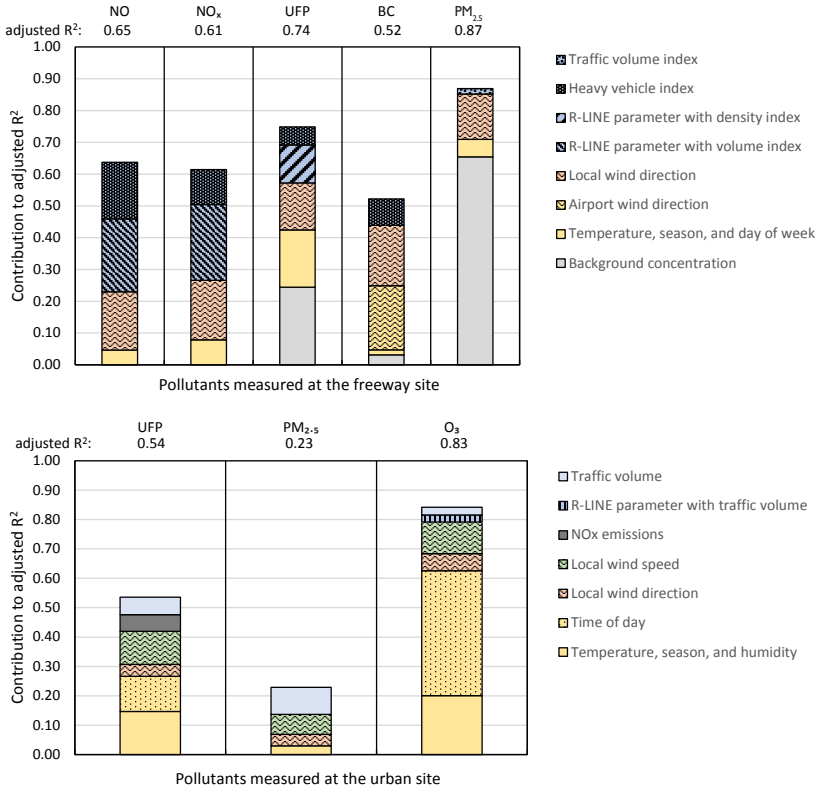

Critique Figure 3. Contributions of selected parameters to statistical model performance (expressed as R^2). The individual contributions to adjusted R^2 do not necessarily add up to the total adjusted R^2 because of correlations among parameters. **Top:** Freeway site. **Bottom:** Urban intersection site. (Source: Adapted from Investigators' Report Figures 19 and 31.)

- At the urban intersection site, the model performance ranged from poor for $PM_{2.5}$ (adjusted $R^2 = 0.23$) to moderate for UFPs (adjusted $R^2 = 0.54$) and good for ozone (adjusted $R^2 = 0.83$) (Critique Figure 3, bottom panel). The parameters contributing the most to the R^2 of the models of air pollutant concentrations measured along the pedestrian sidewalks included traffic on the busy street going through the intersection, time of day, season, and local wind speed for UFPs, and time of day, local wind speed, and temperature for O_3. Unlike at the freeway site, heavy vehicles did not contribute to the adjusted R^2 of the models of air quality at the urban intersection site separately from overall traffic.
- Relative to statistical models that did not include R-LINE dispersion model parameters, the adjusted R^2 of models that included R-LINE model parameters were improved for NO, NO_x, UFPs, and O_3 but were similar for BC and $PM_{2.5}$. The R-LINE model parameter contributed more to the model R^2 of statistical models for pollutants at the freeway site than at the urban intersection site.
- Localized data contributed to the adjusted R^2 of models developed for both sites. However, some other new parameters explored by the investigators (e.g., parameters extracted from LIDAR data) did not contribute to the model adjusted R^2 and were therefore not included in the statistical models. This result most likely occurred because the study areas were not large enough for there to be sufficient variation to observe effects of those new parameters.

HEI REVIEW COMMITTEE'S EVALUATION

To assess whether detailed characterization of various model parameters contributes to increased ability to explain the variability in air quality at two study locations in North Carolina, the investigators compiled a comprehensive database of traffic-related and land use parameters and conducted emissions and air quality measurement campaigns at both sites. They brought measurement methods, datasets, and interpretation from the transportation field to the analysis of near-road air quality through traffic characterization, emissions testing, and quantification of vehicle activity. Relating micro-scale emissions factors to transportation infrastructure and traffic operations contributed to a bottom-up understanding of the effects that individual vehicles and an entire fleet have on local air quality in different meteorological conditions (e.g., in the winter and summer). The two locations allowed analysis of the contributions to near-road air pollution from traffic on a freeway, compared with a busy urban intersection and evaluation of the statistical model performance in those locations. The many components of the complex study design contributed to a rich set of results that demonstrated the application of various innovative methods at two sites with detailed characterizations of the built environments, vehicle fleets, traffic patterns, and exhaust emissions. Other strengths of the study include the use of novel traffic indices and the use of a modeled dispersion parameter as a contributor to statistical models of air pollution. Overall, the study contributes to the discussion of whether more detailed measurements contribute to near-road air quality models with better predictive ability (i.e., higher R^2) by demonstrating that the detailed measurements might be useful in specific situations (as discussed later).

CONTRIBUTIONS OF INTENSE MEASUREMENT CAMPAIGNS

The Committee and investigators reflected on the benefits and limitations of this type of intense and resource-demanding measurement campaign. The Committee agreed with framing this work as a case study with specific results for specific areas because conducting similar measurement campaigns and statistical analyses in different locations could yield different results. Thus, one should use caution in generalizing these results to other study locations.

However, because of the care taken to record and validate data on the built environment and conditions that vary over time (e.g., traffic activity and meteorology), the results may inform observational studies in other locations via comparison of site features. Therefore, some future studies could benefit from intense monitoring of those factors that contributed most strongly to statistical models of air pollutants in this study, based on local understanding of the proposed study sites.

Given that this type of study will be challenging to conduct in a routine manner because of its substantial resource requirements, it will be important to determine whether detailed data collection to develop future models of near-road air pollutant concentrations will be of value. The potentially most important contribution of this study is to weigh the importance of detailed characterization of land use, traffic, emissions, and other determinants to obtain statistical models that are better able to predict variability in near-road air pollutant concentrations. As described below, several of the novel parameters were incorporated into final statistical models, and therefore are potentially valuable in improving very fine-resolution statistical models and are worth further study.

However, even with the detailed characterization of the study areas, the statistical model performance (expressed as R^2) was still lower than what is usually desired for epidemiological studies; performance was higher for the freeway site than for the urban intersection site, which was closer to where people lived. Other questions remain about the applicability of the models for epidemiological studies. For example, it is unclear how the near-road modeling results relate to exposure of nearby populations. This study suggests that efforts to improve traffic and emissions characterization, measure air pollution more intensely, and develop more complex statistical models might all be helpful, but they are unlikely to address all the needs to improve exposure assessment for

health studies. The systematic evaluation of contributors to models and evaluation of the performance and uncertainty in those models is continuing in many research studies, including in ongoing studies funded under HEI's RFA 19-1, "Applying Novel Approaches to Improve Long-Term Exposure Assessment of Outdoor Air Pollution for Health Studies" (see Preface).

VALUE OF NEW MODEL PARAMETERS

The Committee appreciated the comparisons of contributions of parameters in the statistical models to model performance for the freeway and urban intersection site statistical models because the comparisons can be used to identify which parameters were most predictive (i.e., contributed the most to model R^2) of air pollutant concentrations at the freeway site and the urban intersection. This is an important step in identifying where to allocate resources.

Several of the potential statistical model parameters that were tested were included in the final models and demonstrated the value of carefully measured parameters. For example, at both sites the model performance for all the evaluated pollutants improved when local wind measurements were used instead of, or in addition to, regional wind measurements. Additionally, refined traffic-volume indices were incorporated into all the freeway air pollution models: the heavy-vehicle volume index was the traffic parameter that contributed the most to the model R^2 for BC, UFPs, NO, and NO_x, whereas a more general traffic-volume index was a minor contributor to $PM_{2.5}$ model performance. The extent to which real-time traffic data would improve statistical models near urban intersections remains unclear because at the urban intersection site tailpipe emissions of NO_x were included in the UFP models, but traffic indices were not incorporated into any of the final statistical models because they did not contribute to the model R^2. The development of other potential parameters (e.g., those derived from LIDAR) was time intensive, but they did not contribute to the model R^2 because they lacked sufficient variation within each site. Nevertheless, those parameters did allow for relatively complete descriptions of the study areas; they could potentially be used when expanding the study area from the roadside to larger neighborhoods or to entire urban areas.

The new dispersion model parameter based on standardized output from the R-LINE dispersion model captured some features of the near-road environment well, suggesting that dispersion model output could be considered as inputs for statistical models of near-road air quality, particularly at fine spatial resolutions. At the freeway site, the R-LINE model parameter was included in the final statistical models of the traffic-related air pollutants with the strongest near-road gradients (UFPs, NO, and NO_x) but was not included in the statistical models of BC or $PM_{2.5}$ because it did not increase the adjusted R^2 for those pollutants. The R-LINE model parameter was less influential at the urban intersection site, suggesting that dispersion model parameters might contribute more to statistical model R^2 in locations with high traffic volume or free-flowing traffic than in locations where traffic is intermittent; further studies in other locations would be needed to confirm this. The investigators did not directly compare the R-LINE output to statistical models because the R-LINE model parameter was not developed with local meteorology and time-varying emissions to maximize the performance of R-LINE. Nonetheless, the Committee appreciated the investigators' exploration of R-LINE output as a modeled dispersion model parameter that interacts with traffic activity and meteorology in the statistical models.

Given the results of the evaluations of some new model parameters, the Committee thought that additional performance evaluations of air quality models that consider these parameters would be worthwhile. The Committee thought that the reported regression coefficients in the statistical models could potentially be used to describe the air pollution trends in the study locations and that the R^2 and Akaike Information Criterion were appropriate statistics for comparing models. An additional approach they thought would have contributed to the analyses would have been to directly compare statistical models that incorporated different proxies of traffic under conditions experienced at different times of day and seasons, similar to the analyses the investigators conducted for the near-road gradients from the R-LINE output.

SUMMARY AND CONCLUSIONS

The investigators developed and evaluated the performance of statistical models of near-road air quality that incorporated detailed characterization of various parameters, including novel traffic indices. They successfully compiled a comprehensive database of traffic-related parameters and land use parameters from measurement campaigns in two study locations (a freeway and a busy urban intersection) in North Carolina. In these campaigns, they brought measurement methods, datasets, and interpretation from the transportation field directly into the analysis of near-road air quality.

Statistical model performance varied by both pollutant and site. At the freeway site, the models had moderate performance for BC, moderate to good for UFPs, NO, and NO_x, and good for $PM_{2.5}$; whereas at the urban intersection site the models had poor performance for $PM_{2.5}$, moderate for UFPs, and good for O_3. The parameters that contributed the most to the adjusted R^2 of near-road air quality models included distance-weighted traffic-volume indices (especially for heavy vehicles at the freeway site but less so at the urban intersection site) and locally measured wind direction. Localized data on real-time traffic and meteorology contributed to the adjusted R^2 of statistical models of air pollutant concentrations, and local meteorology measurements in particular were more predictive of near-road air pollutant concentrations than were meteorological measurements from farther away. Temperature, background concentrations, and weekend versus

weekday also explained portions of the variability in some of the pollutants.

Some other new potential explanatory parameters explored by the investigators (e.g., land use parameters extracted from LIDAR data) were not included in the final models, most likely because the study areas were not large enough for the variation in these parameters to be sufficient for evaluating their effects. Inclusion of various forms of dispersion model parameters calculated with R-LINE improved the statistical models of the pollutants most strongly related to traffic at the freeway site, but they explained less of the variability in $PM_{2.5}$ concentrations at the freeway site or any of the pollutants measured at the urban intersection site.

Strengths of the study were the detailed characterization of the study areas and incorporation of measurements, methods, and interpretation from the transportation field through traffic characterization, emissions testing, and quantification of vehicle activity, the use of novel traffic indices with distance-weighted traffic activity, and the use of dispersion model parameters calculated with R-LINE as contributors to statistical models of air pollution. Limitations were that the two study sites might not be representative of other locations, and it is unclear how well the models at those two sites actually represent exposure of nearby populations. The large amount of data collected, while a positive aspect of the study, also made it more challenging to fully explore the effects of novel parameters on model accuracy and other interesting issues within the limits of one study.

The HEI Review Committee concurred with the investigators that this study demonstrated that detailed characterization of near-road environments can provide new parameters that could in some cases be used in statistical models to improve estimates of near-road air pollutant concentrations and might add meaningfully to the ability to better understand trends in air pollutant concentrations in the absence of comprehensive measurements. Although the parameters in the models that contributed most strongly to the adjusted R^2 varied by study site and pollutant — so are therefore not generalizable — further study of parameters related to local sources and meteorology might be beneficial. The intense measurement campaigns and assessments of the value of new parameters in this study contribute to an ongoing discussion of which detailed measurements are most valuable for better air quality models of traffic-related air pollutants. Additional studies — including some ongoing studies funded by HEI — will be needed to explore whether the effort put into developing more complex models of traffic-related air pollution will benefit exposure assessment for epidemiological studies.

ACKNOWLEDGMENTS

The Review Committee thanks the ad hoc reviewers for their help in evaluating the scientific merit of the Investigators' Report. The Committee is also grateful to Maria Costantini and Hanna Boogaard for oversight of the study, to Allison Patton for assistance in preparing its Critique, to Carol Moyer for science editing of this Report and its Critique, and to Kristin Eckles and Hope Green for their roles in preparing this Research Report for publication.

REFERENCES

Beelen R, Hoek G, Vienneau D, Eeftens M, Dimakopoulou K, Pedeli X, et al. 2013. Development of NO_2 and NO_x land use regression models for estimating air pollution exposure in 36 study areas in Europe — The ESCAPE project. Atmos Environ; doi:10.1016/j.atmosenv.2013.02.037.

Dons E, Int Panis L, Van Poppel M, Theunis J, Wets G. 2012. Personal exposure to black carbon in transport microenvironments. Atmos Environ; doi:10.1016/j.atmosenv.2012.03.020.

Goldstein AH, Nazaroff WW, Weschler CJ, Williams J. 2021. How do indoor environments affect air pollution exposure? Environ Sci Technol; doi:10.1021/acs.est.0c05727.

HEI (Health Effects Institute). 2010. Traffic-Related Air Pollution: A Critical Review of the Literature on Emissions, Exposure, and Health Effects. HEI Special Report 17. Health Effects Institute:Boston, MA.

HEI (Health Effects Institute). 2013. RFA 13-1 Improving Assessment of Near-Road Exposure to Traffic Related Pollution. Available: *https://www.healtheffects.org/research/funding/rfa/13-1-improving-assessment-near-road-exposure-traffic-related-pollution.*

HEI (Health Effects Institute). 2019. RFA 19-1 Applying Novel Approaches to Improve Long-Term Exposure Assessment of Outdoor Air Pollution for Health Studies. Available: *https://www.healtheffects.org/research/funding/rfa/19-1-applying-novel-approaches-improve-long-term-exposure-assessment-outdoor-air-pollution.*

HEI (Health Effects Institute). 2022. Systematic Review and Meta-Analysis of Selected Health Effects of Long-Term Exposure to Traffic-Related Air Pollution. Special Report 23. Boston, MA:Health Effects Institute.

Hoek G. 2017. Methods for assessing long-term exposures to outdoor air pollutants. Curr Environ Health Rep; doi:10.1007/s40572-017-0169-5.

Karner AA, Eisinger DS, Niemeier DA. 2010. Near-roadway air quality: Synthesizing the findings from real-world data. Environ Sci Technol 44:5334–5344; doi:10.1021/es100008x.

Patton AP, Robinson AL, Boogaard H. 2020. Land use regression models of ultrafine particles for assessment of long-term exposure for health studies. In: *Ambient combustion ultrafine particles and health* (Brugge D, Fuller CH, eds). New York:Nova Science Publishers.

Snyder MG, Venkatram A, Heist DK, Perry SG, Petersen WB, Isakov V. 2013. RLINE: A line source dispersion model for near-surface releases. Atmos Environ 77:748–756; doi:10.1016/j.atmosenv.2013.05.074.

Wallace L. 2000. Correlations of personal exposure to particles with outdoor air measurements: A review of recent studies. Aerosol Sci Technol; doi:10.1080/027868200303894.

Wheeler AJ, Wallace LA, Kearney J, Van Ryswyk K, You H, Kulka R, et al. 2011. Personal, indoor, and outdoor concentrations of fine and ultrafine particles using continuous monitors in multiple residences. Aerosol Sci Technol; doi:10.1080/02786826.2011.580798.

Zhou Y, Levy JI. 2007. Factors influencing the spatial extent of mobile source air pollution impacts: A meta-analysis. BMC Public Health 7:89; doi:10.1186/1471-2458-7-89.

ABBREVIATIONS AND OTHER TERMS

AERMET	meteorological data preprocessor used to prepare input files for an air quality model such as R-LINE
AERMOD	regulatory air quality dispersion model
AIC	Akaike Information Criterion
ANOVA	analysis of variance
AR	autoregressive
ARMA(p,q)	autoregressive moving average with autoregressive order *p* and moving average order *q*
BAM	beta attenuation monitor
BC	black carbon
CALINE	California line-source model
CO	carbon monoxide
CO_2	carbon dioxide
CRONOS	Climate Retrieval and Observations Network Of the Southeast
DSM	Digital Surface Model
GPS	global positioning system
HC	hydrocarbon
HDDV	heavy-duty diesel vehicle
HV	heavy vehicle
ISA	Integrated Science Assessment
LDGV	light-duty gasoline vehicle
LIDAR	light detection and ranging
MSAT	mobile-source air toxic
NAAQS	National Ambient Air Quality Standard
NCCU	North Carolina Central University
NCDEQ	North Carolina Department of Environmental Quality
NCSU	North Carolina State University
NO	nitric oxide
NO_2	nitrogen dioxide
NO_x	nitrogen oxides
O_3	ozone
OLS	ordinary least squares
PEM	personal environmental monitor
POM	portable ozone monitor
PM	particulate matter (typically quantified as particle mass per volume of air)
$PM_{2.5}$	particulate matter ≤ 2.5 µm in aerodynamic diameter
PM_{10}	particulate matter ≤ 10 µm in aerodynamic diameter
PN	particle number (quantified as number of particles per volume of air)
P-Trak	a portable ultrafine particle counter
QA	quality assurance
QC	quality control
R^2	coefficient of determination
R-LINE	Research LINE-source dispersion model
RDU	Raleigh–Durham International Airport
RTMS	Remote Traffic Microwave Sensor
SMPS	scanning mobility particle sizer spectrometer
SOA	secondary organic aerosol
SSE	sum of squared errors
SVOC	semivolatile organic compound
TRAP	traffic-related air pollutant
TD	thermodenuder
UFP	ultrafine particle ($PM_{0.1}$)
U.S. EPA	United States Environmental Protection Agency
VOC	volatile organic compound
vph	vehicles per hour
vpm	vehicles per mile
VSP	vehicle-specific power

RELATED HEI PUBLICATIONS

EXPOSURE TO TRAFFIC-RELATED AIR POLLUTION

Number	Title	Principal Investigator	Date
Research Reports			
202	Enhancing Models and Measurements of Traffic-Related Air Pollutants for Health Studies Using Dispersion Modeling and Bayesian Data Fusion	S. Batterman	2020
199	Real-World Vehicle Emissions Characterization for the Shing Mun Tunnel in Hong Kong and Fort McHenry Tunnel in the United States	X. Wang	2019
196	Developing Multipollutant Exposure Indicators of Traffic Pollution: The Dorm Room Inhalation to Vehicle Emissions (DRIVE) Study	J.A. Sarnat	2018
194	A Dynamic Three-Dimensional Air Pollution Exposure Model for Hong Kong	B. Barratt	2018
183	Development of Statistical Methods for Multipollutant Research		
	Part 3. Modeling of Multipollutant Profiles and Spatially Varying Health Effects with Applications to Indicators of Adverse Birth Outcomes	J. Molitor	2016
179	Development and Application of an Aerosol Screening Model for Size-Resolved Urban Aerosols	C.O. Stanier	2014
175	New Statistical Approaches to Semiparametric Regression with Application to Air Pollution Research	J.M. Robins	2013
152	Evaluating Heterogeneity in Indoor and Outdoor Air Pollution Using Land-Use Regression and Constrained Factor Analysis	J.I. Levy	2010
140	Extended Follow-Up and Spatial Analysis of the American Cancer Society Study Linking Particulate Air Pollution and Mortality	D. Krewski	2009
139	Effects of Long-Term Exposure to Traffic-Related Air Pollution on Respiratory and Cardiovascular Mortality in the Netherlands: The NLCS-AIR Study	B. Brunekreef	2009
131	Characterization of Particulate and Gas Exposures of Sensitive Subpopulations Living in Baltimore and Boston	P. Koutrakis	2005
130	Relationships of Indoor, Outdoor, and Personal Air (RIOPA)		
	Part I. Collection Methods and Descriptive Analyses	C.P. Weisel	2005
	Part II. Analyses of Concentrations of Particulate Matter Species	B.J. Turpin	2007
127	Personal, Indoor, and Outdoor Exposures to $PM_{2.5}$ and Its Components for Groups of Cardiovascular Patients in Amsterdam and Helsinki	B. Brunekreef	2005
Special Reports			
23	Systematic Review and Meta-analysis of Selected Health Effects of Long-Term Exposure to Traffic-Related Air Pollution	HEI Panel on the Health Effects of Traffic-Related Air Pollution	2022
17	Traffic-Related Air Pollution: A Critical Review of the Literature on Emissions, Exposure, and Health Effects	HEI Panel on the Health Effects of Traffic-Related Air Pollution	2010

Copies of these reports can be obtained from HEI; PDFs are available for free downloading at www. healtheffects.org/publications.

HEI BOARD, COMMITTEES, and STAFF

Board of Directors

Richard A. Meserve, Chair *Senior of Counsel, Covington & Burling LLP; President Emeritus, Carnegie Institution for Science; former Chair, U.S. Nuclear Regulatory Commission*

Enriqueta Bond *President Emerita, Burroughs Wellcome Fund*

Jo Ivey Boufford *President, International Society for Urban Health*

Homer Boushey *Emeritus Professor of Medicine, University of California–San Francisco*

Jared L. Cohon *President Emeritus and Professor, Civil and Environmental Engineering and Engineering and Public Policy, Carnegie Mellon University*

Stephen Corman *President, Corman Enterprises*

Martha J. Crawford *Operating Partner, Macquarie Asset Management*

Michael J. Klag *Dean Emeritus and Second Century Distinguished Professor, Johns Hopkins Bloomberg School of Public Health*

Alan I. Leshner *CEO Emeritus, American Association for the Advancement of Science*

Catherine L. Ross *Regents' Professor and Harry West Professor of City and Regional Planning and Civil and Environmental Engineering, and Director of the Center for Quality Growth and Regional Development, Georgia Institute of Technology*

Karen C. Seto *Frederick Hixon Professor of Geography and Urbanization Science, Yale School of the Environment*

Research Committee

David A. Savitz, Chair *Professor of Epidemiology, School of Public Health, and Professor of Obstetrics and Gynecology, Alpert Medical School, Brown University*

Jeffrey R. Brook *Assistant Professor, University of Toronto, Canada*

Amy H. Herring *Sara & Charles Ayres Professor of Statistical Science and Global Health, Duke University*

Barbara Hoffmann *Professor of Environmental Epidemiology, Institute of Occupational, Social, and Environmental Medicine, University of Düsseldorf, Germany*

Heather A. Holmes *Associate Professor, Department of Chemical Engineering, University of Utah*

Neil Pearce *Professor of Epidemiology and Biostatistics, London School of Hygiene and Tropical Medicine, United Kingdom*

Ana Rule *Assistant Professor and Director, Environmental Exposure Assessment Laboratories, Department of Environmental Health and Engineering, Johns Hopkins School of Public Health*

Ivan Rusyn *Professor, Department of Veterinary Integrative Biosciences, Texas A&M University*

Evangelia (Evi) Samoli *Associate Professor of Epidemiology and Medical Statistics, Department of Hygiene, Epidemiology and Medical Statistics, School of Medicine, National and Kapodistrian University of Athens, Greece*

Gregory Wellenius *Professor, Department of Environmental Health, Boston University School of Public Health*

HEI BOARD, COMMITTEES, and STAFF

Review Committee

Melissa J. Perry, Chair *Dean, College of Health and Human Services, George Mason University*

Sara D. Adar *Associate Professor and Associate Chair, Department of Epidemiology, University of Michigan School of Public Health*

Kiros T. Berhane *Professor and Chair, Department of Biostatistics, Mailman School of Public Health, Columbia University*

Michael Jerrett *Professor and Chair, Department of Environmental Health Sciences, Fielding School of Public Health, University of California–Los Angeles*

Frank Kelly *Henry Battcock Chair of Environment and Health and Director of the Environmental Research Group, Imperial College London School of Public Health, United Kingdom*

Jana B. Milford *Professor Emerita, Department of Mechanical Engineering and Environmental Engineering Program, University of Colorado–Boulder*

Jennifer L. Peel *Professor of Epidemiology, Colorado School of Public Health and Department of Environmental and Radiological Health Sciences, Colorado State University*

Eric J. Tchetgen Tchetgen *Luddy Family President's Distinguished Professor, Professor of Statistics and Data Science, The Wharton School, University of Pennsylvania*

Officers and Staff

Daniel S. Greenbaum *President*

Robert M. O'Keefe *Vice President*

Ellen K. Mantus *Director of Science*

Donna J. Vorhees *HEI Energy CEO and Vice President*

Annemoon M. van Erp *Deputy Director of Science*

Thomas J. Champoux *Director of Science Communications*

Jacqueline C. Rutledge *Director of Finance and Administration*

Jason Desmond *Deputy Director of Finance and Administration*

Emily Alden *Corporate Secretary*

Amy Andreini *Communications Assistant*

Ayusha Ariana *Research Assistant*

Palak Balyan *Consulting Staff Scientist*

Hanna Boogaard *Consulting Principal Scientist*

Aaron J. Cohen *Consulting Principal Scientist*

Dan Crouse *Senior Scientist*

Robert M. Davidson *Staff Accountant*

Philip J. DeMarco *Compliance Manager*

Kristin C. Eckles *Senior Editorial Manager*

Elise G. Elliott *Staff Scientist*

Hope Green *Editorial Project Manager*

Yi Lu *Staff Scientist*

HEI BOARD, COMMITTEES, and STAFF

Lissa McBurney *Senior Science Administrator*
Janet I. McGovern *Executive Assistant*
Martha Ondras *Research Fellow*
Pallavi Pant *Senior Scientist*
Allison P. Patton *Senior Scientist*
Quoc Pham *Science Administrative Assistant*
Anna S. Rosofsky *Senior Scientist*
Robert A. Shavers *Operations Manager*
Eva Tanner *Staff Scientist*
Ada Wright *Research Assistant*

HEALTH
EFFECTS
INSTITUTE

75 Federal Street, Suite 1400
Boston, MA 02110, USA
+1-617-488-2300
www.healtheffects.org

RESEARCH
REPORT

Number 207
September 2022